

**ForceArm: a wearable pneumatic gel muscle  
(PGM)-based assistive suit for the upper limb**

(ForceArm: ウェアラブル空気圧ゲル人工筋 (PGM) を用いた  
上肢支援スーツ)

by

**SWAGATA DAS**

**Graduate School of Engineering  
Hiroshima University**

**September 2020**



# Contents

<b>List of Figures</b>	<b>vii</b>
<b>List of Tables</b>	<b>xi</b>
<b>Nomenclature</b>	<b>xiii</b>
<b>1 Introduction</b>	<b>1</b>
1.1 Background and motivation . . . . .	1
1.2 Literature review . . . . .	4
1.2.1 Hard-type wearable robots (HWRs) . . . . .	4
1.2.2 Soft-type wearable robots (SWRs) . . . . .	6
1.2.3 Haptic/ force-feedback . . . . .	7
1.3 Content Outline . . . . .	11
<b>2 System description</b>	<b>17</b>
2.1 Introduction . . . . .	17
2.2 The human upper limb . . . . .	17
2.2.1 Anatomy of the upper limb . . . . .	18
2.2.2 Degrees of freedom (DOFs) considered for the prototype . . . . .	20

---

2.3	ForceArm prototype evolution . . . . .	22
2.3.1	Version 1: ForceHand . . . . .	22
2.3.2	Version 2: ForceArm . . . . .	23
2.4	Pneumatic gel muscle (PGM) . . . . .	28
2.4.1	Overview . . . . .	28
2.4.2	Attachment points of pneumatic gel muscles (PGMs) . . . . .	29
2.5	Control system . . . . .	31
2.5.1	Stretch sensor-based control . . . . .	31
2.5.2	Static wireless control system . . . . .	32
2.6	Discussion . . . . .	33
2.7	Conclusion . . . . .	34
<b>3</b>	<b>System evaluation</b>	<b>35</b>
3.1	Introduction . . . . .	35
3.2	Control system evaluation . . . . .	35
3.2.1	Rising set-point . . . . .	38
3.2.2	Falling set-point . . . . .	38
3.2.3	Pneumatic gel muscle (PGM) switching . . . . .	38
3.3	Pneumatic gel muscle (PGM) force measurement . . . . .	39
3.4	User study for surface electromyography (sEMG)-based evaluation . . .	41
3.4.1	Methodology . . . . .	41
3.4.2	Results . . . . .	44
3.5	Discussion . . . . .	48
3.6	Conclusion . . . . .	50

---

<b>4</b>	<b>Application scenarios and case studies of the ForceArm glove</b>	<b>51</b>
4.1	Introduction . . . . .	51
4.2	CASE STUDY 1: Feasibility study through an elderly exergame . . . . .	53
4.2.1	Development of a Unity-based exergame . . . . .	53
4.2.2	2-month elderly user study . . . . .	54
4.2.3	Parameters chosen for analysis . . . . .	55
4.2.4	Results . . . . .	58
4.2.5	Discussion . . . . .	61
4.3	CASE STUDY 2: Can ForceArm induce motor learning? . . . . .	63
4.3.1	Apparatus . . . . .	64
4.3.2	Participants . . . . .	65
4.3.3	Task and Procedure . . . . .	65
4.3.4	Results . . . . .	67
4.3.5	Discussion . . . . .	68
4.4	CASE STUDY 3: Navigation assistance through ForceArm . . . . .	70
4.4.1	Navigation environment simulated in Unity . . . . .	71
4.4.2	Just noticeable differences (JND) experiment . . . . .	72
4.4.3	Discussion . . . . .	74
4.5	CASE STUDY 4: ForceArm-based feedback in virtual reality (VR) . . . . .	79
4.5.1	Modelling of pneumatic gel muscle (PGM) induced force due to stiffness . . . . .	79
4.5.2	Force-feedback in virtual reality (VR) . . . . .	84
4.5.3	User-study . . . . .	86

---

4.5.4	Open-ended feedback . . . . .	87
4.5.5	Discussion . . . . .	88
4.6	Conclusion . . . . .	90
<b>5</b>	<b>Conclusions</b>	<b>93</b>
<b>6</b>	<b>Future work</b>	<b>97</b>
	<b>Bibliography</b>	<b>101</b>

# List of Figures

2.1	The degrees of freedom (DOFs) associated with the ForceArm prototype.	21
2.2	Placement positions of pneumatic artificial muscles (PAMs) and stretch sensors for each motion [1]. . . . .	22
2.3	Positions of pneumatic gel muscles (PGMs) in the ForceArm prototype associated with each supported motion [2]. . . . .	24
2.4	(a) Extended shoulder brace (b) back view of the shoulder brace (c) front view of the shoulder brace (d) hand-wrap glove (e) attaching the hand-wrap glove in (f) ventral side and (g) dorsal side perspectives; the red circle marks show the points where hook type fabric is attached for facilitating pneumatic gel muscle (PGM) attachment [2]. . . . .	25
2.5	Components used in the ForceArm prototype [2]. . . . .	25
2.6	Working principle involved in the actuation of the pneumatic gel muscle (PGM) [2]. . . . .	28
2.7	Control flow of the stretch sensor-based automated pneumatic artificial muscle (PAM) actuation method [1]. . . . .	31
2.8	Flow diagram of the closed loop PI control system used to maintain stable input air pressure fed to the pneumatic gel muscles (PGMs). Here, POT refers to potentiometer [2]. . . . .	32

3.1	Rising behaviour of the control system with target set-points of (a) final air pressure = 0.1MPa (b) final air pressure = 0.2MPa [2]. . . . .	36
3.2	Control system responses to (a) fall in the set-point (b) switching on one of the pneumatic gel muscles (PGMs) receiving controlled air pressure [2].	37
3.3	Force induced by pneumatic gel muscle (PGM) actuation for two PGM lengths and at two stretched conditions for each PGM [2]. . . . .	39
3.4	Calculation of torque from force induced by pneumatic gel muscle (PGM) actuation; an example of wrist extension where $F$ is the linear force due to the PGM actuation, $r$ is the distance from the axis of rotation to point of application of the force and $\theta$ is the angle shown in the figure [2].	40
3.5	Illustration of various motions associated with pneumatic gel muscle (PGM) actuation. (a) and (b) represent the forearm orientation used for surface electromyographical (sEMG) measurement in wrist flexion-extension (c) and (d) represent the forearm orientation used for surface electromyographical (sEMG) measurement in forearm pronation-supination (e) and (f) show the resultant movement in the arm due to pneumatic gel muscle (PGM) actuation during flexion assistance of the elbow and shoulder joints, respectively. For all measurements, the arm is held against gravity [2]. . . . .	42
3.6	Illustration of the average % maximal voluntary contractions (MVCs) of young subjects for forearm motions with and without assist. . . . .	44
3.7	Average % maximal voluntary contractions (MVCs) of all subjects associated with wrist (a) flexion and (b) extension motions with and without assist. . . . .	45
3.8	Average % maximal voluntary contractions (MVCs) of all subjects associated with forearm (a) pronation and (b) supination motions with and without assist. . . . .	46



---

3.9	Average % maximal voluntary contractions (MVCs) of all subjects associated with (a) elbow flexion and (b) shoulder flexion motions with and without assist. . . . .	47
4.1	(a) Illustration of an elderly gaming session along with various patterns used during the session (b) 60deg (c) inverse 60deg (d) inverse L (e) L (f) O (g) 8 (h) + (i) coordinate reference for LeapMotion measurements [2]. . . . .	53
4.2	Comparing the rates of change of time score with and without suit for various patterns. . . . .	58
4.3	Comparing the rates of change of deviation score with and without suit for various patterns in (a) X-axis and (b) Y-axis. . . . .	59
4.4	Comparing the rates of change of jerkiness score with and without suit for various patterns in (a) X-axis and (b) Y-axis. . . . .	60
4.5	Comparing the rates of change of hand-path ratio score with and without suit for various patterns. . . . .	61
4.6	Materials used for setting up the drumming practice and timing detection	64
4.7	Experiment Settings. . . . .	65
4.8	Drumming scores used for the study. Two easy and six hard patterns.	66
4.9	Results of two-handed drumming study . . . . .	67
4.9	Results of two-handed drumming study (cont..) . . . . .	68
4.10	Degrees of freedom (DOFs) chosen for navigation assistance with positions of the associated pneumatic gel muscles (PGMs) [3]. . . . .	70
4.11	Degrees of freedom (DOFs) considered for use as navigation cues [3]. . . . .	70

4.12	Maze environment simulated in Unity for testing the feasibility of navigation assistance using pneumatic gel muscle (PGM)-based force-feedback [3]. . . . .	73
4.13	User preferences of navigation assistant cue type [3]. . . . .	73
4.14	Error values (%) observed during just noticeable difference (JND) experiment . . . . .	75
4.15	Accuracy (%) plotted against air pressure (kPa) for different resolutions [3]. . . . .	76
4.16	(a) Notations used for forearm dimensions while attaching the pneumatic gel muscles (PGMs) (b) Experimental set-up used to measure force due to stiffness in PGMs [4]. . . . .	79
4.17	Modelling of the force due to stiffness in pneumatic gel muscle (PGM) actuator [4]. . . . .	81
4.17	Modelling of the force due to stiffness in pneumatic gel muscle (PGM) actuator (cont..) [4]. . . . .	82
4.18	Illustration of the control flow used to regulate the air pressure fed to the pneumatic gel muscles (PGMs) [4]. . . . .	84
4.19	Visual representation of the various objects as shown to the users during the study [4]. . . . .	85
4.20	User study to render physicality for objects in virtual reality (VR) [4]. .	86
4.21	Subjective feedback obtained from user-study for various types of feedback	87

# List of Tables

1.1	Comparison of the existing robotic systems for the upper limb with ForceArm. Here, actuation delay refers to the time required to attain the desired torque after receiving the command. Abbreviations used: FE - flexion-extension, AA - adduction-abduction, F - flexion, RT - rotation, PS - pronation-supination. © 2020 IEEE . . . . .	15
2.1	List of components used in the ForceArm prototype with their respective weights [2]. © 2020 IEEE . . . . .	27
2.2	Comparison of the contraction and elongation ratios of pneumatic gel muscle (PGM) and its commercially available soft actuator equivalent PM-RF10 at a fixed air pressure input of 0.2MPa. . . . .	29
4.1	Actuation sequence of pneumatic gel muscle (PGM) for various feedback types in binary and pulse width modulation (PWM) actuation methods [4]. © 2020 IEEE . . . . .	85



# Nomenclature

## Acronyms / Abbreviations

AD Anterior Deltoid

AR Artificial reality

BB Biceps Brachii

BPM Beats per minute

BRC Brachialis

BRD Brachioradialis

DAC Digital to analog converter

DOF Degree of freedom

EAS Exoskeleton Actuated by the Soft Modules

ECR Extensor Carpi Radialis

EMG Electromyography

EMS Electrical muscle stimulation

FCU Flexor Carpi Ulnaris

HEXORR Hand Exoskeleton Rehabilitation Robot

HWR Hard-type wearable robots

ITI Inter-tap interval

JND Just noticeable difference

MVC Maximal voluntary contractions

NTG Nippon Tansan Gas Co.Ltd.

PAM Pneumatic artificial muscle

PGM Pneumatic gel muscle

PM Upper Pectoralis Major

PN Pneumatic networks

PT Pronator Teres

PWM Pulse width modulation

QoL Quality of life

ROM Range of motion

sEMG Surface electromyography

SENIAM Surface electromyography for the non-invasive assessment of muscles

SL Supinator Longus

SMA Shape memory alloy

SWR Soft-type wearable robots

VR Virtual reality

WFD World's fastest drummer

# Chapter 1

## Introduction

### 1.1 Background and motivation

The upper limb of the human body plays a vital role in our day to day life. It is an essential part of the body to maintain a good quality of life (QoL). Any injury or weakness in the upper limb can result in unsatisfactory living conditions leading to mental and additional physical illnesses. We perform many small yet fundamental tasks such as navigation inside a building by opening and closing doorknobs, lifting objects, typing, changing clothes, taking a shower, holding phones to talk and more using our upper limb. Therefore, disorders in the upper limb of patients and older adults can adversely affect their QoL. Frequently performing physically demanding activities often leads to wearing down of the muscles in our body, which in turn, makes regular performance in day to day activities difficult and time taking due to successive pain and numbness. Other reasons for similar irregularity in muscular functioning may also result from repetitive motions involved in sports such as tennis, badminton, cricket and others. The upper limb comprises of three joints, namely the wrist, elbow and shoulder. These are very complicated joints when it comes to recovery and rehabilitation. Besides, the complexity of the wrist joint often makes it challenging to design a rehabilitation or assistive device. Additionally, the wrist dynamics play a significant role in the decisions

taken to design a product. We developed a soft, and wearable robotic assist prototype called the ForceArm glove by carefully considering such constraints related to the wrist and upper limb dynamics.

The speciality of these types of robotic systems is that they can have multiple numbers of applications and not limited to use in the medical field. Such additional applications may include usage in entertainment through virtual, augmented, and mixed reality, enhancing physical and cognitive abilities of human, resistive training for healthy individuals and more. In this work, the prototype that was initially designed for rehabilitation and providing physical assistance, was then also tested and tried for the following enlisted applications:

- using force-feedback to induce motor learning (two-handed drumming)
- using force-feedback assistance to provide navigation cues
- provide force-feedback in virtual reality (VR)

The first application we considered for study was the prototype's ability to induce motor learning in individuals. We often realize that learning dexterous physical tasks such as playing musical instruments, handling chopsticks, and painting requires plenty of time to master due to the need for auditory and multi-limb coordination. To accelerate the learning process, we can use the force-feedback technique of providing training. Recently, haptic interfaces are being deployed to achieve such motor learning by actuating human body parts. However, this field has not been studied in abundance so far as no device has successfully shown learning effect. Therefore we consider this topic as our additional area of research. For this study, we chose two-handed drumming as the learning task.

The second application tested using the ForceArm prototype was navigation assistance. We all use navigation aids in our day to day lives. A previously unseen path is undoubtedly challenging to navigate through. Such paths demand immense attention



which may also lead to a reduced concentration on other engagements or tasks. For example, it is quite cognitively demanding if someone wants to navigate through a new route using a map-based application and talk over the phone at the same time. Such situations even cause serious accidents due to the high cognitive load. Humans have used maps and compasses as conventional methods of navigation during olden days. These methods were replaced by auditory and visual methods such as mobile phone-based navigation assistance during recent times. If we observe, it can be said that prolonged usage of such audio-visual information transfer often leads to confusion and frustration, resulting in reduced efficiency. Also, visually challenged individuals do not have the privilege to use such systems except through the audio channel. Research has proved the tactile channel to be the most suitable way of cue-transfer for humans. It was shown in many recent pieces of research that haptic feedback has advantages over other types of information transfer channels when it comes to navigation assistance [5]. Moreover, tactile feedback was proved to have the least reaction time while responding to warning signals as compared to visual and audio feedback types in a recent study [6]. All these observations from the recent advances in literature led us to test our prototype for feasibility as a navigation assistance device.

The third application scenario examined for the ForceArm prototype was providing force-feedback in VR at the wrist joint. We have seen remarkable advances in the field of VR by simulating different types of environments to let users feel immersed. In addition, VR has also been used as a training or learning tool in fields such as rehabilitation [7], gaming [8], art [9], and medicine [10]. Good haptic feedback provided to convey information about contact with the physical objects in the virtual worlds can increase realism in VR [11]. Through this research, we aim to use one part of the ForceArm prototype to provide realistic force-feedback at the wrist joint. We chose the wrist joint primarily because there is very less work done that focuses on providing force-feedback at this joint of the upper limb.

## 1.2 Literature review

With an increasing population of elderly in the world [12], assistive devices are likely to have a significant role to play. Rehabilitation is done to recover from joint and muscle disorders in the body. However, the success rate of physical rehabilitation mainly depends on factors such as intensity, orientation and duration of training as well as the patient's health condition, attention, and effort [13, 14]. The burden on caregivers significantly increases if patients depend on human assistance for their active recovery, which is possible only with repetitive and sincere training sessions. Besides, it also adversely affects the financial condition of the patient. These issues have been addressed over the recent years by researchers who developed robotic systems that provide physical rehabilitation [15, 16]. It has been proved that robotic rehabilitation can accelerate recovery [17].

Park *et al.* classified wearable robots into hard-type wearable robots (HWRs) and soft-type wearable robots (SWRs) according to the materials used in the system and their manoeuvring method [18]. HWRs or rigid type robotic systems [19] often contain joints with rigid links, thus with increased costs and weight. Besides, the rigid structure reduces compliance and the overall comfort of the system when directly worn by the users. Patients or elderly individuals look for comfort when opting for solutions with daily life usability. Therefore, such rigid systems are often not preferred for the elderly or patients. Soft actuators [20] allow us to overcome the issues mentioned above, thereby enabling the implementation of safe and comparatively inexpensive systems. This section carefully discusses the different types of wearable robots developed so far for the upper limb.

### 1.2.1 Hard-type wearable robots (HWRs)

There are several hard-type wearable exoskeletons for different joints of the upper limb. Some of those from the last two decades are summarized in this section. The

desired qualities in a typical hard exoskeleton are discussed in [21], and following those qualities, a haptic arm exoskeleton with five degrees of freedom (DOFs) was designed. The same prototype was upgraded to RiceWrist [22] later. The design, control and performance are also discussed, and the prototype is applied for rehabilitation and training. A seven DOF upper limb powered exoskeleton called CADEN-7 is proposed for rehabilitation and VR simulations [23]. Another seven-DOF hard exoskeleton called SUEFUL-7 was used to assist shoulder, elbow, forearm and wrist motions actuated through electromyography (EMG)-based control method [24]. Other typical upper extremity hard exoskeletons are mentioned in [25, 26, 19, 27].

Pneumatic actuators have been often combined with rigid structures to achieve higher power to weight ratios as compared to pneumatic actuators alone. Such combinations were also used to realize upper limb exoskeletons in the recent past. Tsagarakis *et al.* developed a low weight pneumatic artificial muscle (PAM)-based exoskeleton combined with a rigid frame to support seven DOFs of the upper limb [28]. Another upper limb exoskeleton called Pneu-WREX using PAMs was combined with a rigid frame with a precise control mechanism, as discussed in [29]. Similar work focussing on forearm-wrist rehabilitation was also accomplished [30]. Structural components made of graphite composite materials were combined with PAMs to develop an upper extremity therapy robot called RUPERT [31]. Such components could reduce the overall weight of the prototype. Grounded type of upper-limb rehabilitation systems was also developed. One such system fixed to the patient's bed was made using PAMs to increase the wearability factor [32]. Combination of actuation systems with pneumatic and electric components was used to develop an upper-body exoskeleton robot in [33]. Electric components were used to drive Bowden cables to transmit the force generated by the PAMs to the joints of the robot.

Various control systems have also been implemented to control the actuation of the exoskeletons. One type of motion control has been shown using a PID-based control algorithm to drive the two DOF robotic exoskeletal prototype called EXOWRIST,

which also uses PAMs [34]. EMG-based control methods were implemented to actuate the upper limb exoskeleton called SUEFUL-7 [24] and a wrist exoskeleton [35].

Exoskeletons to support only the digits of the hand fingers were also developed. One such prototype to provide a full range of motion (ROM) called Hand Exoskeleton Rehabilitation Robot (HEXORR) for all hand digits was successfully tested for rehabilitating stroke survivors [36]. A systematic review on hand exoskeletons proposed for both rehabilitation and haptic applications can be found in [37] and [38].

### 1.2.2 Soft-type wearable robots (SWRs)

Researchers introduced many novel approaches over the past decade due to the rising interest in soft robotics. One recent work used a fabric type soft actuator composed of shape memory alloy (SMA) spring bundles to develop a soft wearable robotic suit [18]. Soft exosuits were developed using Bowden cable-driven actuation with geared motors for walking-assist [39] and for upper limb augmentation [40, 41]. Another novel soft actuation method comprised of moulded elastomeric chambers with fibre reinforcements was used to develop a glove intended for hand rehabilitation. These actuators were named pneumatic networks (PneuNets). The glove could induce specific bending, twisting, and extending trajectories under fluid pressurization [42, 43]. Soft Modules actuated by pneumatic control were used to develop an Exoskeleton Actuated by the Soft Modules (EAsoftM) aimed at reaching movement [44]. Another recent work used 0.25-inch thick PAMs to augment flexion-extension and pronation-supination of the wrist and forearm respectively [45]. Additional fabric type soft actuators were discussed in [46, 47]. Upper-limb focused robotic research using soft actuators has progressed significantly. However, the majority of research focuses on hand or finger rehabilitation [37, 38].

### 1.2.3 Haptic/ force-feedback

Haptic feedback providing devices have been a challenging subject for roboticists in the recent past. Haptic feedback given to users is highly essential to make the interaction between the computer and human more acceptable and realistic. Phantom [48] and SPIDAR [49] are primarily developed grounded types of haptic feedback providers. They need to be placed on the firm ground to be used. This type of systems is suitable for generating large haptic forces. CyberGrasp and CyberGlove by CyberGlove Systems are ungrounded type haptic feedback providers. The CyberGrasp is a full hand force-feedback exoskeletal device, worn over the CyberGlove. The advantages of ungrounded type are their wearability and portability, although CyberGrasp cannot generate high forces. Electrical muscle stimulation (EMS) has also been applied as a source of haptic feedback [50]. A systematic review of different exoskeleton robots used in conjunction with VR, augmented reality (AR), and gamification to realize complicated applications for motor recovery, augmentation, gaming, and more are shown in [51].

Haptic or force-feedback has been applied to multiple applications in entertainment as well as the medical field. Some other application types include human augmentation to enhance or support physical or cognitive human abilities. In this work, we utilize our prototype in three additional applications other than rehabilitation, namely motor learning, VR feedback and navigation assistance. The literature review for each of these applications is discussed next.

#### Motor learning

Muscle memory is created by motor learning that involves step by step consolidation of the desired motor task into memory through repetition. The use of augmented feedback, through which the user is provided with external information about the desired motion, can facilitate motor learning. Such feedback is supplemental to our intrinsic sensory such as vision or proprioception of limbs. Several studies have investigated the type

or frequency of augmented feedback that facilitates the retention of motor skill. The influential guidance hypothesis postulates that too much feedback is detrimental to motor skill learning. One of the assumptions of the guidance hypothesis is that a reduced frequency of augmented feedback (providing feedback on every alternate training trial) may facilitate learning because it promotes the learner to use their intrinsic knowledge during the no-feedback trials [52, 53]. The no-feedback trials also provide the learner with the opportunity to integrate information from previous feedback trials, with information derived from their inherent feedback. The active use of inherent feedback during the no-feedback trials may help the learner form a motor command to execute a target movement without relying on the augmented feedback [52, 53]. In general, inherent feedback can enhance performance in the acquisition phase of learning. However, the performance gains are lost in the retention phase. That is also explained in the guidance hypothesis. The type of guidance, such as visual feedback, forces learners to ignore their intrinsic feedback or proprioception. However, while learning dynamic tasks, proprioception is more important than vision. A healthy person can learn dynamic tasks equally well with or without vision. However, someone who lost proprioception may have particular difficulty controlling the dynamic properties of their limbs or learning new dynamic tasks without vision [54, 55].

Xiao *et al.* proposed a design framework for music learning and explained that embodiment is one of the essential aspects to acquire perception and motor skills, especially for music learning [56]. They also pointed out that novel interfaces may go beyond using learning videos by supporting imitation, although videos are already a popular medium for people to learn new skills. Some researchers also try to accelerate motor learning by approaches based on embodied feedback, for example, Feygin *et al.* demonstrated that active force guidance could be beneficial for learning a 3D trajectory following task, particularly in timing-related aspects [57]. Vibrotactile feedback was used to foster rhythm skills and multi-limb coordination through a drumming task in [58]. Many researchers tried to accelerate the learning process of musical instruments, such as piano, and they presented multiple interactive systems

for this purpose. Tamaki *et al.* used EMS to guide users in learning a new Japanese traditional stringed instrument called *Koto* [59]. EMS was also applied to teach how to use different home tools, such as spray can and avocado knife [50]. EMS is beneficial for activating human muscles. However, using electricity on the muscles is not entirely innocuous for the human body, and there are both ethical and safety concerns [60].

### **Haptic feedback**

Haptic feedback through force actuation has also been widely considered recently for a substantial number of applications such as medical training, industrial machinery simulation, sports training and more. Some of the related work is discussed in this section. AcceleGlove was a gesture recognition glove [61] used as a controller of robotic devices and by replicating grasping and lifting arms. NuGlove [62] can be used either as a gesture recognizer or as a controller for robotic devices or to track individual hand movements. Another work proposed by Kim *et al.* [49] describes a vibrotactile feedback method to assist writing texts and drawing shapes in the air. The review by Pacchierotti *et al.* [37] discusses a wide range of available wearable haptic systems for the fingertip and the hand. These haptic systems are categorized into two categories, grasping and manipulating, based on cutaneous and kinesthetic stimuli on the fingertips and whole hand. Wrist rehabilitation has been attempted through interactive gaming by vibrotactile actuation in the E-Glove [63].

Recent researches in the field of haptic technology mainly focus on replication of haptic properties of objects by simulating the contact of user's fingertips with different types of surfaces or textures [64, 65]. Interaction with objects have force effects on the wrist or the forearm of the user, but such effects are not yet thoroughly studied. A conventional table-top force-feedback device, Phantom [48] could render such forces on the user's forearm. However, due to its grounded configuration, it can be utilized only for stationary applications. Another approach for realizing force-feedback effects on the forearm was using SPIDAR [66] and SPIDAR-W [67], the prior being grounded

type and the latter, wearable type with a carry-on cage on the user's hand. EMS was also used to realize force-feedback effects on the arm and foot [68].

## Navigation

For the past two decades, the field of human-computer interaction has expanded the scope of applications to different fields that include physical as well as cognitive assistance to humans. One such emerging field of application is assistance in navigation. Some of the recently developed hand-held devices in this field are discussed next. A four DOF hand-held motion guidance system was developed by making use of finger movements to convey navigation cues to users [69]. Another interesting idea of a shape-changing haptic interface was developed for blind and sighted pedestrian navigation [70]. A navigation tool for cyclists was developed by utilizing vibration-based cues [71]. Majority of the work in this field utilized hand-held devices and vibration-based cues. Research also says that haptic or force-feedback can further enrich vibration-based feedback for richer interaction [72]. Conventional force-feedback devices include table-top systems such as the Phantom [48] and SPIDAR [49]. An example of a force-feedback system to implement wearability is the CyberGrasp. There is much scope to realize wearability and force-feedback through the same system without compromising the comfort of the user.



## 1.3 Content Outline

The literature study implied that the most commonly used components for SWRs were Bowden cables, SMA, soft pneumatic modules, pneumatic and hydraulic actuators. Bowden cables require heavyweight motors for their operation. Besides, SMA-based actuators are significantly expensive due to their manufacturing procedure [73]. A notable drawback of hydraulic actuators is fluid leakage even though they are capable of producing larger forces as compared to pneumatic actuators [74]. Rigid components combined with pneumatic modules provide benefits to the system such as higher force, stability and better control. Many researchers have also used PAMs for upper limb rehabilitation in combination with rigid structures. However, a significant drawback of using pneumatic actuators is the need for heavyweight compressors. Also, soft pneumatic actuators are unable to produce large forces when compared to their counterparts.

In terms of motor learning, the approach based on soft exoskeleton has several benefits compared with EMS and rigid exoskeleton. Soft actuators do not restrict our body movement like a rigid exoskeleton or HWRs, and it is easier to resist the provided force. EMS also allows us to resist the provided force, but it is difficult to oppose when a large amount of electric current flows through and shrinks our muscle. Furthermore, the pneumatic gel muscle (PGM) that we use in this study can be driven by relatively low air pressure. This quality of the PGMs allows us to use small air tanks to provide compressed air to the pneumatic actuator and enable us to provide substantial force-feedback to the users. It is also easier to realize the system with a wearable form factor.

Wide variations in the types of rendering force-feedback can be observed during the past decade's literature. Some of the force-feedback applications are to replicate hand movements to control robotic devices, and others focus on the detection of proper motions of arm, hands and finger. On the contrary, force-feedback rendering at the wrist to enable rehabilitative and assistive applications have not been deeply considered

yet. Based on such facts, we developed a wearable glove-type force-feedback device for the entire arm. We prioritized to make the system lightweight, portable, wearable and not restricting natural human motions. The fundamental concept of this glove was presented in [75]. The second version of the glove that could actively support users who need assistance in performing necessary wrist motions through automatic actuation of PAMs was named ForceHand [1]. Such active support can enable users to rehabilitate themselves through repetitive training at home with minimal investment. Additionally, it was made sure that the components used in the prototype were commercially available at affordable rates. Therefore, the system can become a prospective low-cost solution for rehabilitation and force-feedback applications.

The ForceHand glove was further improvised to bring the final version of an upper limb wearable assistive suit called ForceArm [2]. This system supports the majority of the DOFs of the arm, including wrist flexion-extension, forearm pronation-supination, elbow flexion, and shoulder flexion. First, we evaluated the ForceArm suit using muscle activity measurement to verify the effects of muscle unloading in elderly subjects for the forearm DOFs. The other two DOFs shoulder and elbow flexion were measured on younger subjects because we could not get permission to measure back and thorax muscles in the elderly participants. Following muscle activity measurement, a gaming scenario was developed using Unity software. This application was mainly intended to identify the effectiveness of the prototype in motor rehabilitation for elderly individuals against time. The major component of the ForceArm suit is PGM [76]. The speciality of these actuators is their ability to produce higher force at lower air pressure requirement compared to similar commercially available counterparts. This quality of the PGMs enables us to use the system as a standalone, without the need for a heavyweight air compressor for extended time-periods. Table 1.1 compares the ForceArm suit with selected previously developed prototype counterparts. At lower operating air pressure, ForceArm achieved equivalent force density output, when compared to the selected prototypes using pneumatic actuators. Moreover, the ForceArm suit was built with only

soft components giving the advantage of comfort, especially to the elderly individuals and patients.

The qualifications which were prioritized during the design and are vital to fulfilling the aspirations of patients, medical and technical communities [77] include:

- Minimized restriction of natural movements
- Donning and doffing made easy
- Wearable even with loose normal clothing externally
- Reduced worn weight: ForceArm weighs 2100g, and only 214g is worn on the arm
- Low complexity with reduced engineering and manufacturing cost
- Flexible behaviour of actuators thus providing minimum restriction
- Reduced maintenance after acquiring the product
- Does not get affected by environmental factors such as dust, moisture, and water.
- Standalone: the use of low-pressure type actuators enables the system to be used with portable canisters for long hours
- Associates to a multiple DOFs of the upper limb

This thesis is divided into six chapters. The introduction chapter is followed by system description which explains the DOFs associated with the prototype, along with system configuration, the introduction of PGMs, the control system, and the integration of the ForceArm with a static control system. The third chapter describes the technical evaluation of the system, precisely, the control system and force measurement due to PGM actuation. This chapter also includes the surface electromyography (sEMG)-based evaluation of the ForceArm prototype in both young and elderly subjects. The next chapter describes the application scenarios related to the ForceArm prototype in

the form of four user studies conducted to evaluate the prototype. This is followed by the conclusions drawn from the various user studies and prototype evaluation. Finally, the future work prospects of this research are discussed in the last chapter.

Table 1.1 Comparison of the existing robotic systems for the upper limb with ForceArm. Here, actuation delay refers to the time required to attain the desired torque after receiving the command. Abbreviations used: FE - flexion-extension, AA - adduction-abduction, F - flexion, RT - rotation, PS - pronation-supination. © 2020 IEEE

Actuation method	Weight (grams)	Operating air pressure (MPa)	Torque/Force Density or Torque (Nm)	Maximum force (N)	Actuation delay	DOF	Additional components
Bowden cable [40]	2085 (motors) + 387	-	-	-	-	Shoulder FE, AA + elbow FE	Motors
SMA [18]	960	-	125N/Kg	120N	1s (90% contraction)	Elbow F	BOA ratchets + cables
Pneumatic soft modules [44]	967	0.03	8.79Nm/Kg	8.5Nm	> 3s for 10 to 20kPa change	Shoulder FE + elbow FE	ABS printed structures
PAMs [28]	<2000	0.6	-	-	-	Shoulder FE, AA, RT + elbow FE + Forearm PS + Wrist FE, AA	Mechanical structures
PAMs [45]	2260	0.4	35.4N/Kg	80N (two in parallel)	-	Forearm PS + Wrist FE	BOA ratchets
PGMs (ForceArm)	2100	0.2	38.1N/Kg	80N (two in parallel)	<50ms	Wrist FE + forearm PS + shoulder F	Completely soft except controller components



# Chapter 2

## System description

### 2.1 Introduction

This section begins with a short description of the various DOFs of the upper limb, followed by a summary of the characteristics and components involved in the prototype design. The prototype uses a low-pressure type artificial muscle called PGM, which is also explained. The wearable portion of the system and the components used to control the air pressure fed to the PGMs are also described orderly. Furthermore, the limitations of the current prototype are also discussed in detail.

### 2.2 The human upper limb

The upper limb of the human includes the hand, arm and the shoulder. The hand is the most evolved organ in the upper limb. Generally, shoulder and forearm are used to position the hand at the desired spot. The upper limb is crucial in performing daily life activities such as sports, handling tools, wearing clothes, gestures, lifting objects, and cleaning. This section describes the various upper limb motions along with the associated muscles.

### 2.2.1 Anatomy of the upper limb

The upper extremity in human begins with the shoulder joint, which is the only ball and socket joint in the human body other than the hip joints. Because of the type of joint, a wide range of motions is permitted by our shoulder. The shoulder is followed by the elbow joint, which is a hinge joint and joins the upper arm to the forearm. As it is a hinge type joint, it allows only flexion and extension motions. Finally, there is the wrist joint which joins the forearm and the hand. The wrist joint is an ellipsoidal type synovial joint that allows movement along two axes. In other words, flexion, extension, adduction, and abduction can all occur in this joint [78].

#### Shoulder joint

Because of the type of joint, it allows a wide range of movement. However, the shoulder joint is less stable due to its shallow glenoid cavity of the scapula [78]. The possible movements occurring at the shoulder joint with acting muscles are as follows [79]:

- Flexion - Range of motion is  $0^{\circ}$ - $180^{\circ}$ . The major acting muscles are Anterior Deltoid and Coracobrachial. The minor acting muscles include Pectoralis Major (upper), Middle Deltoid and Serratus Anterior.
- Extension - Range of motion is  $0^{\circ}$ - $60^{\circ}$ . The major acting muscles are Latissimus dorsi, Posterior Deltoid and Teres Major. The minor acting muscle includes Triceps Brachii (long head).
- Scaption - Range of motion is  $0^{\circ}$ - $170^{\circ}$ . The major acting muscles are Deltoid and Supraspinatus.
- Abduction - Range of motion is  $0^{\circ}$ - $180^{\circ}$ . The major acting muscles are Deltoid (middle fibres) and Supraspinatus.



- Horizontal abduction - Range of motion is  $0^{\circ}$ - $130^{\circ}$ . The major acting muscle is Deltoid (posterior fibres). The minor acting muscles include Teres Minor and Infraspinatus.
- Horizontal adduction - Range of motion is  $0^{\circ}$ - $130^{\circ}$ . The major acting muscle is Pectoralis Major. The minor acting muscle includes Deltoid (anterior fibres).
- External rotation - Range of motion is  $0^{\circ}$ - $90^{\circ}$ . The major acting muscles are Infraspinatus and Teres Major. The minor acting muscle includes Posterior Deltoid.
- Internal rotation - Range of motion is  $0^{\circ}$ - $90^{\circ}$ . The major acting muscles are Subscapularis, Pectoralis Major, Latissimus Dorsi and Teres Major. The minor acting muscle includes Anterior Deltoid.

### **Elbow joint**

The elbow joint has a single DOF because of the joint type except for forearm supination and pronation [78]. The possible movements occurring at the elbow joint with acting muscles are as follows [79]:

- Flexion - Range of motion is  $0^{\circ}$ - $150^{\circ}$ . The major acting muscles are Biceps Brachii, Brachialis and Brachioradialis. The minor acting muscles include Pronator Teres, Extensor Carpi Radialis Longus, Flexor Carpi Radialis and Flexor Carpi Ulnaris.
- Extension - Range of motion is  $150^{\circ}$ - $0^{\circ}$ . The major acting muscle is Triceps Brachii. The minor acting muscle includes Anconeus.
- Forearm supination - Range of motion is  $0^{\circ}$ - $80^{\circ}$ . The major acting muscles are Supinator and Biceps Brachii.
- Forearm pronation - Range of motion is  $0^{\circ}$ - $80^{\circ}$ . The major acting muscles are Pronator Teres and Pronator Quadratus. The minor acting muscle includes Flexor Carpi Radialis.

## Wrist joint

The wrist joint comprises of three joints altogether, namely the radiocarpal joint, the ulnocarpal joint and the distal radioulnar joint. It has eight small bones called carpal bones. The acting muscles of this joint are as follows [79]:

- Flexion - Range of motion is  $0^{\circ}$ - $80^{\circ}$ . The major acting muscles are Flexor Carpi Radialis and Flexor Carpi Ulnaris. The minor acting muscles include Palmaris Longus, Flexor Digitorum Superficialis, Flexor Digitorum Profundus, Abductor Pollicis Longus and Flexor Pollicis Longus.
- Extension - Range of motion is  $0^{\circ}$ - $70^{\circ}$ . The major acting muscle is Extensor Carpi Radialis Longus, Extensor Carpi Radialis Brevis and Extensor Carpi Ulnaris. The minor acting muscles include Extensor Digitorum, Extensor Digiti Minimi and Extensor Indicis.

### 2.2.2 Degrees of freedom (DOFs) considered for the prototype

ForceArm is a four-DOF assistive suit enforced with PGMs. Fig. 2.1 shows the DOFs that can be assisted by the current design of the ForceArm suit. The ForceHand glove [1], which is the first version of ForceArm, was designed to support two DOFs of the wrist and forearm namely, flexion-extension and pronation-supination. Additional DOFs were introduced in ForceArm, namely elbow and shoulder flexion, as shown in Fig. 2.1. Shoulder and elbow extension of the human body is significantly supported by gravity in most real-life scenarios. Therefore, the current design is restricted to elbow and shoulder flexion and not extension. Wrist abduction-adduction motions were also not included in this version of the prototype because of the limited ROM involved in this DOF.

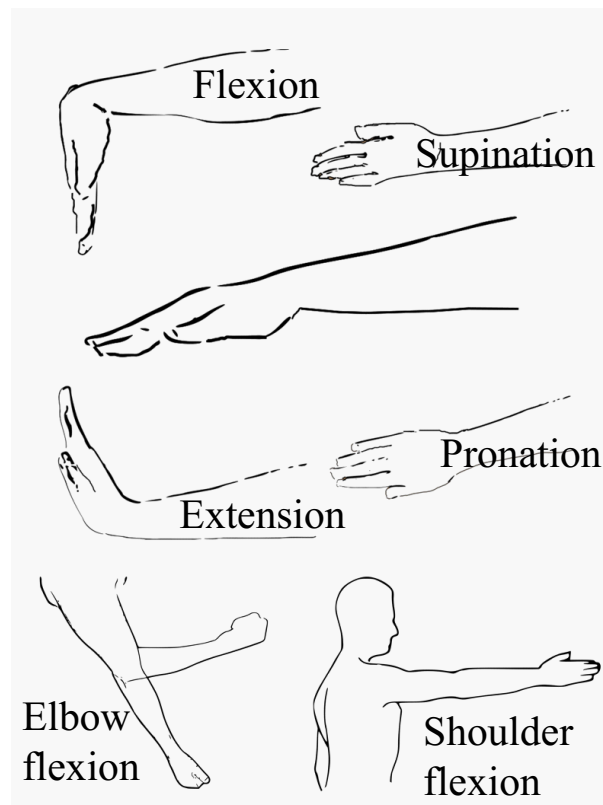


Figure 2.1 The degrees of freedom (DOFs) associated with the ForceArm prototype.

## 2.3 ForceArm prototype evolution

This section describes the two versions of the prototype that were developed by considering user feedback and various other technical and physical constraints and requirements.

### 2.3.1 Version 1: ForceHand

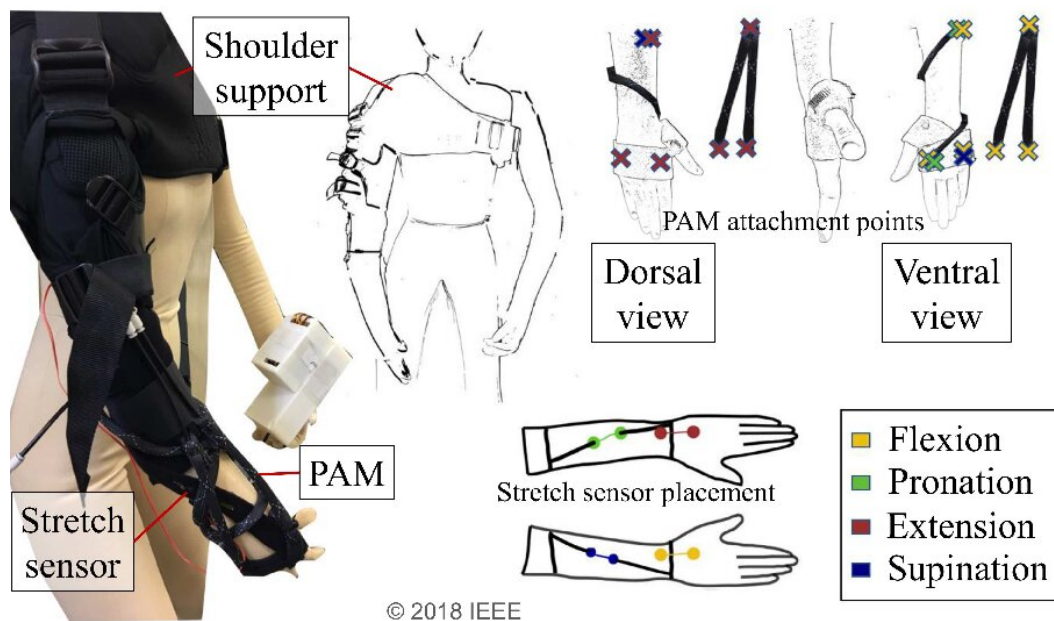


Figure 2.2 Placement positions of pneumatic artificial muscles (PAMs) and stretch sensors for each motion [1].

ForceHand was the first version of the prototype that was designed to support the wrist joint only. It was completely built with commercially available components. The base was a thin glove extending from the hand towards the elbow. This glove was used to attach the stretch sensors (YAMAHA) to sense the flexion and extension motions at the wrist joint. There were two more stretch sensors for sensing pronation and supination motions of the forearm. These sensors were however fixed to two separate elastic bands that were in turn attached on the base sleeve through hook and loop fasteners as shown in Fig. 2.2. Additionally, there was a shoulder attachment with an

elongated sleeve towards the elbow joint. Another clothing component was a thin wrap around glove for the hand that was used to attach the PGMs and pronation-supination stretch sensors through hook and loop fasteners. All components are illustrated in Fig. 2.2 from both dorsal and ventral viewpoints.

The total weight of the prototype was 395g. However, for this version of the prototype, we used a heavyweight grounded compressor (Meiji) due to which the prototype cannot be called entirely portable. Compared to the prototype before ForceHand that was reported in [75], ForceHand could realize better overall performance with improved wearability and user satisfaction. The ForceHand glove could support two wrist motions, namely flexion and extension and the forearm motions of pronation and supination. This support was implemented through the actuation of soft actuators called PAMs. PAMs are the earlier version of PGMs with similar composition. Unlike PGMs, the PAMs that we used for this prototype were not made of the customized inner tube. Therefore, these artificial muscles were not operable at air pressure as low as 0.1MPa. However, the functionality of the PAMs is same as PGMs that is they can contract or extend based on the compressed air fed to one of the ends [75]. Since this prototype used stretch sensors for detection of human intentions, whenever any of the sensors detected motion, the corresponding set of actuators were programmed to get actuated so that the user feels assisted while completing the motion and muscle fatigue is ultimately reduced.

### 2.3.2 Version 2: ForceArm

ForceArm prototype is the improvised and neater version of ForceHand glove [1] with two added DOFs. The complete prototype is illustrated in Fig. 2.3. Besides, we removed the stretch sensors because they did not meet the requirements of the prototype in terms of time delay. The prototype is built from commercially available materials. Table 2.1 shows the list of components used to build the ForceArm prototype in the same order as described in this section. The shoulder brace is extended towards

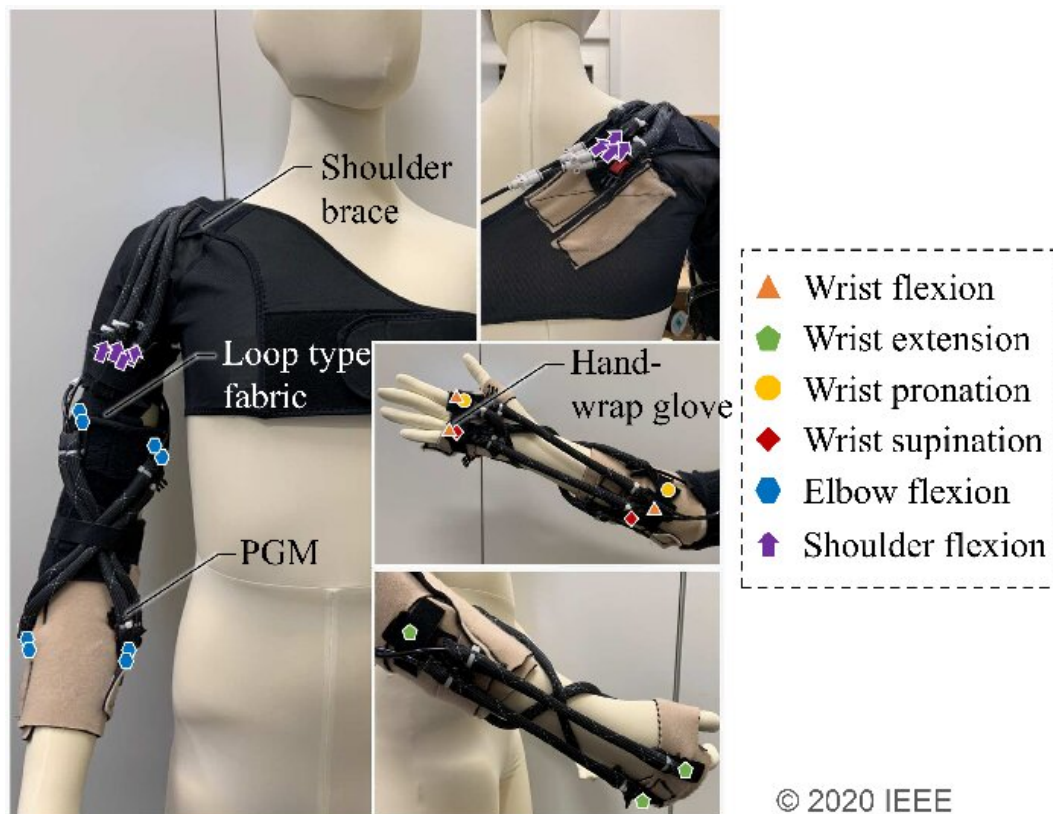


Figure 2.3 Positions of pneumatic gel muscles (PGMs) in the ForceArm prototype associated with each supported motion [2].

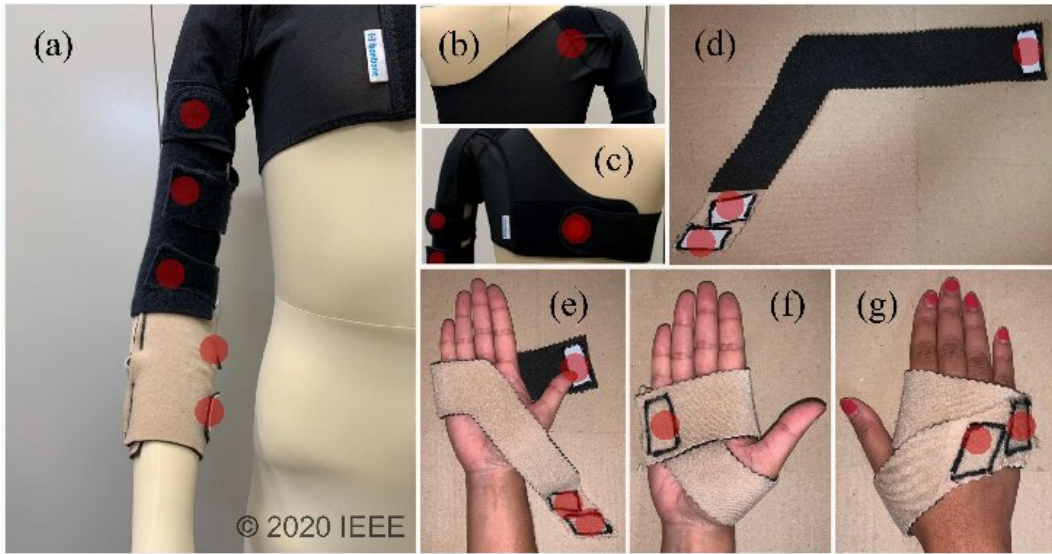


Figure 2.4 (a) Extended shoulder brace (b) back view of the shoulder brace (c) front view of the shoulder brace (d) hand-wrap glove (e) attaching the hand-wrap glove in (f) ventral side and (g) dorsal side perspectives; the red circle marks show the points where hook type fabric is attached for facilitating pneumatic gel muscle (PGM) attachment [2].

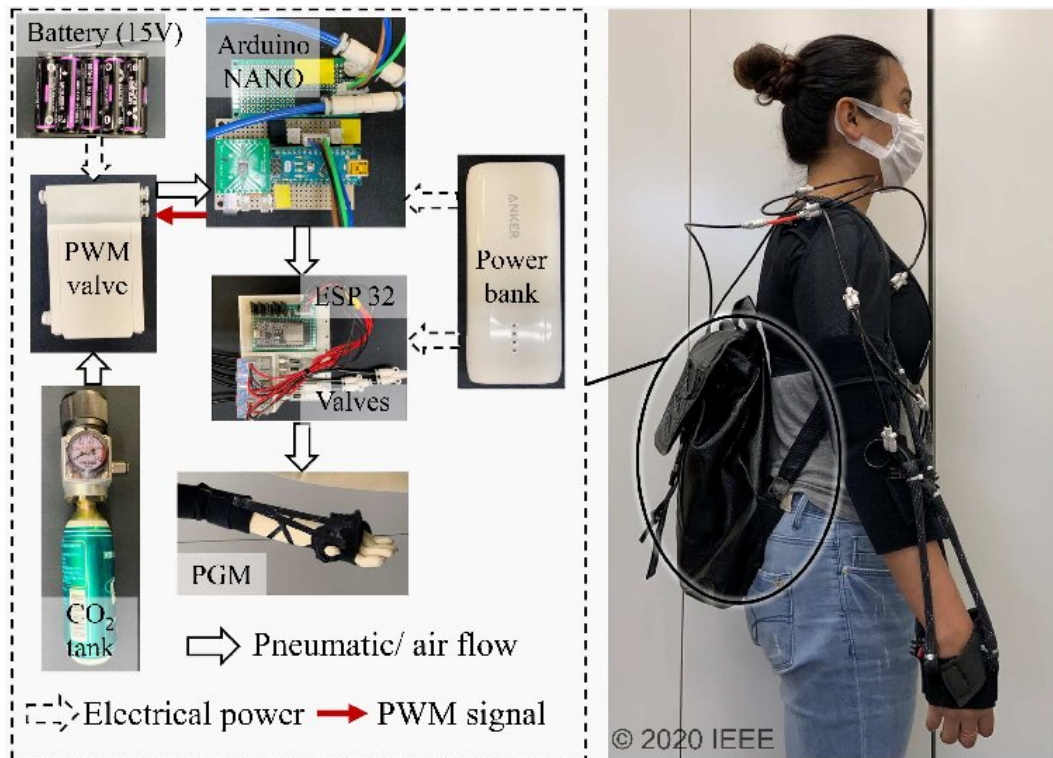


Figure 2.5 Components used in the ForceArm prototype [2].

the forearm crossing the elbow joint of the arm using loop type fabric. This fabric enables the attachment of PGMs to the fabric with hook type fabric fasteners. An additional wrap type glove is worn on the hand which will be called as the hand-wrap glove. Fig. 2.4 illustrates the shoulder brace and the hand-wrap glove. 14 PGMs are used in total for the whole prototype. A compressed air source is required for the actuation of PGMs. Therefore, a portable canister from Nippon Tansan Gas Co.Ltd. (NTG) CO<sub>2</sub> is used for this purpose. The operating time of these canisters changes according to the length of PGMs and the frequency of actuation. Upon observation, one canister could actuate a 30cm and a 20cm PGM for 1280 and 2240 times, respectively. During the elderly gaming application scenario, uninterrupted operating time-period of about 15 minutes was observed using one canister. The canister was used with an attached regulator for coarse air pressure control. For a precisely tuned supply of air pressure, we built a static control system using Arduino Nano microprocessor and an SMC ITV series PWM valve (SMC Corporation manufactures pneumatic control valves). A digital to analogue converter (DAC) attached to the microprocessor is required to provide analogue signals to the PWM valve. This valve also needs a 15V DC power supply which was provided by an external battery. We used a pressure sensor read by the Arduino microprocessor for sensing the air pressure to provide feedback to the control loop. Six solenoid valves (binary control for each motion) were used to control the PGMs at the end of the control system. These SMC SYJ series pneumatic valves were controlled through an ESP32 microprocessor board wirelessly through an embedded Bluetooth module. Therefore, the final binary control signals were sent from the main computer (which is not a part of the wearable system) to the ESP32 through Bluetooth. The wireless reception enabled the wearable system to be operated as a standalone unit. A power bank was used to power the Arduino Nano and ESP32 boards. All electronic components were enclosed in a leather backpack so that the user can carry them around during usage. Fig. 2.5 illustrates the components used to design the complete prototype.



Table 2.1 List of components used in the ForceArm prototype with their respective weights [2]. © 2020 IEEE

<b>Component name</b>	<b>Specification</b>	<b>Weight (grams)</b>
Shoulder brace	Fabric	140
Hand-wrap glove	Fabric	14
PGM	Multiple length	60
NTG CO <sub>2</sub> tank	74g capacity	300
Pressure regulator	0-0.5 MPa	340
PWM controller	Arduino NANO and a DAC	79
PWM valve	SMC ITV0031-2L	168
Battery	DC15V	220
Pressure sensor	ADP5160-Panasonic	2
Switching controller	Six SMC SYJ312M valves with ESP32	337
Power bank	5200mAh	120
Backpack	leather	320
Net weight	Wearable part: 214g	2100

## 2.4 Pneumatic gel muscle (PGM)

A select type of artificial muscle is used to build the ForceArm prototype that requires low air pressure for actuation. This behaviour of the artificial muscles enables users to use the prototype for longer hours with portable canisters.

### 2.4.1 Overview

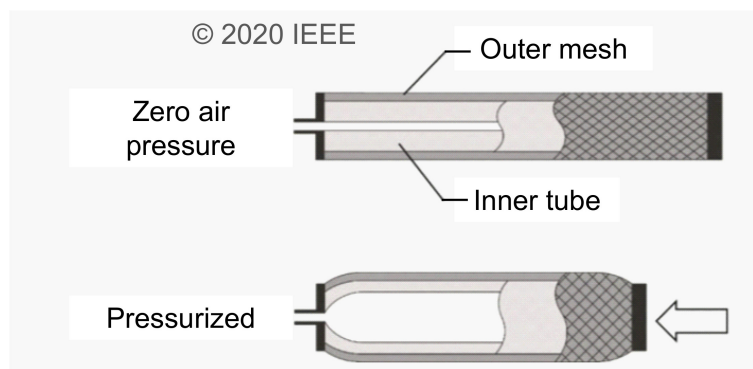


Figure 2.6 Working principle involved in the actuation of the pneumatic gel muscle (PGM) [2].

The ForceArm glove was comprised of low air pressure type actuators called PGMs. PGMs, being the main component of the prototype, could provide assistive force when attached to different parts of the arm. The DAIYA industry, Japan develop these actuators. When compared to commercially available soft actuators, PGMs can produce more significant force at comparable air pressure values. This quality is due to the presence of a customized styrene-based thermoplastic elastomer as the inner tube of the actuator. The composition of PGMs is comparable to conventional McKibben actuators. A braided mesh conceals the inner tube on the outside. Fig. 2.6 shows the layers of the PGM along with its functioning. When compressed air is inserted to the inner tube through the external pneumatic tubing, the inner tube inflates like a balloon. However, this inflation is limited by the outer mesh, which in turn reduces the length of the PGM itself. The presence of the braided mesh results in a linear contraction of

Table 2.2 Comparison of the contraction and elongation ratios of pneumatic gel muscle (PGM) and its commercially available soft actuator equivalent PM-RF10 at a fixed air pressure input of 0.2MPa.

Attached load (N)	Contraction ratio (%)		Elongation ratio (%)	
	PM-RF10	PGM	PM-RF10	PGM
0	32	36	–	–
10	14	29	29	11
20	3	23	41	20

the PGM. PGMs can generate forces of up to 40N at an input air pressure of as low as 0.1MPa [76]. This force depends on the length of the PGM and the input air pressure.

Previous literature [76] proves that PGM can generate more force as compared to a commercially available soft artificial muscle counterpart called PM-RF10. PGMs have the benefit of longer operating hours while using portable CO<sub>2</sub> canisters as a source of compressed air. Table. 2.2 shows the comparison of contraction and elongation ratios of PGM and PM-10RF at an input air pressure of 0.2MPa. We can observe that both contraction and elongation ratios are better for PGM even at an attached load condition of 20N.

### 2.4.2 Attachment points of pneumatic gel muscles (PGMs)

ForceArm uses a total of 14 PGMs. Four PGMs each are used in association with elbow and shoulder flexion, two PGMs each for wrist flexion and extension and one PGM each supports forearm pronation and supination motions. Two different lengths of PGMs are used. There are eight 20cm and six 30cm PGMs. The 30cm PGMs support forearm pronation and supination and shoulder flexion. The 20cm PGMs support the remaining DOFs. Fig. 2.3 shows the attachment points of all PGMs used in ForceArm. The PGMs associated with wrist flexion are placed on the ventral side of the forearm. One end of each of those two actuators attaches to the palm, just below the little finger and the index finger, respectively. The other ends are attached to a common

point near the elbow joint towards the ulnar side. The PGMs associated with wrist extension are placed on the dorsal side of the forearm. One end of those two PGMs related to wrist extension motion is attached to the hand, just below the endpoints of the knuckle, that is, near the index finger and the little finger. The remaining ends of the PGMs are attached to the radial side of the forearm near the elbow joint. The PGM that supports pronation runs spirally from the point on the palm just below the index finger to the elbow joint. Similarly, the PGM that supports supination motion runs spirally from the palm, just below the little finger to the elbow joint, spiralled in a direction opposite to the pronation associated PGM. The PGMs that support elbow flexion are attached on the ventral side of the arm, making a cross pattern such that the point of intersection is just above the ventral side of the elbow joint. The PGMs supporting shoulder flexion are attached parallelly, from the back to the biceps of the arm. Fig. 2.3 illustrates the attachment points and orientation of all PGMs associated to each DOF. All attachment points of the ForceArm suit are enabled with loop type fabric as a part of the shoulder brace and the hand-wrap glove.

## 2.5 Control system

This section describes the evolution of the control system from ForceHand prototype to ForceArm with changed components and overall control flow.

### 2.5.1 Stretch sensor-based control

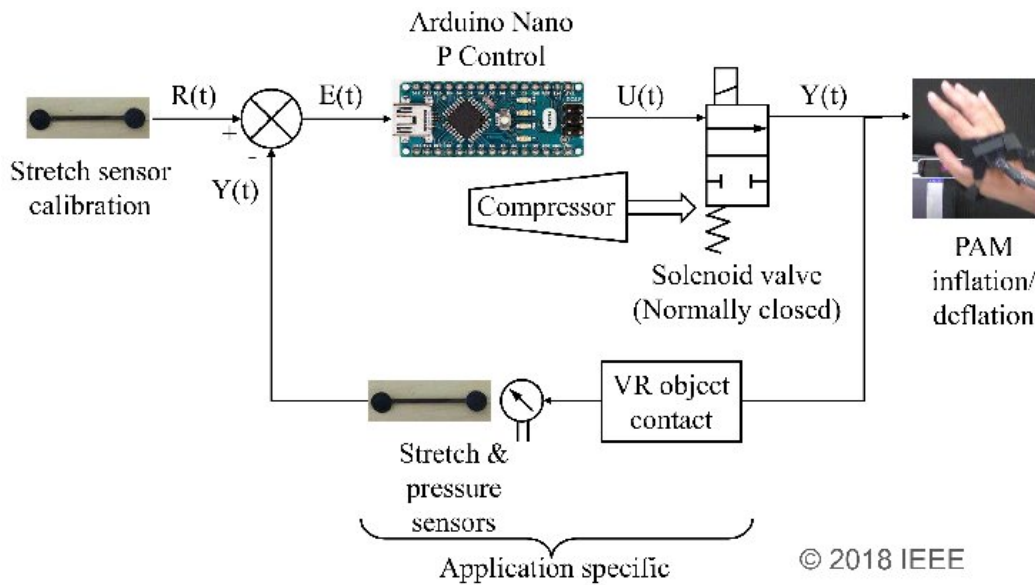


Figure 2.7 Control flow of the stretch sensor-based automated pneumatic artificial muscle (PAM) actuation method [1].

The control flow of the FH glove's stretch sensor-based sensing mechanism is illustrated in Fig. 2.7. The continuous process of P control is realized by the Arduino Nano board that monitors the data from the stretch sensor associated with each motion. The first step of the control flow is the identification of the reference value or the set-point from the stretch sensor data. The reference value identification is followed by calibration where the Arduino Nano board reads the stretch sensor output. Based on this output, the corresponding PAM group is either actuated or deflated through the designated solenoid valve (KOGANEI G010E1). These valves operate in a normally closed configuration. The pressure sensing is done by ADP5160-Panasonic sensor to

monitor the input pressure supplied by the compressor at the same time. The following equations represent the control loop:

$$E = R - Y \quad (2.1)$$

$$U = k_p E \quad (2.2)$$

where  $E$  denotes the error signal,  $R$  is the calibrated reference value and  $Y$  represents the analog value of stretch sensor,  $U$  is the input to the solenoid valve and  $k_p$  is the P-gain, respectively.

### 2.5.2 Static wireless control system

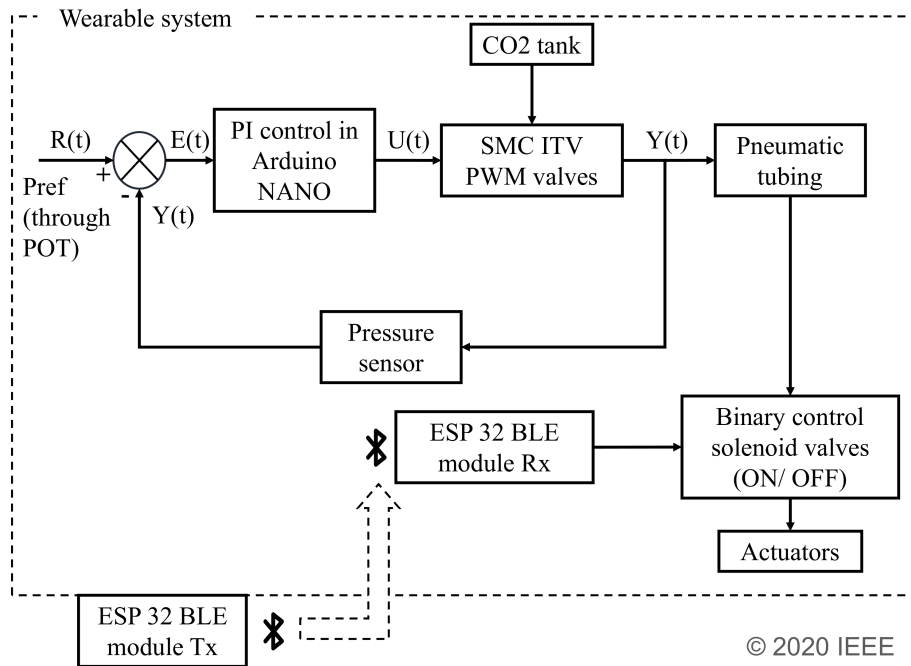


Figure 2.8 Flow diagram of the closed loop PI control system used to maintain stable input air pressure fed to the pneumatic gel muscles (PGMs). Here, POT refers to potentiometer [2].

A static control system regulates the compressed air supply. Fig. 2.8 illustrates the control system in detail. The CO<sub>2</sub> canister continuously supplies compressed air.

A PI control loop is used to monitor and regulate the input air pressure fed to the pneumatic actuators. The presence of a control loop ensures the safety and controlled supply of air pressure to the PGMs.

At first, a potentiometer is used to set the reference value or the set-point,  $R(t)$ . The set-point of the system is then mapped to the target air pressure. When the pressure sensor reads the out pressure,  $Y(t)$ , this value is then compared to the target air pressure. If the values are different, the ITV PWM valve is manipulated to match the target air pressure value. The proportional and integral gains were set to  $k_p = 5$  and  $k_i = 5$ , respectively, after careful consideration and adjustment. We ensured zero overshoot and minimum possible rise time. The variables  $R(t)$  and  $Y(t)$ , are analogue values read by the Arduino pins and these values were always mapped to a range of 0-255 to provide commands to the PWM valve.

After obtaining a regulated input air pressure from the PI loop, a binary switching system was used. The binary switching for each PGM was done by using SMC SYJ series valves. During the sEMG measurement task, the binary switching was implemented by push-button switches given to the users in their non-assisted hand. On the other hand, for the gaming task, as described later, the actuation of the desired PGMs was implemented by sending out a signal whenever the LeapMotion sensor detected the user's hands. In other words, user support was turned on whenever the game detected a hand in front of the LeapMotion sensor.

## 2.6 Discussion

We built a stretch sensor-based actuation mechanism for the artificial muscles. However, due to limitations of the stretch sensors, it is not advisable to use this control method by users of special needs such as elderly and disabled. The limitations of the sensors include sensing delay, hysteresis and fragility. We are, therefore considering additional possibilities of deploying automatic actuation control by sensing the joint angle.

A static air pressure control system was built using commercially available materials. The current limitation of the control system is that it does not consider the real-time motions of the human arm that can be dynamic. To address such issues, we need real-time motion sensing of the complete upper-limb and design a dynamic control method to deploy higher levels of compliance.

## **2.7 Conclusion**

This section described the anatomy of the human upper limb, followed by the building components of the prototype. We used a customized, low air pressure PAM called PGM to enable the portability of the prototype by using small CO<sub>2</sub> canisters that can function for a considerable amount of time without replacement.



# Chapter 3

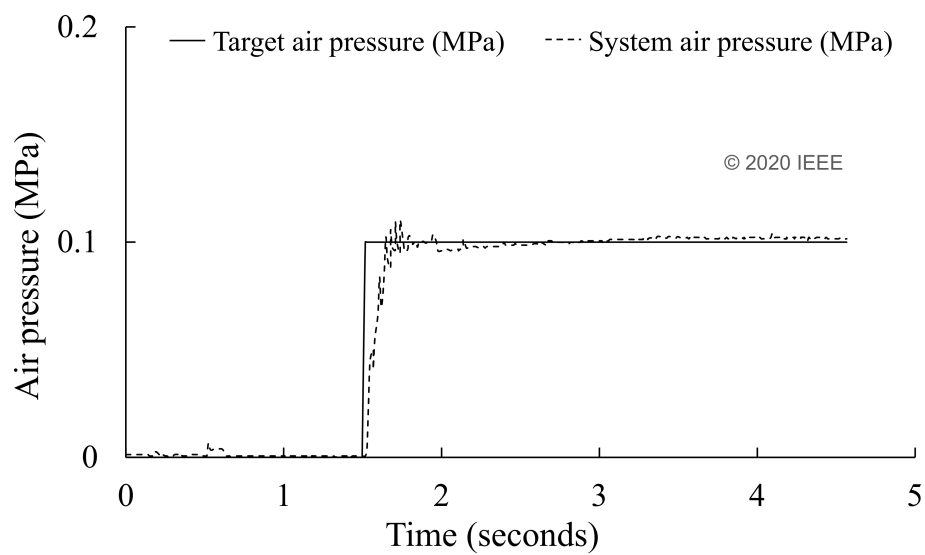
## System evaluation

### 3.1 Introduction

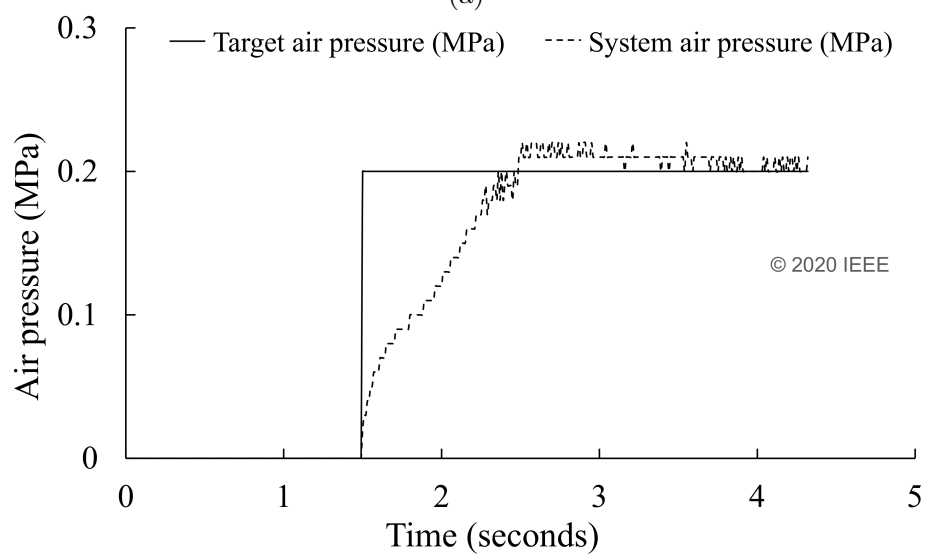
Technical evaluation of assistive or rehabilitation technologies is a vital step to approve of its use by any subject or user. We must be answerable to any information that may affect the performance of the prototype in both positive or negative ways. Therefore a systematic evaluation of the ForceArm prototype was done by measuring various delays involved in the control system and the force induced by the PGM actuation. Besides, we measured the muscle unloading effects in elderly and young users to verify the usability of the prototype as assistive support. This evaluation is detailed in this section.

### 3.2 Control system evaluation

In this section, we evaluate the static control system used to maintain stable air pressure at the output. Three significant aspects were evaluated, namely, the system's response to rising set-point, falling set-point, and PGM switching.



(a)



(b)

Figure 3.1 Rising behaviour of the control system with target set-points of (a) final air pressure = 0.1MPa (b) final air pressure = 0.2MPa [2].

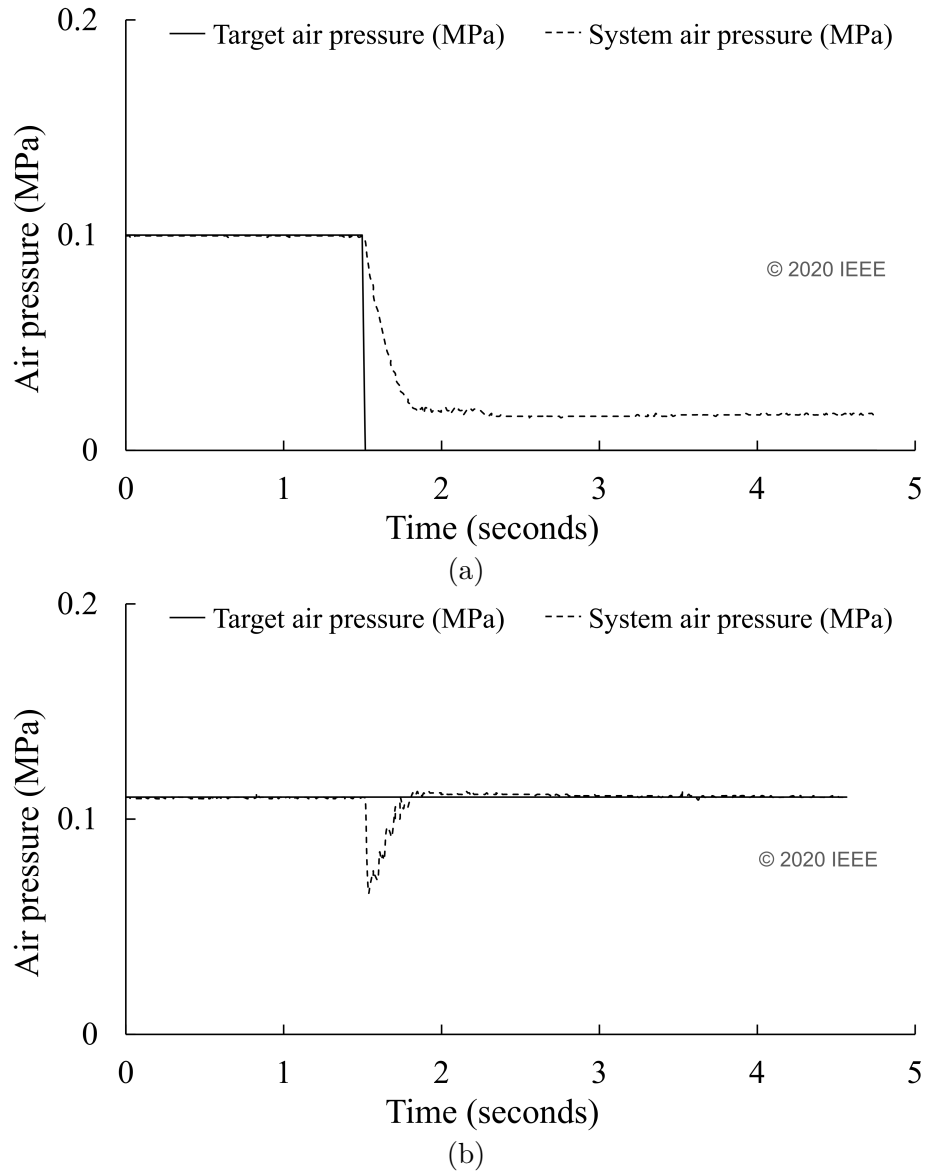


Figure 3.2 Control system responses to (a) fall in the set-point (b) switching on one of the pneumatic gel muscles (PGMs) receiving controlled air pressure [2].

### 3.2.1 Rising set-point

Fig. 3.1 illustrates the response curves of the control system to a rise in the set-point. In Fig. 3.1a, the target set-point or air pressure value is 0.1MPa. In this case, the system's settling time (time required to reach  $\pm 10\%$  of the final value) is around 700ms. In Fig. 3.1b, the final value of air pressure is 0.2MPa. The settling point, in this case, rises to around 900ms which is considerably high. However, no overshoot was observed in the rising behaviour for both air pressure values. PGMs provide an acceptable amount of assistive force at 0.1MPa and the highest air pressure for the safe operation of PGMs is 0.2MPa, which also induces the highest force. Therefore, the operating range of air pressure was set from 0.1MPa to 0.2MPa for various applications discussed in this work and the control system responses for these values are illustrated in Fig. 3.1.

### 3.2.2 Falling set-point

For the case of falling set-point (as shown in Fig. 3.2a with final air pressure = 0MPa), the settling time was observed as around 200ms. Some residual air pressure can be seen at 0MPa. This residual air pressure is due to the leftover air inside the PGM, which can be released entirely only by stretching the actuator further. However, when the PGM is at rest, this residual air pressure remains inside the actuator. Therefore, in a real usage scenario, the residual air pressure is a negligible issue.

### 3.2.3 Pneumatic gel muscle (PGM) switching

PGM switching is the condition where multiple PGMs use the regulated air pressure from the static control system, and one of those PGMs is either switched on or off. Fig. 3.2b illustrates the system's response to PGM switching. If an additional PGM receiving the controlled air pressure was turned on, this behaviour was observed. The settling time was around 200ms.

The control system showed significant delay ( $< 900\text{ms}$ ) for different changing conditions of the set-point. The delay in settling time for the PGM switching condition was around  $200\text{ms}$ . Since currently, constant air pressure was used as the final source; the delay in rising and falling set-point is of less importance. Moreover, in an actual scenario, when a potentiometer is used to make any changes in the set-point, gradual change in the resultant air pressure is acceptable. Therefore, the delay did not have any adverse effect on the system in the current applications.

### 3.3 Pneumatic gel muscle (PGM) force measurement

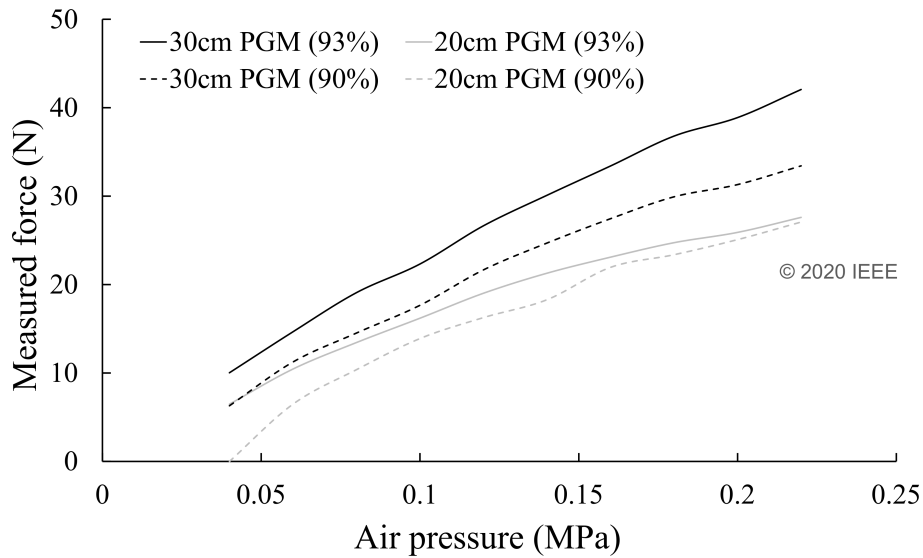


Figure 3.3 Force induced by pneumatic gel muscle (PGM) actuation for two PGM lengths and at two stretched conditions for each PGM [2].

Estimating the force acted by any assistive wear on the user is an important assessment. Therefore, we measured the resultant force from PGM actuation. The two types of PGMs used in ForceArm were of maximum stretchable lengths, 30cm and 20cm. PGMs show spring-like behaviour on applying zero pressure. Therefore, the actuator length can change with change in joint angles of the user. However, under

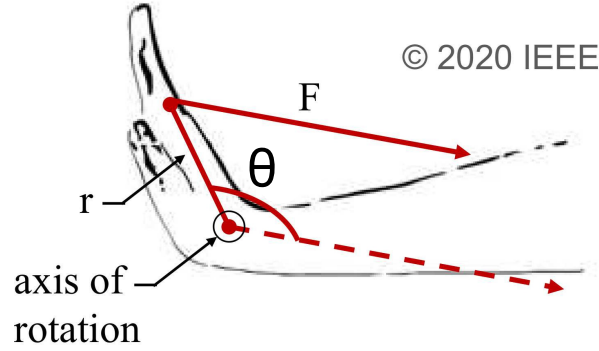


Figure 3.4 Calculation of torque from force induced by pneumatic gel muscle (PGM) actuation; an example of wrist extension where  $F$  is the linear force due to the PGM actuation,  $r$  is the distance from the axis of rotation to point of application of the force and  $\theta$  is the angle shown in the figure [2].

pressurized condition, PGMs cannot be stretched easily due to increased stiffness, which means, joint angles do not affect the length of the actuators as much. For ForceArm related experiments, PGMs were used at stretched lengths of 90% to 93% of their maximum lengths. Therefore, we measured the resultant force while actuating these PGMs for the stretched lengths of 90% to 93%. Fig. 3.3 illustrates the force measured by actuating the PGMs in a linear orientation. The input air pressure was varied from 0.04MPa to 0.22MPa to acquire this data. Our fixed operating range of air pressure was set from 0.1MPa to 0.2MPa. We used a calibrated force transducer (Leptrino FS080YA501U6) for the measurement of force due to PGM actuation. Torque was not measured for each use case. However, the resultant torque can be calculated by referring to the force information illustrated in Fig. 3.3. An example use-case is provided in Fig. 3.4 where the torque can be derived from the linear force as:

$$\tau = rF\sin\theta \quad (3.1)$$

## 3.4 User study for surface electromyography (sEMG)-based evaluation

An sEMG-based user study was conducted to evaluate the effectiveness of the ForceArm prototype as assistive wear. An ethics committee approved the study. This section describes the methodology followed during the study.

### 3.4.1 Methodology

We had initially evaluated the two-DOF muscle unloading effects of ForceArm on the forearms of young subjects [1]. However, for real validation, it was vital to evaluate the prototype for physically challenged individuals. The additional DOFs, elbow and shoulder flexion also needed to be evaluated. Therefore, muscle unloading effects in the forearm were first evaluated through sEMG measurement in elderly subjects. Since consent was not received to measure sEMG on the back and upper thorax portions in elderly participants, we conducted the sEMG evaluation experiment for elbow and shoulder flexion on young individuals. This section briefly describes the methods and results of the two sEMG experiments.

Six young (all males) and six elderly (one female and five males) participants consented to participate in the sEMG experiment. The average age of the elderly participants was  $84.5 \pm 6.5$  years old with typical characteristics of weakness due to ageing factors and occasional pain in their muscles and joints. The Japanese elderly care insurance identifies each elderly patient with a rating on a scale from 1 to 5 (5 defines the highest care requirement) [80]. The average care requirement level of our participants was 1.5. The average age of the young subjects was  $23.8 \pm 1.2$  years old who were all physically active and never used PGMs for elbow and shoulder motion assistance before this user study. The experimental protocol was identical for both experiments. A push-button switch panel was held by the non-assisted hand of the users which was used by the participants themselves to actuate the PGMs. The switches in

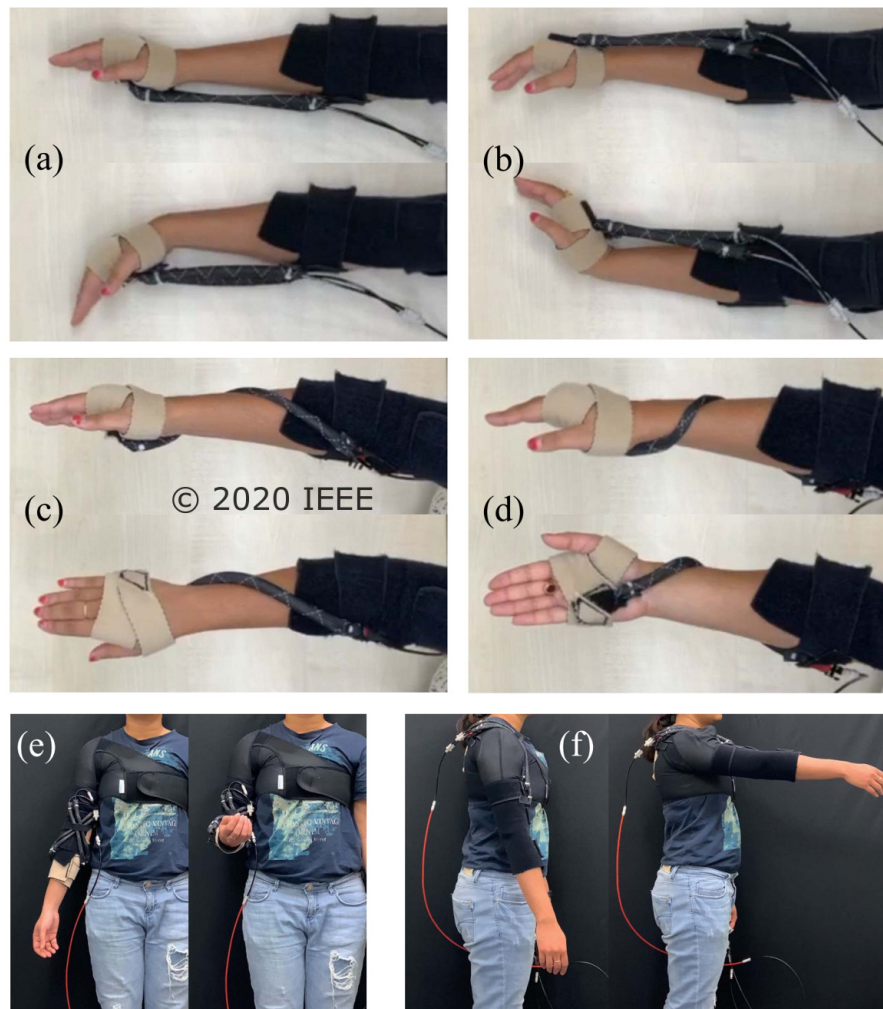


Figure 3.5 Illustration of various motions associated with pneumatic gel muscle (PGM) actuation. (a) and (b) represent the forearm orientation used for surface electromyographical (sEMG) measurement in wrist flexion-extension (c) and (d) represent the forearm orientation used for surface electromyographical (sEMG) measurement in forearm pronation-supination (e) and (f) show the resultant movement in the arm due to pneumatic gel muscle (PGM) actuation during flexion assistance of the elbow and shoulder joints, respectively. For all measurements, the arm is held against gravity [2].



the panel were directly connected to the pneumatic valve actuation circuit which could control the binary actuation. The latency in this actuation was measured as 50ms. We used Oisaka P-EMG Plus measurement system for sEMG recording. The guidelines provided by the surface electromyography for the non-invasive assessment of muscles (SENIAM) project [81] were sincerely followed to maintain the standards of sEMG data recording during both experiments. The participants' skin was carefully cleaned using alcohol tissues and shaved as well, if necessary, before attaching the self-adhesive electrodes. The forearm muscles chosen in elderly participants were Flexor Carpi Ulnaris (FCU), Extensor Carpi Radialis (ECR), Pronator Teres (PT), and Supinator Longus (SL). For elbow flexion, we measured sEMG in Brachioradialis (BRD), Biceps Brachii (BB), and Brachialis (BRC) muscles in the younger participants. Muscles recorded for shoulder flexion were Anterior Deltoid (AD), BB, and Upper Pectoralis Major (PM).

First, the maximal voluntary contractions (MVCs) were recorded by asking the participants to perform motions concerned with each muscle, while an experimenter resisted those motions. This data was used for normalizing the remaining data in order to account for various EMG interferences. The subjects were then instructed to wear the shoulder brace and the hand-wrap glove.

Since PGMs show a spring-like behaviour during the non-pressurized condition, they can be expanded while attaching to the forearm. However, if the actuator is overextended, then the user may feel restricted while performing natural motions and may also receive too high forces on actuation. For this reason, the ROM of each elderly subject was determined at first. The tension in each PGM was adjusted while attaching them on the user's arm according to the determined ROM. This procedure was carefully done manually through trial and error in the current situation to avoid any injury. All participants (young and elderly) were given ample time to get habituated to the PGM actuation and thus adjust the air pressure by themselves through the potentiometer attached to the control system. Next, the subjects were instructed to perform the motions to cover their maximum ranges of motions with PGM actuation. Fig. 3.5

shows the orientation of the forearm, while all concerned motions were executed. Each motion was asked to perform for 5 seconds duration twice within a total of 25 seconds duration. The sEMG data were recorded at all times during all conditions over the 25 second periods. Each 25-second task was repeated three times in total for each motion. Two consecutive tasks were separated by a time gap of at least 20 minutes to nullify the effects of fatigue and learning. Also, the sequence of motions was randomized for all subjects. Finally, all wearable attachments were removed, and sEMG was recorded while the subjects performed the same task without any augmentation or assistance. Therefore, sEMG data for two conditions, assist and no-assist was obtained. Half of the subjects performed the no-assist task before the assist task. All motions were performed against gravity for both and young and elderly participants, as shown in Fig. 3.5.

### 3.4.2 Results

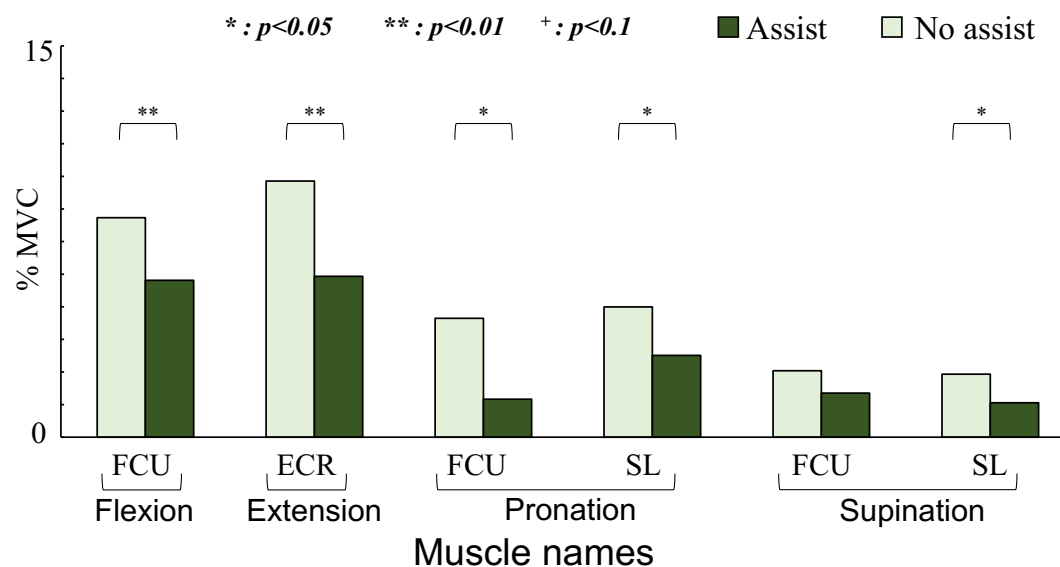


Figure 3.6 Illustration of the average % maximal voluntary contractions (MVCs) of young subjects for forearm motions with and without assist.

We smoothed the raw sEMG data by using a second-order low-pass filter with a cut-off frequency of about 4.8Hz by the P-EMG measurement system. Next, the

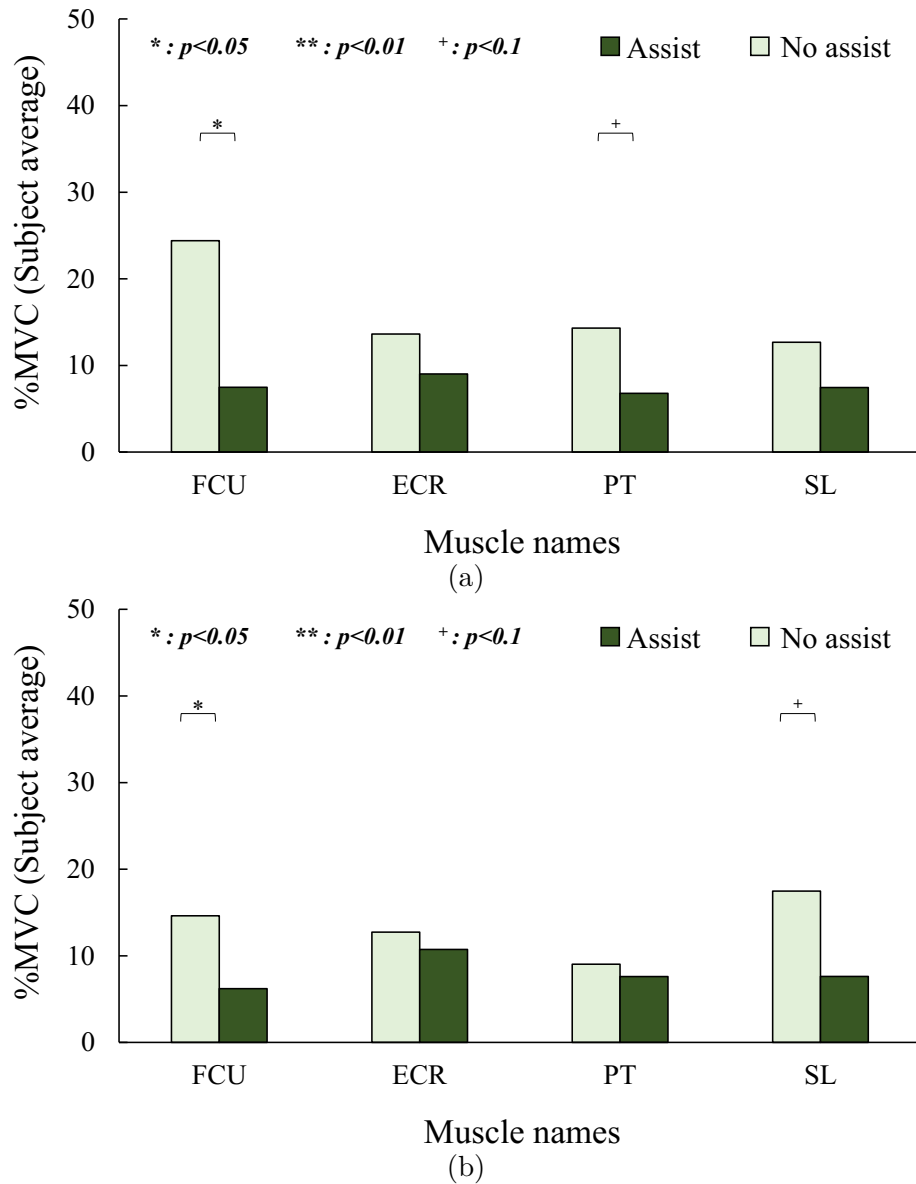


Figure 3.7 Average % maximal voluntary contractions (MVCs) of all subjects associated with wrist (a) flexion and (b) extension motions with and without assist.

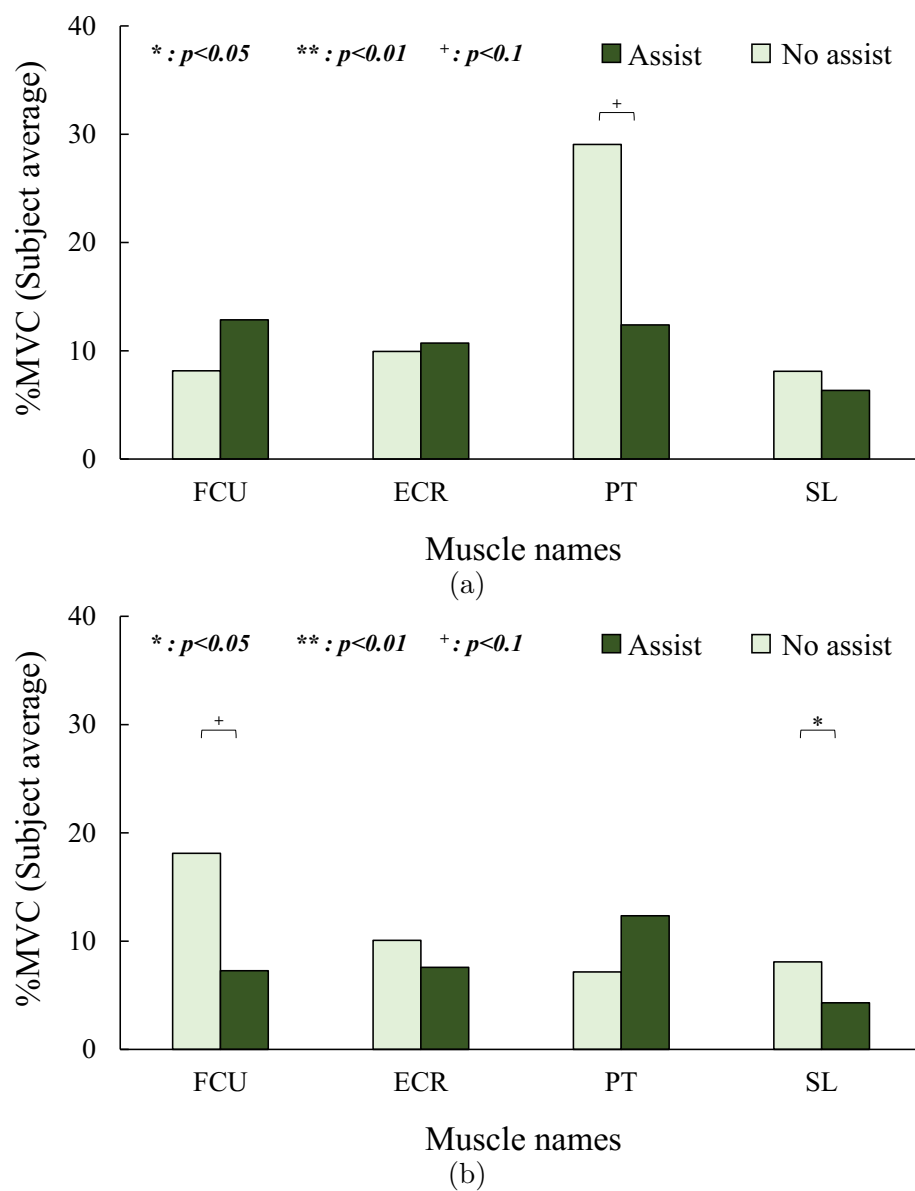


Figure 3.8 Average % maximal voluntary contractions (MVCs) of all subjects associated with forearm (a) pronation and (b) supination motions with and without assist.

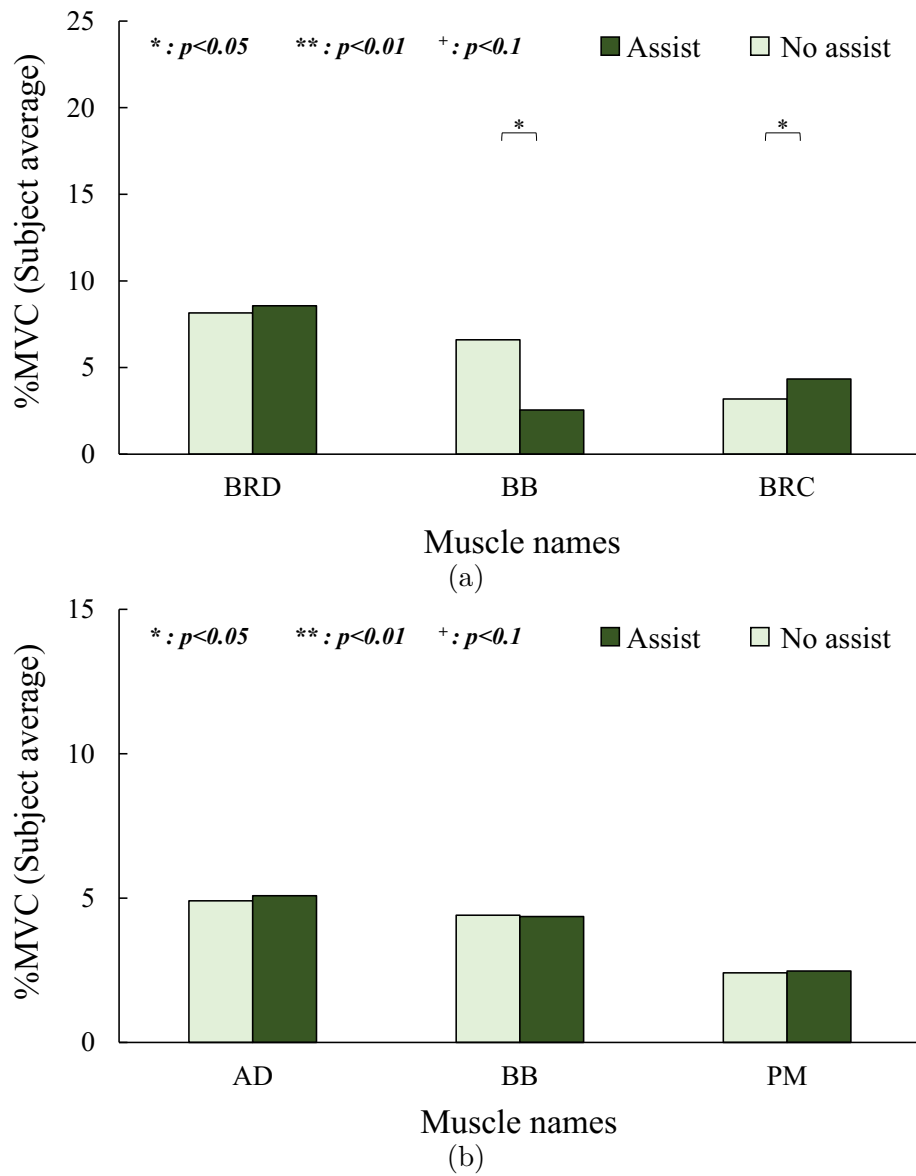


Figure 3.9 Average % maximal voluntary contractions (MVCs) of all subjects associated with (a) elbow flexion and (b) shoulder flexion motions with and without assist.

segmentation of the data was done. For each 5-second task data, we used 1-second sEMG data from the middle portion of the actuated duration (duration of motion). All segmented data were then normalized using the MVC values of the respective muscles of each subject. Normalization was done by calculating the sEMG as % of the MVC. A normality check was then performed using the Shapiro Wilk test before performing the significance tests. Conventionally, sEMG data is analyzed for significant differences using a paired t-test method. Therefore, a paired t-test was used to compare assist and no-assist conditions for individual subject data. If the subject data was not normally distributed, we applied logarithmic transformation for normalizing the data. The average of all subjects was also considered for the t-test. However, since, normality check was substantially negated in this case, a non-parametric test called Wilcoxon Signed Rank test was used to check the significance in differences. Previous work [1] proved the effectiveness of the forearm section of ForceArm on young subjects, as shown in Fig. 3.6. The average %MVC data for all motions measured are shown in Fig. 3.7, 3.8 and 3.9. These figures show the average subject data for all representative muscles.

### 3.5 Discussion

During wrist flexion, average subject data shows that FCU and PT are the two muscles with reduced muscle activity in assisted condition as compared to unassisted condition. For wrist extension, the average subject data show reduced %MVC in assisted condition for two muscles, FCU and SL. In the case of forearm pronation motion, average data implied reduced muscle activity for PT muscle only. For supination motion, reduced %MVC in two muscles FCU and SL for the assisted condition was observed. Therefore, it can be said that on average, ForceArm could result in muscle unloading for at least one associated muscle in all motions of the wrist and forearm in elderly subjects. This statement holds for all motions except wrist extension.

For elbow flexion, average data implied significant differences in muscle activity in BB and BRC muscles. BB shows reduced muscle activity in case of the assisted condition, but BRC shows the opposite result. Besides, we could not achieve muscle unloading in any average subject data for shoulder flexion. However, there were two individual subject cases of reduced muscle activity in AD for assisted shoulder flexion.

The ForceArm was developed and evaluated for elderly individuals. The first experiment using sEMG emphasizes the fact that the ForceArm can be helpful in muscle unloading for use on the human forearm, and this is also applicable to elderly individuals. Since we could not receive consent for recording the sEMG of muscles located on the back and upper thorax regions in elderly participants, we evaluated our prototype for elbow and shoulder flexion in young subjects. We achieved reduced muscle activity for elbow flexion in case of one muscle. However, the results of shoulder flexion were not as expected. In this experimental evaluation, we used fixed-length PGMs with fixed points of attachment for all subjects, and this may be a reason for failure in achieving muscle unloading effects in some subjects while they performed different motions with the assistance from ForceArm. Some subjects might need different length PGMs or different force values according to their arm specifications. Therefore, we plan to resolve this problem in the future by finding the optimum length and placement positions of PGMs for different motions in different users through simulation techniques. One of the observed limitations of the PGMs in the current configuration is the insufficient force for supporting shoulder flexion in young subjects. Therefore, we also plan to integrate multiple numbers of PGMs combined other wearable actuation techniques to realize higher forces in supporting shoulder flexion. Optimum alignment of the actuators also needs to be ensured for adequate shoulder support and avoid an increase in muscle activity in other associated muscles (which happened in the case of elbow flexion) due to the PGM actuation. Such solutions can be attempted through simulation techniques before measurement of sEMG on the subjects.

## 3.6 Conclusion

ForceArm prototype was tested for muscle unloading effects through sEMG measurement in both young and elderly subjects. The elderly subjects participated in this experiment only for the forearm part due to constraints related to ethics. As we could not receive consent for recording the sEMG of muscles located on the back and upper thorax regions in elderly participants, we evaluated our prototype for elbow and shoulder flexion in young subjects. Additional DOFs of shoulder and elbow flexion were evaluated through the participation of young subjects.



# Chapter 4

## Application scenarios and case studies of the ForceArm glove

### 4.1 Introduction

Wearable technology can be utilized in multiple scenarios for human ability enhancement. These scenarios can include both medical and entertainment fields. The ForceArm prototype was designed to support up to three degrees of freedom (DOFs) in the upper limb. According to these applicable DOFs, the prototype was tested in four different application scenarios. As explained in the previous chapter, it was proved that we could achieve muscle unloading in both younger healthy and elderly users with the ForceArm prototype. Therefore, we justified the use of the prototype in assisting users with weak or non-functioning arms. In this chapter, we describe the use of the prototype in four additional scenarios of application.

The first application is providing a necessary push to elderly participants in the form of force-feedback in a gaming scenario during a two-month study. The participants in this study were two elderly patients, and the goal was to perform rehabilitation exercises for the upper limb with motivation provided by the exergame. The second

application is using the prototype to induce motor learning. Motor learning is a complex process in the human body that involves the gradual acquisition of motor ability related to any dexterous tasks such as playing musical instruments, swimming, riding a bicycle and more. Human beings learn such tasks at an individual pace which may differ from person to person. However, if there are techniques that could accelerate this process of learning, it could be both motivational and augmenting in nature for that particular skill. Therefore, in this study, we verify if providing force-feedback through the ForceArm prototype could accelerate the process of learning two-handed drumming. The third application considered for study was using force-feedback acquired from the prototype to provide navigation assistance. The conventional methods of navigation assistance can often create confusion if the information channels are limited to visual and audio. Therefore, in this user study, we test force-feedback as a channel to provide navigation cues on the arm. Besides, we experiment to identify the ability to differentiate between two force-feedback intensities which can potentially be used to provide complex navigation cues. The fourth study is about using the ForceArm glove to provide force-feedback in virtual reality (VR). We compared two types of force-feedback for four different object types in VR.

## 4.2 CASE STUDY 1: Feasibility study through an elderly exergame

### 4.2.1 Development of a Unity-based exergame

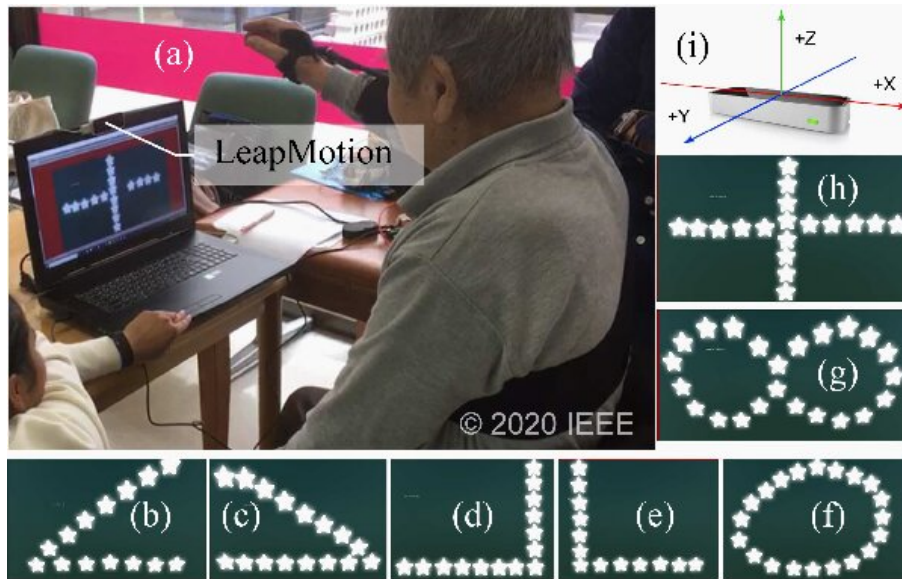


Figure 4.1 (a) Illustration of an elderly gaming session along with various patterns used during the session (b) 60deg (c) inverse 60deg (d) inverse L (e) L (f) O (g) 8 (h) + (i) coordinate reference for LeapMotion measurements [2].

We designed a gaming task to verify the effects of introducing soft actuator-based force-feedback on the upper limb, especially for older adults. In this task, a Unity environment was combined with LeapMotion sensor to create a gaming scenario. The task of the participants was to reach for various patterns shown on the computer screen through their virtual hand, which was detected through the LeapMotion sensor. All patterns consisted of a fixed number of stars. When the user would touch the stars with their virtual hand, they would disappear. We did not provide haptic feedback to the user when the touch or the collision of the virtual hand with the stars was detected. Fig. 4.1 illustrates the patterns used during the gaming task, along with a shot captured during one of the elderly sessions. The palm position and velocity of the user in X, Y, and Z axes were recorded for all sessions and later used for data analysis.

We ultimately compared the performance of the users who participated in this task. Our motive was to compare the change in performances over time and identify the improvement due to PGM-based enforcement.

### 4.2.2 2-month elderly user study

Fixed number of stars were used to form different patterns in the Unity environment. The subjects could virtually touch these stars. The final goal was to be able to touch all the stars to make all of them disappear by following the trace of the patterns. Seven patterns were designed for this task after referring to literature [82]. Fig. 4.1 illustrates the patterns and their given names which will be referred to later.

Two participants approved for this feasibility experiment. One participant performed all tasks without PGM while the other participant performed all tasks with PGM. The age of the participants were 87 and 79. Both participants were rated “1” according to the Japanese nursing care requirement. They performed the task thrice a week for two months. The sequence of the patterns was randomly chosen during each day’s session. Each pattern was ensured to be repeated three times each day. The normalized values of the palm position, velocity and timing data were recorded during each training session using the LeapMotion sensor positioned in front of the user. Since both participants had heart diseases in their medical records, they had weak arm movements. Physical therapists monitored the task during all sessions. During the entire duration of the session, the participants were not receiving any additional training or rehabilitation associated with their upper limb. For all sessions, the LeapMotion sensor was positioned on the top of the laptop screen, as illustrated in Fig. 4.1. The figure also shows the orientation of X, Y, and Z coordinates used to obtain the position and velocity data from the sensor. Before starting each session, a calibration procedure was performed to ensure that a fixed distance of the user’s hand from the leap motion was maintained along the Z-axis. We also ensured that the user could reach all corners of the virtual screen through the virtual hands while they were

seated on a chair. The PGM-based assistance provided to one participant included elbow and shoulder flexion and wrist extension DOFs. The actuation in PGMs was turned on whenever the LeapMotion sensor detected the virtual hand.

### 4.2.3 Parameters chosen for analysis

Different movements involved during this feasibility task execution along X and Y axes gave us information related to motor recovery. This data was converted to various parameters to study the learning or recovering curve in each participant. Four parameters were considered for evaluating the performance of the subjects in this feasibility assessment task, namely:

- Time score
- Deviation score
- Jerkiness score
- Hand-path ratio score

**Time score** The time score does not associate to the motor ability of the subject. This score was directly related to the performance, which means, a higher value of the parameter indicates good performance. The time score mainly considers the timing-based performance of the participant. It is calculated based on the number of stars hit by the participant, the time required to hit each star, and the total time consumed to perform the task. The following equation was used to calculate the score:

$$Time\ score = \frac{\frac{S_h}{S_t}}{T_{max} + T_{avg} + 0.2T} \quad (4.1)$$

Here,  $S_h$  represents the total number of stars hit,  $S_t$  is the total number of stars presented in the concerned pattern,  $T_{max}$  denotes the maximum hitting time for

touching a star in the concerned pattern, and  $T_{avg} = \frac{T}{S_h}$  denotes the average time required to hit each star, such that, T is the total time required to hit  $S_h$  stars. We selected coefficient 0.2 for the third term of the denominator to fix the range of the time score from 0 to 0.2. The time-related terms that have lower values for better performance were kept in the denominator so that the score is directly related to the performance.

**Deviation score** This score is inversely proportional to performance, which means, the higher this parameter is, the lower the performance. The deviation score is calculated by comparing the x-y trace of the subject with that of a healthy subject trace for the respective patterns. The healthy subject pattern was recorded by considering the following restriction criteria: a) all stars should be touched at a single attempt to trace the pattern b) time taken to complete the pattern should be less than 10 seconds c) calibration process followed for elderly subjects should also be followed for the healthy user before recording the trace data. The healthy subject trace helped us identify the best path to cover all stars nearest to the target path. A higher value of this parameter indicates more deviation from the ideal trace. The equations to calculate the deviation score for X and Y axis, respectively, are:

$$Deviation\ score_x = \sum_{i=1}^T \min|x_{ideal}(t_i) - x_{sub}(t_i)| \quad (4.2)$$

$$Deviation\ score_y = \sum_{i=1}^T \min|y_{ideal}(t_i) - y_{sub}(t_i)| \quad (4.3)$$

Here,  $x_{ideal}$  and  $y_{ideal}$  represent the position data measured from the trace of a healthy individual and  $x_{sub}$  and  $y_{sub}$  are the position data measured during sessions with elderly participants.

**Jerkiness score** This parameter is also inversely proportional to the performance. It indicates the gradual weakening or shaking in the arm movements. This measure was widely adopted by robotic rehabilitation literature and can be measured by different methods [83]. For this work, the jerkiness was calculated using the integral of the squared magnitude of jerk value in X and Y axes. In physics terms, jerk is the time-derivative of acceleration or the third derivative of position. Before taking the third derivative, the acceleration data were low-pass filtered for high-frequency noise reduction. The following equation represents the calculation of the jerkiness score for X and Y axes, respectively:

$$Jerkiness\ score_x = \sum_{i=1}^T \ddot{x}(t_i)^2 \quad (4.4)$$

$$Jerkiness\ score_y = \sum_{i=1}^T \ddot{y}(t_i)^2 \quad (4.5)$$

Here,  $\ddot{x}(t_i)$  and  $\ddot{y}(t_i)$  are the third derivatives of the position data in X and Y axes, respectively. A higher value of this score represents increased jerk and thus relating to bad performance.

**Hand-path ratio score** This score is directly related to the subject's performance, which means, the higher this parameter is, the better the performance. We first calculated the ratio of the shortest path to the hand path used by the subject and multiplied it by 100 (converted to a percentage score) to determine the final score value. Sometimes, there were short path data without hitting a sufficient number of stars to complete the entire task. So we adjusted the resultant term again with the number of stars hit by the subject during the specific trial. The equation, therefore, is given as:

$$Hand - path\ ratio\ score = \frac{Shortest\ path}{Hand\ path} \frac{(100S_h)}{S_t} \quad (4.6)$$

Here,  $S_h$  denotes the total number of stars hit, and  $S_t$  is the total number of stars in the concerning pattern.

#### 4.2.4 Results

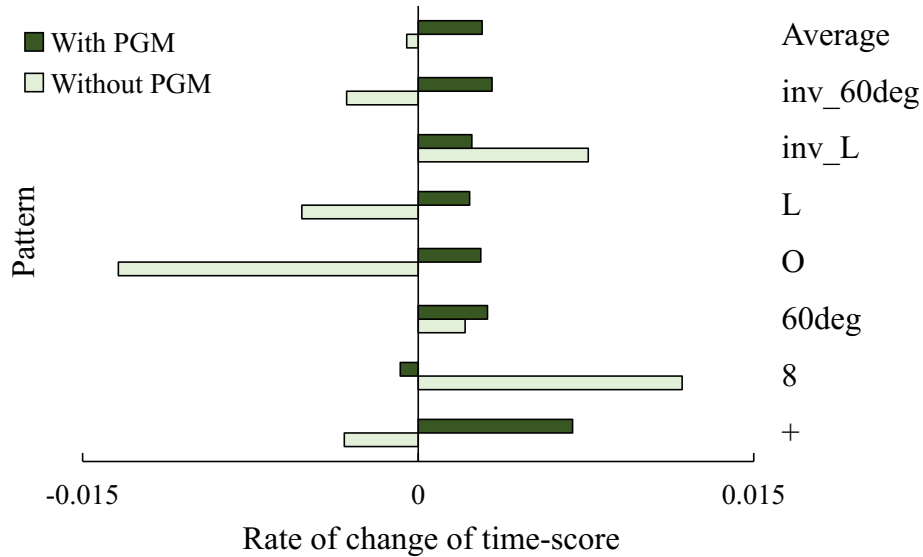
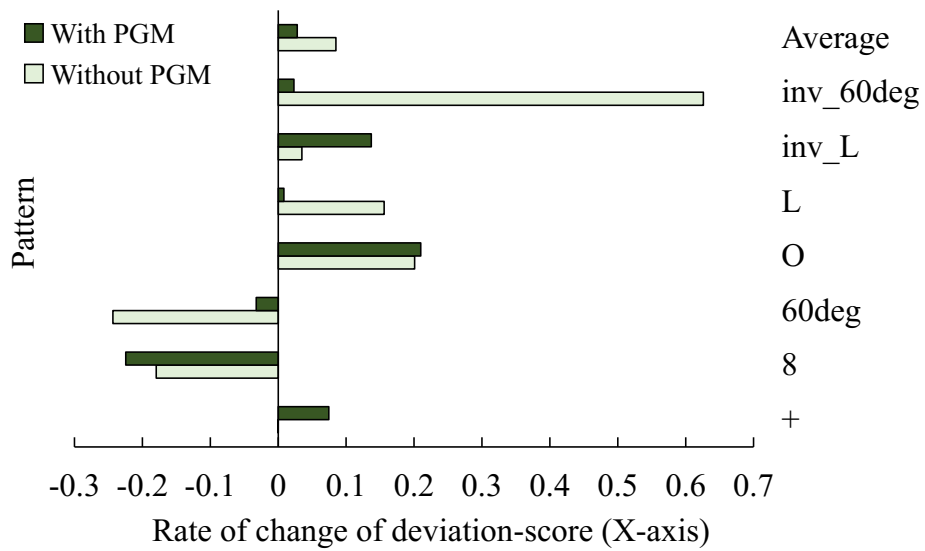


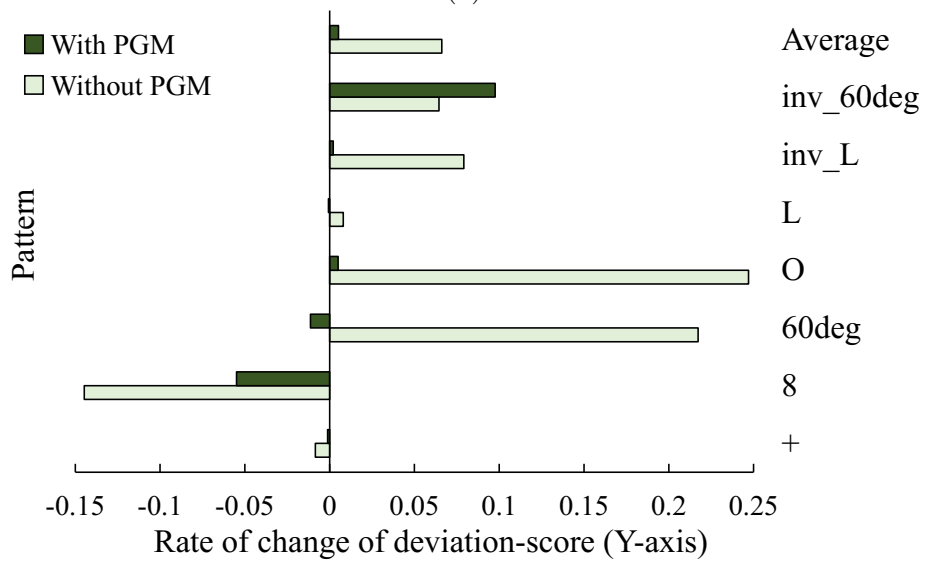
Figure 4.2 Comparing the rates of change of time score with and without suit for various patterns.

The four scores were each carefully calculated from the recorded data for each session. After getting the score values, we plotted them against the session progression. Those plots were then curve fitted using a linear trend-line. The slope values of each linear trend-line indicated the change in performance of the subjects over time. Therefore, those values were recorded. We calculated slope values in all patterns and parameters for the two participants. For all parameters, a negative slope value denotes that the score is reducing over time, whereas a positive value means the opposite. Fig. 4.2 illustrates the rates of change of time score over time for different patterns in case of both participants. Since time score is directly proportional to the performance, a positive value in the plot indicates better performance. Fig. 4.3 illustrates the rates of change of deviation score in X and Y axes over time. Fig. 4.4 represents the rates of change of jerkiness score in X and Y axes over time for different patterns. Since



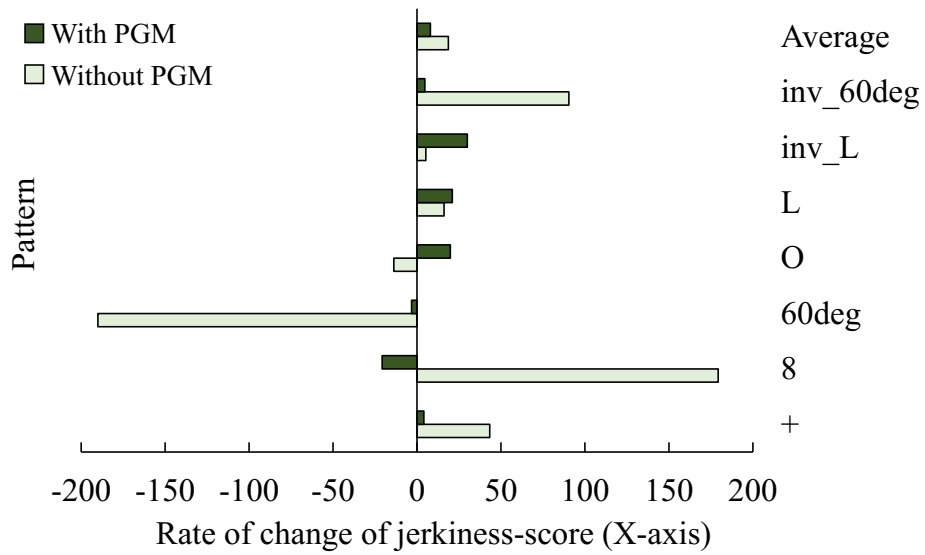


(a)

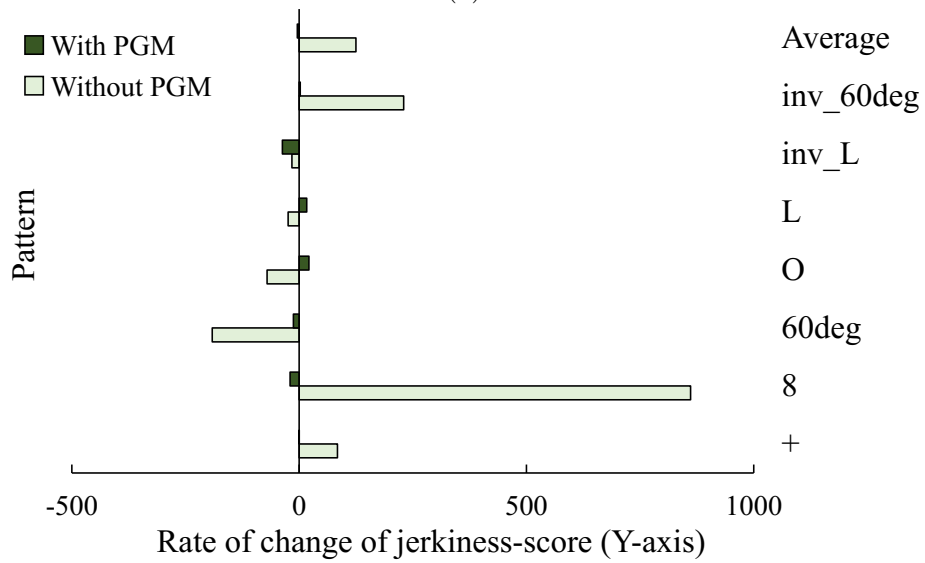


(b)

Figure 4.3 Comparing the rates of change of deviation score with and without suit for various patterns in (a) X-axis and (b) Y-axis.



(a)



(b)

Figure 4.4 Comparing the rates of change of jerkiness score with and without suit for various patterns in (a) X-axis and (b) Y-axis.

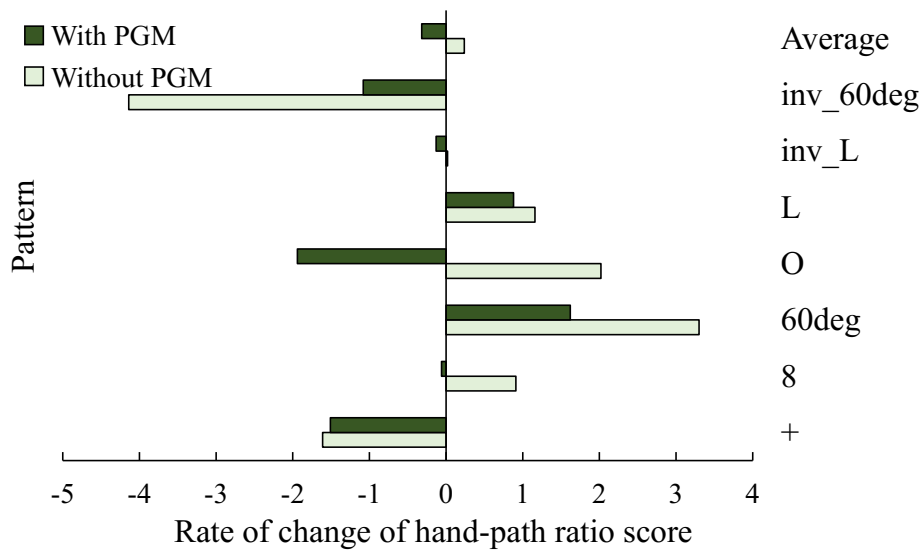


Figure 4.5 Comparing the rates of change of hand-path ratio score with and without suit for various patterns.

deviation and jerkiness scores are inversely proportional to the performance itself, a positive and a positive higher value in the plot indicates poor performance over time, whereas a negative or a lower value indicates the opposite. Fig. 4.5 illustrates the rate of change of hand-path ratio score over time. Since this score is directly proportional to performance like time score, a higher value indicates a better improvement in performance.

#### 4.2.5 Discussion

We developed a gaming task to identify the effects of ForceArm on motor recovery in elderly individuals. Four different parameters were selected and calculated from the task data collected over two months. It can be observed that the rate of change of time score for the subject who was supported by PGM remained positive in all patterns except the pattern “8”. On the other hand, the unsupported subject showed a negative change or decline in time score for four out of seven patterns. The deviation score for the X-axis was found to increase in both participants for five out of seven patterns. Looking at the average data, the rate of increase was lesser for the subject with PGM.

In the case of Y-axis, the subject who was assisted with PGM showed a negative rate of change of deviation score in four patterns. The subject without PGM showed patterns of increase at a significant rate for up to three patterns. In the case of the jerkiness score, similar to the deviation score, the value expected to fall with progressing sessions. For X-axis, both participants showed a minimal increase in the jerkiness score. However, the subject without PGM showed a sharp rise in case of pattern “8” for both X and Y axes. Not much improvement was observed in the hand-path ratio for the participant who used PGM as compared to the other participant. If the average values are carefully observed, the improvement in the performance of the subject with PGM was better concerning all scores taken into consideration in this study except hand-path ratio score. It was also noted that pattern “8” appeared to be the hardest to master for both participants. Open feedback was also collected from the participants after the end of all sessions. The positive opinion from the participant who used PGM was that he felt “motivated” to continue using his arm when he performed those exercises with the suit, as it provided him with the “necessary push”.

At this stage, we can say that ForceArm can also be used in integration with gaming environments to provide repetitive training resulting in motor rehabilitation and recovery. It was already proved by previous research [84] that as compared to conventional treatment, robot-assisted repetitive movement training can induce better improvements in terms of decreasing impairment, increasing reach extent and improving strength. We observed that the gaming task designed for the elderly in this work showed better improvements in the participant who was assisted through the ForceArm prototype. Therefore, the prototype gives a substantial possibility of providing positive results in the long term as compared to conventional rehabilitation.

## 4.3 CASE STUDY 2: Can ForceArm induce motor learning?

Muscle memory is created by motor learning that involves step by step acquisition of the concerned motor task into memory through repetition. Motor tasks that involve complex learning, such as playing musical instruments, take more extended periods. One such task is drumming. Gaining expertise in drumming requires an abundant amount of repetitive training. The training may also involve getting acquainted with different rates of drumming beats, commonly termed as beats per minute (BPM). The human voluntary rhythmic movement, like uni-manual tapping, is limited to 5-7 Hz. However, the winner of a recent contest to find the world's fastest drummer (WFD) could perform such movements using a hand-held drumstick at 10 Hz, which corresponds to an inter-tap interval (ITI) of 100 ms [85]. Therefore, individual limitations in maximum voluntary rhythmic motion may differ from person to person.

In this study, we verify if force feedback can be used as a training method in two-handed drumming. We then compare it with audio feedback in the same context of learning two-handed drumming. We use the ForceArm glove to provide force-feedback, which is, in turn, synchronized to the drumming patterns to be taught. Besides, the utilized augmentation method in the form of the soft exoskeleton is highly flexible, wearable and restricts our body movement to a minimum extent. We chose two-handed drumming patterns since such patterns are hard to master in drumming for beginners. Participants were asked to play the drum while looking at the score or the musical notation of the drumming pattern. This prototype is the first wearable pneumatic system to be attempted to train rhythm sense by actuating the user's arm. To evaluate force-feedback-based learning, we used audio feedback as a modality of comparison for the users.

### 4.3.1 Apparatus

The materials used for setting up the user study of learning to drum through force-feedback is shown in Fig. 4.6. Participants wore the ForceArm glove with two DOF support, namely pronation and supination for both hands. Two PGMs were spirally attached around their forearm. Drumming movement corresponds to pronation and supination motions which is why we used these two motions. We prepared a drum practice pad and two sticks covered with copper foil as illustrated in 4.6. The participants had the practice pad placed in front of them. We logged the time stamp whenever contact between the tip of the sticks and the surface of the practice pad was detected. We placed armrests of equal heights to ensure a fixed posture of all participants. Besides, noise-cancelling headphones were used to play white noise during the experiments to cancel external noise. During the task time duration, they were provided with a metronome on the same headset. The headphones prevented the participants from hearing PGM decompression noises which could create disturbance in remembering the musical scores. The experiment recording scenario can be seen in Fig. 4.7.

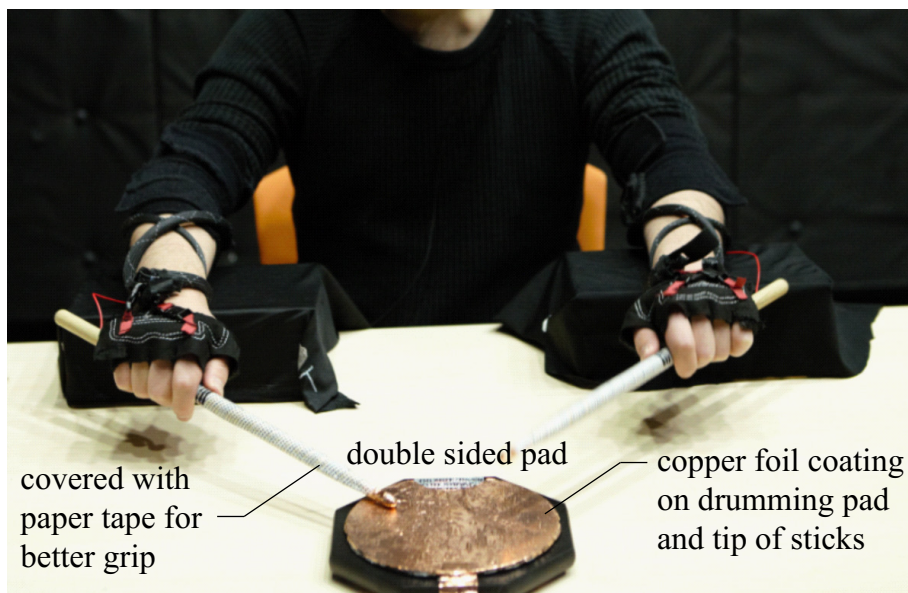


Figure 4.6 Materials used for setting up the drumming practice and timing detection

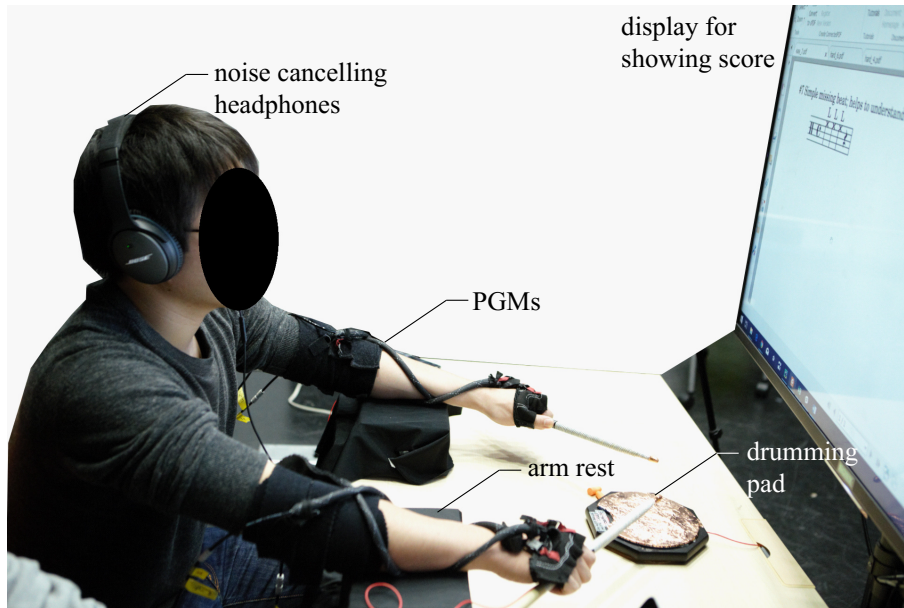


Figure 4.7 Experiment Settings.

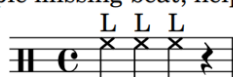
### 4.3.2 Participants

We recruited four participants for the initial study (two females and two males, aged from 23 to 31). One of the participants P1 was an experienced guitarist that made him acquainted with rhythm training. The other participants were all amateurs who were never trained to play any musical instrument. Half of the participants trained with PGM first, and the other half trained with audio first for counter-balancing.

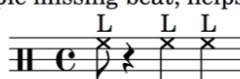
### 4.3.3 Task and Procedure

The participants were first given time to get acquainted with the whole system with a brief description of the experiment. We introduced our soft exoskeleton and attached it to the participants' forearm while they tried to play the drum with force-feedback provided the actuated PGMs. The tasks of this user study are shown in 4.8). The first two scores are basic beats that are very easy to remember. Therefore we chose complicated patterns for the remaining tasks that included off-beat and missing beat type patterns. For each pattern type, a short practice session was provided with force

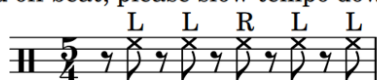
#7 Simple missing beat; helps to understand timing



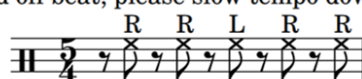
#8 Simple missing beat; helps to understand timing



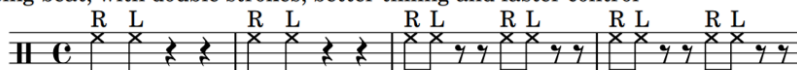
#4 Hard off beat; please slow tempo down to 80 or less



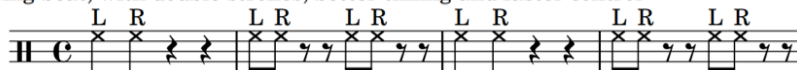
#5 Hard off beat; please slow tempo down to 80 or less



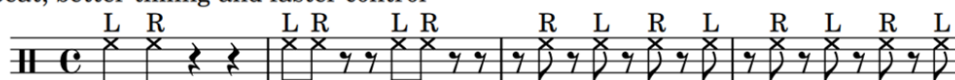
#6 Missing beat; with double strokes; better timing and faster control



#7 Missing beat; with double strokes; better timing and faster control



#9 Off beat; better timing and faster control



#10 Off beat; better timing and faster control

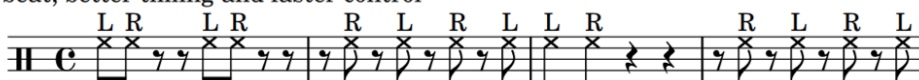


Figure 4.8 Drumming scores used for the study. Two easy and six hard patterns.

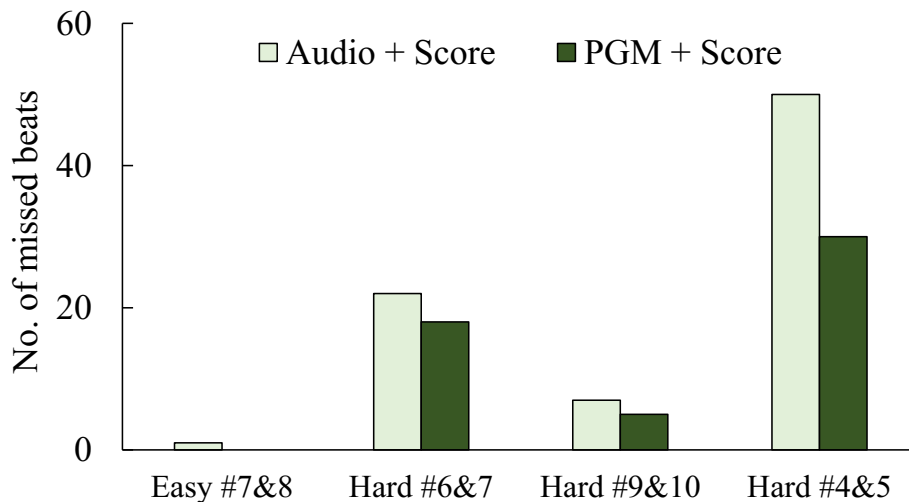


or audio feedback (with a visual display of the pattern) which was followed by repeating the same pattern without feedback (without visual display of the drumming score). Therefore, the participants had to remember the drumming pattern during the practice session with audio or force feedback that comprised of three repetitions for each task.

As a measure of efficiency, we counted the number of missed beats in the tasks. When participants drummed in wrong timing or missed a drum beat, it was counted as a missed beat. The duration of the error time width was set to  $\pm 62.5$  milliseconds from the desired hitting timing. This time width was determined from the shortest difference between two consecutive notes in all tasks.

We measured the number of missed beats during both training and testing sessions. Training sessions refer to the practice session, and the testing session refers to the sessions without feedback-based assistance.

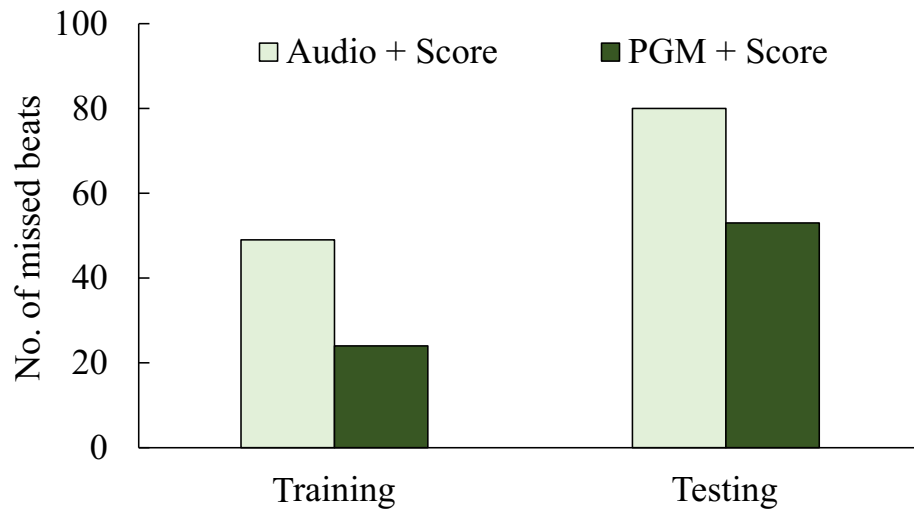
#### 4.3.4 Results



(a) Average missed beats for audio and force-feedback type testing sessions

Figure 4.9 Results of two-handed drumming study

The efficiency measure used to evaluate the two types of force-feedback methods was counting the number of missed beats for each type of score practice. Fig. 4.9 shows the results of the user study in a conclusive manner. Fig. 4.9a shows the average



(b) Average missed beats during training and testing sessions

Figure 4.9 Results of two-handed drumming study (cont..)

number of missed beats of all subjects for the four different difficulty level-based scores. Fig. 4.9b shows the average missed beats for the whole training and testing sessions compared for the two types of feedback provided.

### 4.3.5 Discussion

The prototype was also pondered for the possibility of use as a device that can accelerate the process of learning complex motor tasks. In this case, two-handed drumming was considered, and a fundamental user study was conducted. Force-feedback provided by actuating PGMs on the forearm was used to provide training sessions and compared with audio-feedback for providing the same training. It was observed that PGM-based training resulted in the lesser average number of missed beats which was used as a measurement of efficiency of the training method. This observation gives us hope that such wearable force-feedback systems that can actuate our body parts in synchronization with a complex task could train us faster to perform those tasks as compared to conventional training methods. If this is true, it could be revolutionary because we can implement such training methods in any environment such as in moving trains, in the woods, and break time at the workplace. Since the system is wearable

and portable, there is not much liability of carrying materials around. However, this work was a fundamental user study, and more data needs to be collected and verified in order to prove the concept.

## 4.4 CASE STUDY 3: Navigation assistance through ForceArm

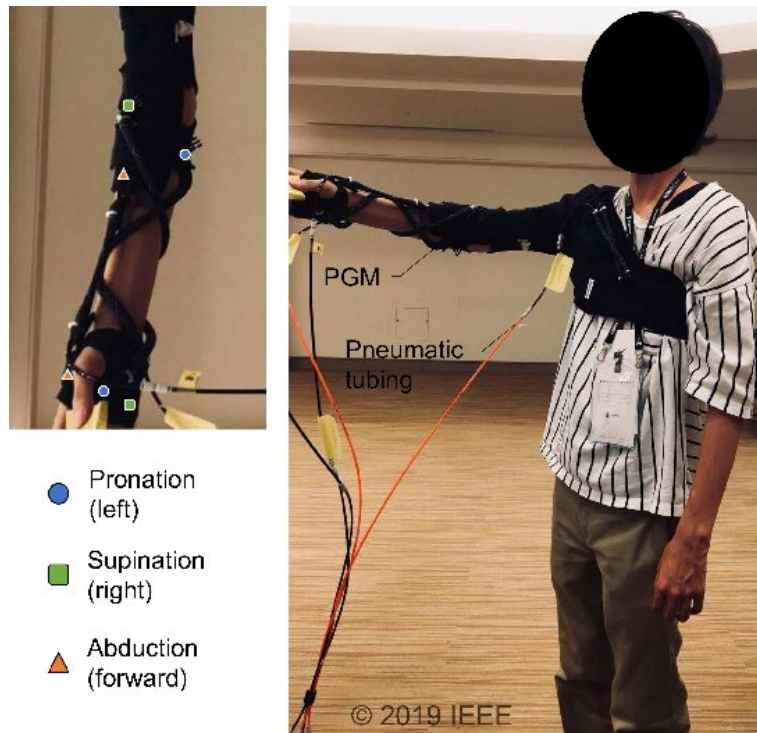


Figure 4.10 Degrees of freedom (DOFs) chosen for navigation assistance with positions of the associated pneumatic gel muscles (PGMs) [3].

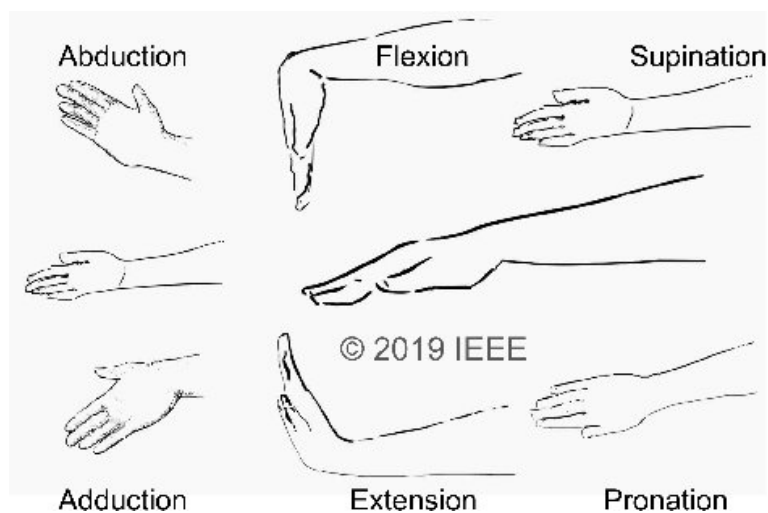


Figure 4.11 Degrees of freedom (DOFs) considered for use as navigation cues [3].

The third case study was about testing the feasibility of using our prototype for navigation assistance. Wearable force-feedback was rarely used as a real-time navigation cue provider which has been attempted in this case study. The first version of the prototype called ForceHand glove [1] was used for this application. The system was mainly designed to provide navigation cues to the forearm part of the upper limb. Fig. 4.10 shows the different motions or DOFs used for providing navigation cues to the users. Since it was a feasibility test, we kept it simple with only three types of cues, namely left, right and forward. However, we considered various additional DOFs, as shown in Fig. 4.11 in the forearm portion and chose pronation supination and abduction based on user feedback and preferences. The respective PGMs to induce force-feedback for these motions were positioned according to the points of attachment shown in Fig. 4.10. The feasibility test involved an extensive user study containing a simulated navigation environment. The navigation environment was simulated using Unity. Wide variations of users were included during this study, and their subjective feedback was collected. In addition to this feasibility study, a just noticeable difference (JND) experiment was also conducted in order to identify the ability of the prototype to provide precise navigation cues during situations with multiple possible navigation choices such as multi-forked roads and intersections.

#### 4.4.1 Navigation environment simulated in Unity

This experiment aimed to identify the preferred type of cue, while navigation assistance is provided in a simulated environment.

##### Methods

The Unity-based simulation mainly included a previously unseen maze for the subjects to navigate through. An animated character was spawned at different locations of the maze to represent the presence of cues. Fig. 4.12 illustrates a bird's eye view of the entire maze. The image also shows the start and end points given to the user.

The user's task was to navigate themselves from the start point to the endpoint by collecting various collectables along the way. The animated characters guided them through navigation cues of various types: force-feedback, audio and visual. The users could see the first-person view on the computer screen while they controlled their movement inside the simulated environment through an Xbox gaming console. The collectables were placed inside the maze such that the users have to carefully follow the navigation cues in order to obtain high points. Points acquired depends on the number of collectables gained. The direction cues using force-feedback were provided upon colliding with the animated characters using PGMs attached to the dominant hand of the users, as shown in Fig. 4.10. Audio and visual cues were also provided during a few collision instances with the animated characters. There were fifty-seven participants in total who provided their valuable feedback after actively taking part in this feasibility experiment.

### **User experience evaluation**

All participants had to choose their preferred types of cues after playing the game. Fifty-one out of fifty-seven participants chose force-feedback, which is 89.5%. Visual or auditory type of feedback was chosen over force-feedback by only one participant. Five other participants were unsure about their preferences. The results are illustrated in Fig. 4.13.

#### **4.4.2 Just noticeable differences (JND) experiment**

Distinct cues provided for each direction often have the possibility of misleading us in situations where there can be multiple choices in a single direction. In real-life scenarios such as multi forked roads and intersections, we need more precise cues to understand the navigation. This experiment was conducted in order to identify human's ability to distinguish between two different forces. Such combinations of different forces can be used to provide precise navigation cues for further advancement of the prototype

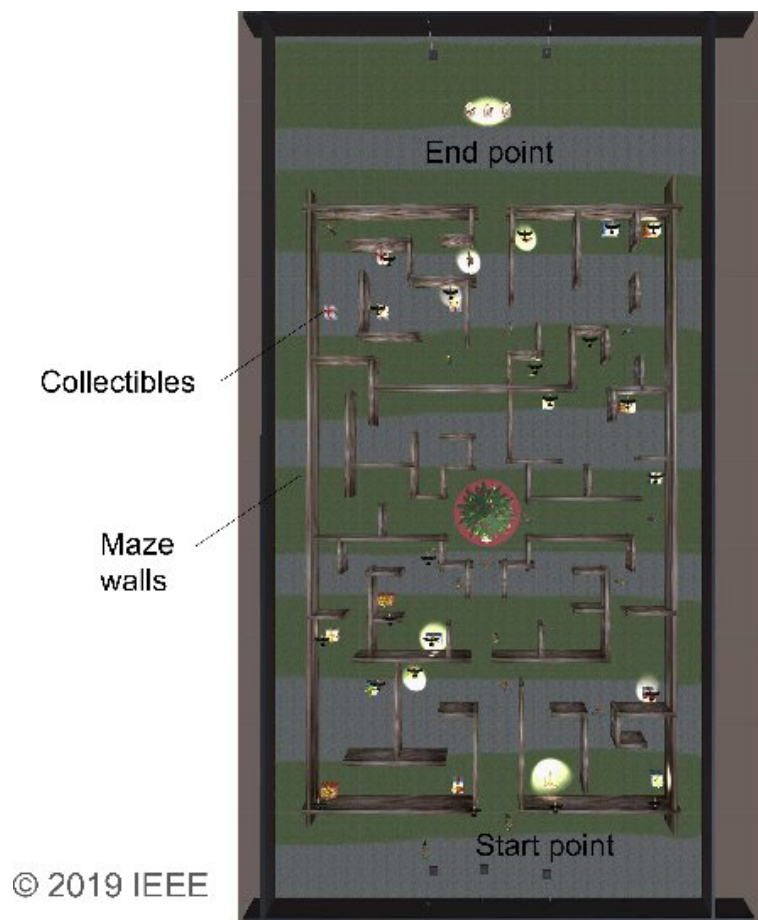


Figure 4.12 Maze environment simulated in Unity for testing the feasibility of navigation assistance using pneumatic gel muscle (PGM)-based force-feedback [3].

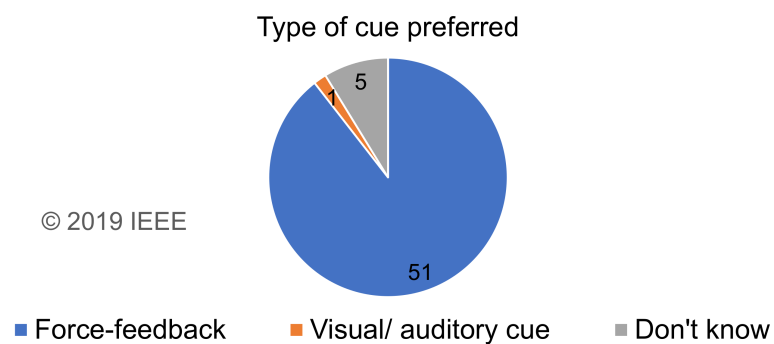


Figure 4.13 User preferences of navigation assistant cue type [3].

applications. Eight participants consented for this experiment. The subjects wore the glove to receive only a single type of cue but with different force intensities. The force intensities were varied through a pulse width modulation (PWM) type valve that could control the air pressure precisely. The participants received two different types of force intensities and were asked to identify the larger force. We varied the air pressure values with resolutions of 20, 15, 10 and 5 kPa. We selected ten pairs of force values for each resolution. These ten pairs called as one trial were repeated five times for each subject.

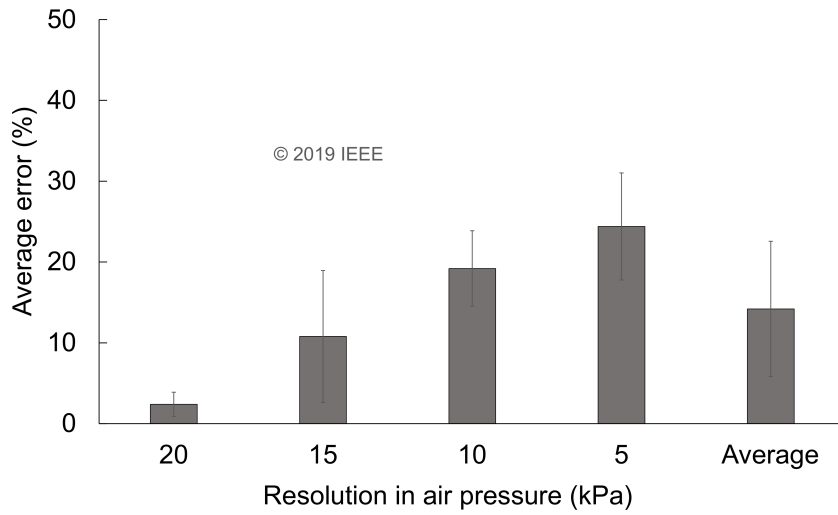
### **Results of the just-noticeable differences (JND) experiment**

The results of this experiment were quite similar to our expectations. We evaluated the results based on the number of mistakes made by the subjects. Each trial consisted of 10 pair of forces. Therefore, the mistakes made by the subjects were counted out of 10 and then converted into a percentage. The summarized results are illustrated in Fig. 4.14. Fig. 4.14a shows the average error of all subjects for each resolution. Five subject data are separately illustrated in Fig. 4.14b. We also analyzed the data from a different perspective. For each pair, there was a lower force value. The entire accuracy data were plotted against this lower force value for each resolution in Fig. 4.15. Here accuracy represents the percentage of correct responses out of 10 pairs in each trial for all subjects. This illustration shows the effect of different force values of input air pressure on the accuracy of force identification. It was observed that the accuracy tends to decrease with the increase in air pressure value provided. This fact remains true for all resolutions except 5kPa.

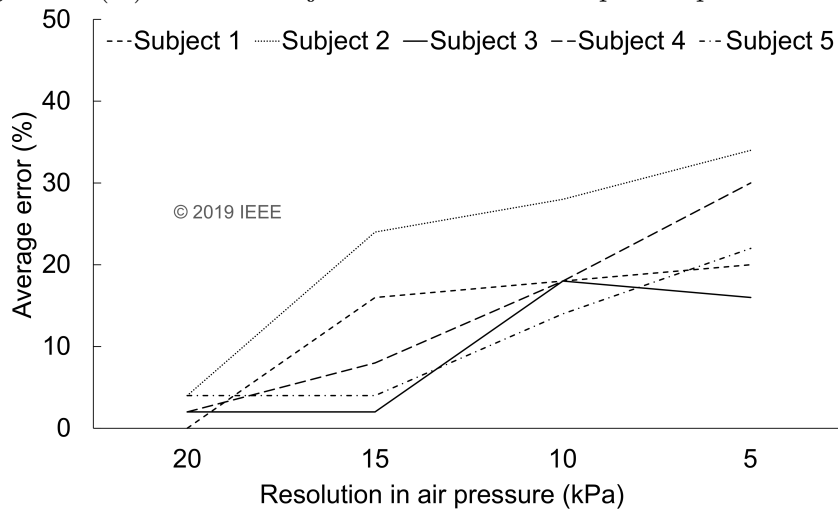
### **4.4.3 Discussion**

A section of the ForceArm suit was tested for feasibility as a navigation assistant through two user studies. We also received subjective feedback from participants who tried the simulated navigation scenario in Unity with PGM-based force-feedback navigation cues. Also, another user study was conducted to identify human's ability to identify





(a) Average error (%) for each subject with increase in input air pressure resolution [3].



(b) Average error (%) values with respect to increase in resolution of input air pressure [3].

Figure 4.14 Error values (%) observed during just noticeable difference (JND) experiment

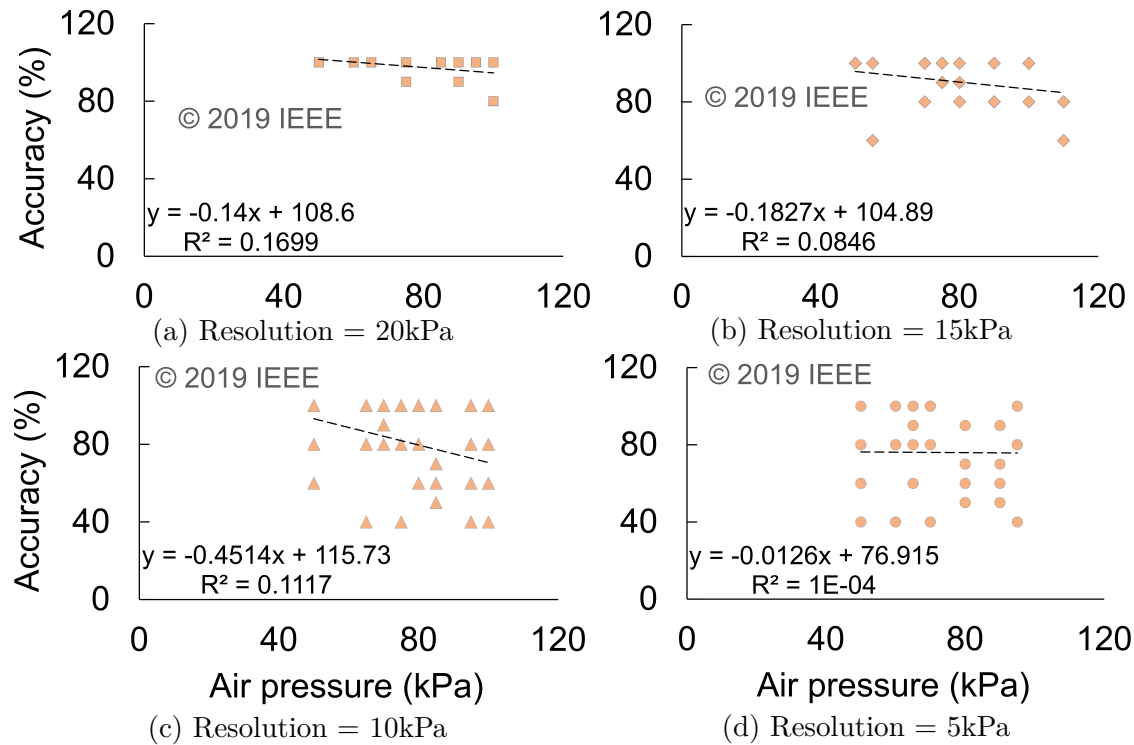


Figure 4.15 Accuracy (%) plotted against air pressure (kPa) for different resolutions [3].

differences between two different force levels for different resolutions. During the first user study, the vast majority of the participants preferred force-feedback over audio and video types of cues for navigation assistance. Some of the users suggested using both arms for providing the navigation cues. Even though the information provided to the user will be redundant in this case, providing force-feedback to both arms may have an additional positive effect. Some users also suggested for the independent choice of the types of motions associated with each direction. Such requirements can be implemented by including an additional calibration session where the users can choose their preferred DOFs and associate those to the navigation cue types through self trial. Some users found the pronation and supination cues quite similar and therefore took some extra time to get familiar to the cues. This issue can be solved if independent choices are given, and some extra time is given to the user for getting acquainted with the cue types. The time consumed by each participant for learning or getting acquainted was different. Therefore, it is essential to identify the higher limit of the

learning time required. Other subjects also mentioned the possibility of including additional cues other than left, right and forward, which is a part of the future work of this case study. The force-feedback was too strong for some subjects who also suggested the need to tune the force to the most comfortable range before beginning the task. Soft wearable force-feedback was quite a different and new experience for most of the users, especially for navigation assistance. Therefore, many of them agreed that PGMs were the right choice for providing sensory feedback in navigation scenario. One of the interesting observations made by two of the participants was that the force-feedback received by their arm resembled the feeling of the presence of a second person in the scenario who pulled their arm to provide the necessary guidance. This response was very thought-provoking and sharp observation. The guiding presence was felt due to the complementary appearance of the animated character and force-feedback. This kind of virtual environment simulation can be further improved by including tactile feedback on the fingertips. This type of feedback will be particularly suitable for gaming applications. One other user mentioned that it was difficult for him to concentrate because he was too engaged in the game through visual senses. Multiple sensory channels are difficult to tackle for such individuals. Another vital aspect mentioned by some participants was about the aesthetics of the current glove design. They mentioned that there is a tremendous scope of improvement, especially in the sleeve part. The type of hook and loop type fabric used to attach the PGMs in this user study was a quite low quality that made it time-taking to don and doff. Also, many users did not prefer hook and loop fabric because it tended to catch dirt and grab onto other unwanted objects, which might even cause damage to those objects. Such issues can be solved by replacing hook and loop fabrics with buckles and other kinds of fabric attachments.

Regarding the second experiment, as expected, subjects showed similar patterns of accuracy for different resolution values. However, individual differences in the levels of accuracy were present for each subject due to differences in concentration and other

cognitive parameters. Some of the critical observations made during this experiment are pointed out as follows:

- It was easier to identify differences for lower values of forces
- 20kPa was the highest resolution considered for this study associated with an average accuracy of 97.6%
- Accuracy for other resolutions 15kPa, 10kPa and 5kPa were 89.2%, 80.8% and 75.6%, respectively.

## 4.5 CASE STUDY 4: ForceArm-based feedback in virtual reality (VR)

The study is about using the ForceArm glove to provide force-feedback in VR. We compared two types of force-feedback for four different object types in VR.

### 4.5.1 Modelling of pneumatic gel muscle (PGM) induced force due to stiffness

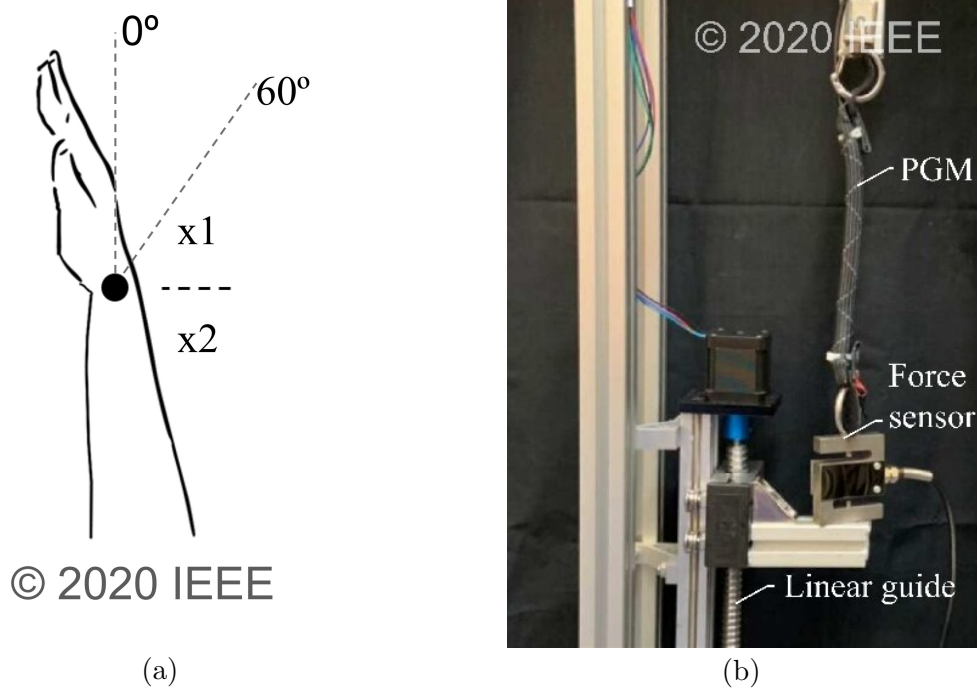


Figure 4.16 (a) Notations used for forearm dimensions while attaching the pneumatic gel muscles (PGMs) (b) Experimental set-up used to measure force due to stiffness in PGMs [4].

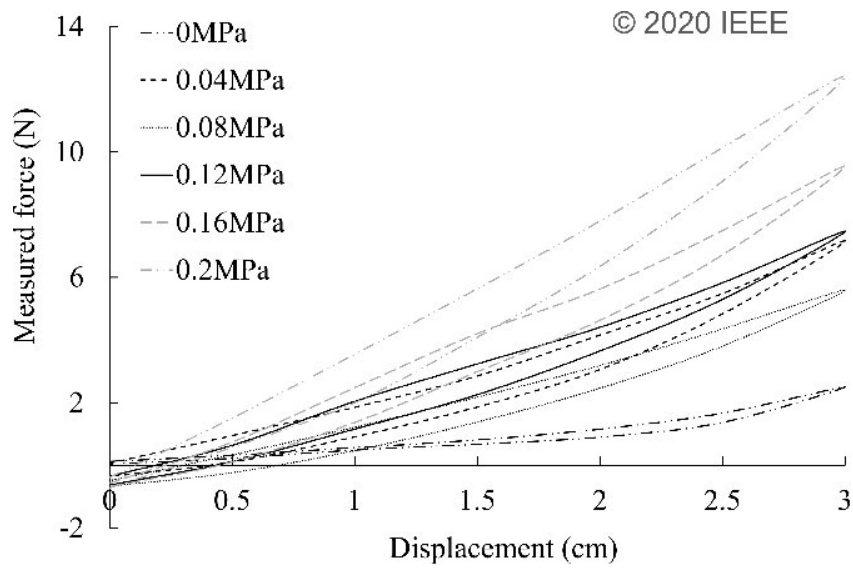
Modelling and estimation of the forces induced by the PGM actuators is a vital step when it comes to using those actuators to provide force-feedback in virtual environments. The proper estimation of the forces enables us to keep the system within the desired physical properties. It also helps to ensure the reproducibility of the

force-feedback during different instances. Therefore, we measured the force received from PGM actuation and modelled it using a spring model. The following equation represents the modelled force behaviour of the PGM as a function of displacement and applied air pressure.

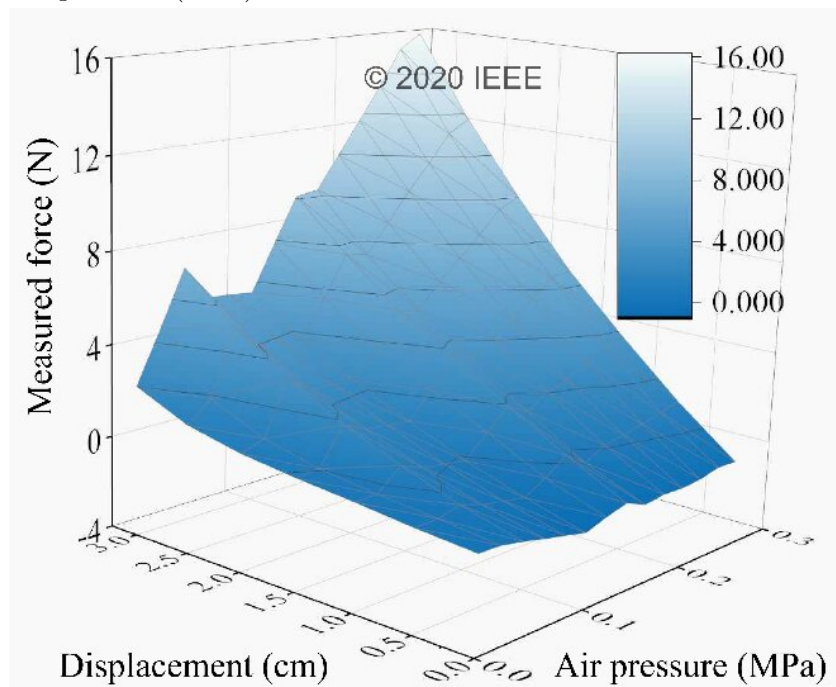
$$F_s = f(x, P) = (a_0 + a_1P)x + a_2 \quad (4.7)$$

Equal length PGMs were used during the entire study. Therefore, we modelled the force characteristics of the specific length used for the study. The length of the actuator at rest was measured as 30cm. Fig. 4.16b shows the experimental set-up used to measure force resulting from contracting behaviour of the PGMs through the insertion of varying levels of input air pressure and displacement. The range of air pressure considered for force modelling was 0MPa to 0.26MPa with 0.02MPa steps. The displacement was increased step-wise from 0cm to 3cm and then back to 0cm for each air pressure value. Here, the displacement indicates an expansion of the PGM. A two-dimensional representation of the force characteristics plotted against displacement for different levels of air pressure can be seen in Fig. 4.17a. A three-dimensional representation of the force characteristics plotted against displacement and air pressure is shown in Fig. 4.17b. The force tends to increase with increasing levels of air pressure as well as displacement. We can observe hysteresis in the two-dimensional representation of the force due to the damping properties of the PGM. In other words, the loading and unloading force characteristics of the PGM form a hysteresis loop for each value of air pressure. The equation 4.7 was used to model the force characteristics with coefficients  $a_0 = 0.956$ ,  $a_1 = 15.71$ , and  $a_2 = -0.803$ . The modelled force and residual error for each data point are illustrated in Fig. 4.17c. The r-squared value for this plot was 0.95.

In this work, we developed two different PGM actuation methods to create realistic force-feedback in virtual environments. A user study was conducted to compare the two methods. We used simple binary switching of high-speed solenoid valves SMC

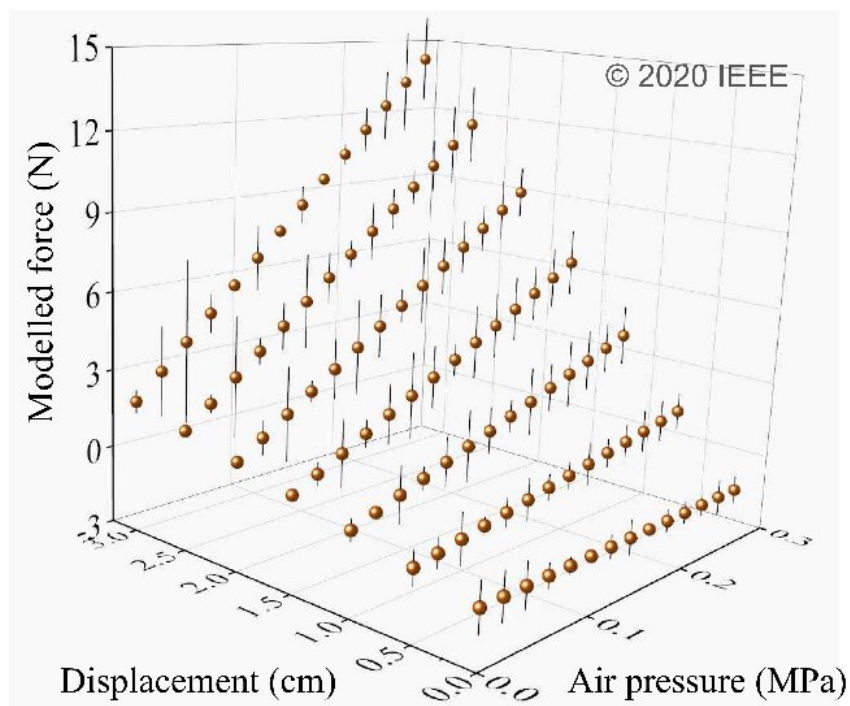


(a) Measured force (N) with respect to change in displacement (cm) for varying levels of air pressure (MPa)



(b) 3-D representation of measured force (N) plotted against displacement (cm) and air pressure (MPa)

Figure 4.17 Modelling of the force due to stiffness in pneumatic gel muscle (PGM) actuator [4].



(c) Modelled force (N) with residual error

Figure 4.17 Modelling of the force due to stiffness in pneumatic gel muscle (PGM) actuator (cont..) [4].



SYJ312M in the first method. The valves were turned on or off per contact status of the user's virtual hand with the objects. Fixed air pressure of 0.2MPa was provided to the input side of the valves. This value is the highest air pressure that can be fed to the PGMs, creating maximum contraction without causing any damage. The second method of providing force-feedback was by using PWM-based switching of the air pressure fed to the actuators. We used the SMC ITV0031-2L PWM valve for this method of control. This PWM valve can precisely regulate the output air pressure (0-0.5MPa) while the DC voltage applied to the valve is changed from 0-5V. However, the air pressure in this study was limited to 0-0.25MPa because of the physical limitations of PGM. All users tend to extend their wrist voluntarily when they are asked to make contact with the objects in the VR environment. This voluntary wrist movement results in the negative displacement of the PGMs that, in turn, reduces the stiffness force at the wrist. The range of wrist extension range 0-60° for all users. We used the control method to maintain a minimum force of 0.5N using the wrist extension actuators at all times of no-contact state. This slightly stiff state of the PGMs helped increase the concentration and engagement in the users. Moreover, the 30cm PGM was attached on the forearm such that,  $x_1 = 7\text{cm}$  and  $x_2 = 26\text{cm}$  at 0MPa. Here,  $x_1$  and  $x_2$  are dimensions illustrated in Fig. 4.16b. We calculated these values using the equation 4.7 to ensure that a stiffness force of maximum 2N (0MPa) is maintained at the wrist during no-contact states. For better force-feedback feeling, we observed that maintaining the stiffness force at the wrist at all conditions creates a positive effect. Therefore, we used the control mechanism to regulate the air pressure such that a minimum force of 0.5N was maintained at the dorsal side of the wrist. The air pressure required for this condition was observed as 0-0.15MPa at a minimum positive displacement of 0.3cm. At no-contact states, a closed-loop PI control was used to regulate the air pressure through an ESP32. A stretch sensor was used to identify the degree of wrist extension at all times. We placed the sensor on the ventral side of the wrist through a stretchable band extending from the palm towards the elbow. Before starting the user study, a calibration process was conducted for every user to

set the stretch sensor range for the particular user's wrist extension from  $0^\circ$  to  $60^\circ$ . This range was then mapped to the PGM air pressure range of 0-0.15MPa. The control flow used in the system is illustrated in Fig. 4.18. The stretch sensor is used to set the reference  $R(t)$  which is then compared to the pressure value read by the pressure sensor at the output  $Y(t)$ . The PI controller then minimizes the error,  $E(t) = R(t) - Y(t)$  by changing the analogue voltage fed to the PWM valve.

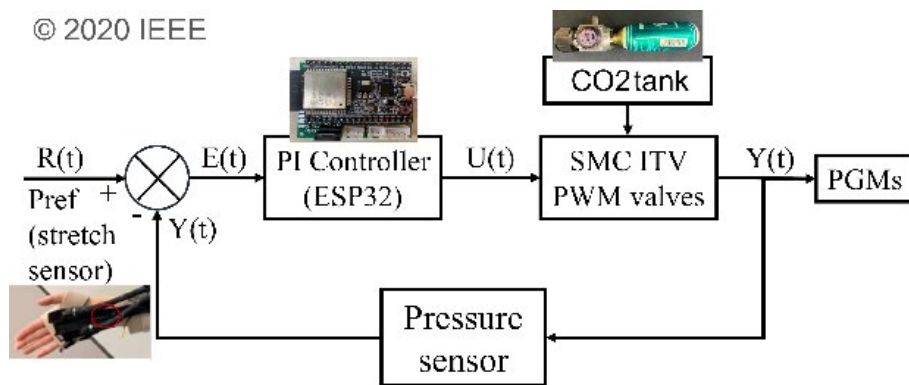


Figure 4.18 Illustration of the control flow used to regulate the air pressure fed to the pneumatic gel muscles (PGMs) [4].

#### 4.5.2 Force-feedback in virtual reality (VR)

There were four types of force-feedback in this user study. Each of them was designed using both binary and PWM-based actuation methods. The visual information shown to the users for each type of feedback is depicted in Fig. 4.19. We used both wrist flexion and extension associated PGMs to realize these feedback types. Table 4.1 represents the timing information for both actuation methods associated with each force-feedback type. For the binary actuation method, all PGMs were driven by commands 0 for low and 1 for high. For the PWM-based actuation method, the flexion associated PGMs were controlled using binary commands while the extension associated PGMs were actuated using the PWM-based control. During contact mode of PWM-based actuation method, the air pressure was raised by 0.1MPa.

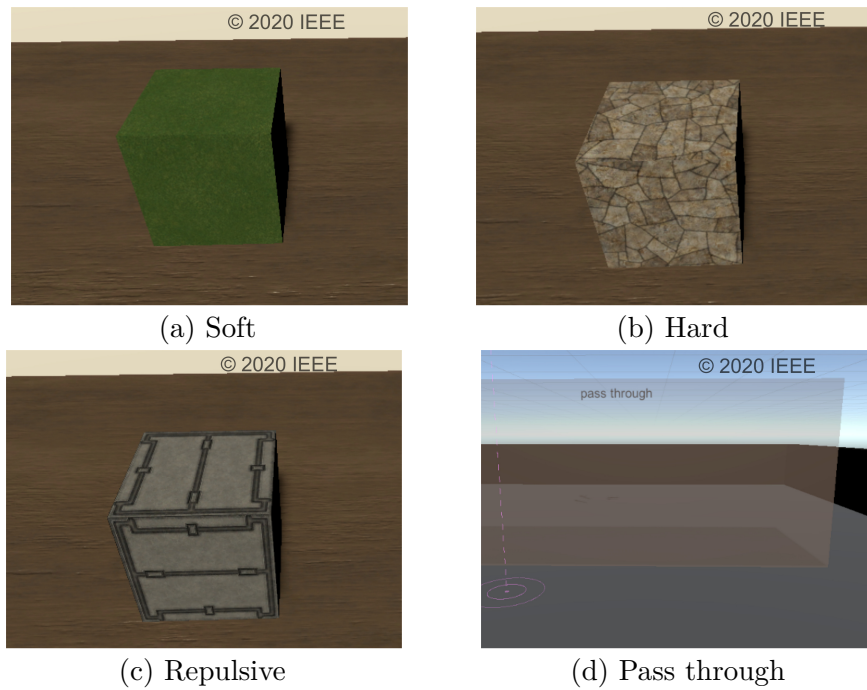


Figure 4.19 Visual representation of the various objects as shown to the users during the study [4].

Table 4.1 Actuation sequence of pneumatic gel muscle (PGM) for various feedback types in binary and pulse width modulation (PWM) actuation methods [4]. © 2020 IEEE

<b>Binary</b>	<b>Actuation sequence</b>
Soft	Flex (150ms), delay (150ms), Flex (150ms)
Hard	Extend (150ms), delay (150ms), Extend (150ms)
Repulsive	Extend (500ms)
Pass through	Extend (150ms), Flex (150ms)
<b>Pulse width modulation (PWM)</b>	<b>Actuation sequence</b>
Soft	Flex (300ms), delay (300ms), Flex (300ms)
Hard	Extend (1000ms), delay (1000ms), Extend (1000ms)
Repulsive	Extend (2000ms)
Pass through	Extend (500ms), Flex (300ms)

### 4.5.3 User-study

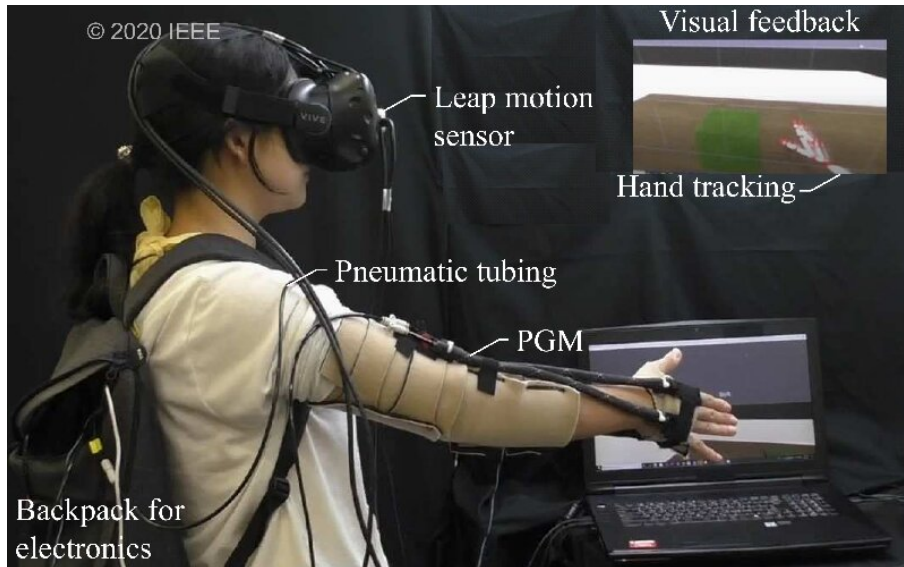


Figure 4.20 User study to render physicality for objects in virtual reality (VR) [4].

This section describes the various experiments carried out to verify the experiences of using the two actuation methods used for providing force-feedback at the wrist using PGMs.

#### Methods

Five participants consented for this experiment. They were first instructed and then placed in the virtual environment prepared using Unity software. The participants were all experienced in using VR headsets. One session each was conducted for binary and PWM-based actuation. We ensured a time separation of 24 hours between the two sessions for each subject. The time separation between the two sessions was to ensure the absence of bias of one session on another. The objects in VR scenes were all labelled so that the participants can recognize the type of feedback and the corresponding object type. Only right-handed participants were chosen for this experiment, and their dominant hands were used to reduce set-up time. Participants were given 30 seconds for evaluating each type of feedback. If needed, we provided multiple iterations of

the objects to judge the feedback types. After the end of each session, participants rated the objects based on a Likert scale [86] rating from 0 to 7 with 7, meaning the most realistic rating. They also selected their favourite type of feedback and provided open-ended feedback after both sessions.

## Results

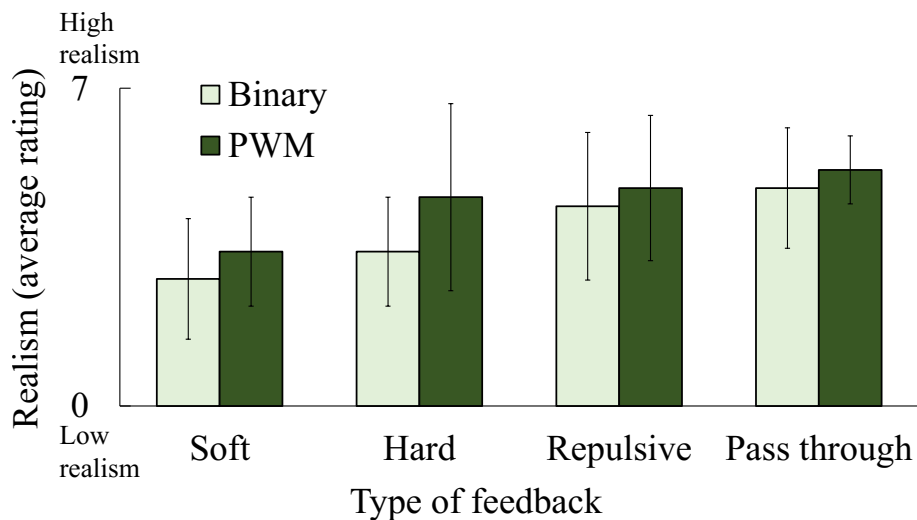


Figure 4.21 Subjective feedback obtained from user-study for various types of feedback

Fig. 4.21 illustrates the average rating of all types of feedback using the two methods of PGM actuation. PWM-based feedback was rated higher than binary actuation. On average, pass-through was the highest-rated type of feedback. Most participants chose pass-through as their most satisfactory or realistic type of feedback during the study.

### 4.5.4 Open-ended feedback

PWM-based force-feedback was generally rated more realistic as compared to the binary method. Some open-ended comments from various participants are listed as follows [4]:

- “During the PWM session, PGM contracted slower, but the movements felt real”. This was stated by P1, who is highly experienced in VR.
- “Short term stimulus is not suitable for haptic feedback. The continuous feedback during the second session felt like touching objects. It was good. In the case of *pass through*, it felt similar to passing through an object. So, I think it would be nice to see translucent objects in VR”. This was stated by P2, who has sufficient experience with PGMs as well as haptic feedback.
- P3 was also experienced in both VR and PGMs and mentioned, “The on-off (binary) feedback is good to realize high reaction forces. However, the soft feeling felt strange in the case of binary feedback. PWM felt more natural compared to binary, especially the soft feedback was better and more realistic”.
- P4 and P5 were satisfied most by the pass-through type feedback.

#### 4.5.5 Discussion

We modelled the actuator called PGM in this case study and used it in a VR force-feedback application. The wrist flexion-extension DOF was mainly used for this application. We attempted to relate the force-feedback with heavy object handling sensation, especially at the wrist. The major benefits of utilizing PGMs in this kind of applications is their wearability and low weight. Besides, the portable nature of the prototype enables any application that demands non-stationary usability, such as walk-around virtual environments. We tested four types of object feedback, namely soft, hard, repulsive and pass-through. We designed two different methods of obtaining force-feedback in virtual environments, namely binary switching and PWM-based switching. The spring model of the PGM induced force characteristics was used for the PWM-based control method of air pressure. Participants were asked to rate each force-feedback experience using a Likert scale rating of 0 to 7. From user-feedback, soft type feedback was rated as the most realistic, followed by hard, repulsive, and

pass-through. PWM-based actuation method was generally rated better than binary type by all participants. Here are some observations from the open-ended comments of the participants:

- “Force-feedback types that demand higher reaction forces should be implemented using higher values of actuation forces”. Binary type actuation method can realize higher forces as compared to the PWM-based control. Therefore, based on the types of feedback, different actuation types are suitable. Such requirements can also be fulfilled by integrating the two types of feedback methods.
- “Soft-type feedback is better using PWM-based control”. This was an expected observation of the subjects because the rise time in the PWM-based control method was higher than binary actuation. This difference in the rise time results in a mild force effect in case of the PWM-based control, which is more relevant for soft feedback. Moreover, soft type feedback is considered as the hardest to be rendered in VR [68]. So more extensive research needs to be done for better acceptability of this force-feedback type.

## 4.6 Conclusion

We tested the ForceArm glove and parts of it to identify its role in different kinds of application scenarios. There were explicitly four different application scenarios. The first was elderly rehabilitation which involved a two-month study in verifying if a user wearing the prototype while performing repetitive motions will eventually have better performance of the arm compared to a control subject. We could observe better improvement in the elderly user who used PGM assistance compared to the other participant. However, more detailed user study involving a more substantial number of participants needs to be done to hold the assumption. The second study was to identify if providing force-feedback using the ForceArm prototype can induce motor learning effects in human subjects. A primary study was done to prove this hypothesis by considering two-handed drumming as the motor learning task. The training was provided using force-feedback and audio separately and resulted in the two situations were compared. Force-feedback showed better results which meant participants made lesser mistakes when they learnt the drumming lessons through the wearable force-feedback. The third study was about using the ForceArm glove as a navigation assistant. A simulated environment in Unity was designed to be used by participants for navigation like a task where they compared different types of navigation cues, audio, visual and force-feedback type. Majority of them preferred force-feedback because it was relatable to the navigation directions, and the response time was faster than the other two types of feedback cues. The fourth study was about using the ForceArm prototype in a VR environment to provide force-feedback. We designed two types of force-feedback using binary and PWM solenoid valves and asked participants to compare between the two. The feedback type was different from the existing literature because heavyweight object handling feedback is very less approached in VR haptics field due to the involvement of the wrist joint. Haptic feedback on the fingers is commonly available and abundantly approached. Therefore, through this



study, we attempted to address this issue and provide an idea of force-feedback in VR explicitly focused on the wrist joint.



# Chapter 5

## Conclusions

This work of the pneumatic actuator-enabled force-feedback generating suit for the arm of the human body prioritizes wearability and user-friendliness for rehabilitation through gaming and other multiple possible force-feedback applications. The human body can achieve restoration of motion functionality only through repetitive and efficient training. Often, people who suffer from accidents or post-stroke weakness have to go through a tedious process of rehabilitation through long training sessions. If these sessions are made more stimulating and interactive through real-time force-feedback in gaming, physical training can be achieved along with cognitive training. In the future, we intend to improve our wearable device to support full three DOFs of the arm and use it in conjunction with an appropriate gaming environment application, especially for the elderly.

The ForceArm prototype was also tested for elderly usage. An experiment was conducted to verify the muscle unloading effects of the prototype on elderly participants. This assessment was done through sEMG measurement. The forearm DOFs were only evaluated in elderly participants as we could not receive consent to measure the back and upper thorax muscles. Therefore, the shoulder and elbow motions were evaluated in young subjects. Muscle unloading was observed in all motions except shoulder flexion in case of younger participants and wrist extension in case of elderly

individuals. Besides, a gaming task was developed to evaluate the prototype's ability to enhance motor recovery in elderly participants. Data were collected for various patterns of the task, and the data were analyzed using four specific parameters related to motor characteristics. The obtained data showed that ForceArm assisted individual showed better improvements in all patterns except for the hand-path ratio score. The conclusions drawn are:

- ForceArm can be used to assist the forearm motions of wrist flexion, forearm pronation and supination, and elbow flexion in young as well as older adults. The remaining motions supported by ForceArm are wrist extension and shoulder flexion, which were also successfully assisted in selected individuals during the study. The ability of assistance was proved through sEMG measurement in both young and older adults.
- The prototype can also assist in motor recovery in older adults with decreased arm functionality which was proved through a gaming task in this work.

We also evaluated how pneumatic artificial muscles impact skill acquisition of two-handed drumming. Pneumatic muscles are a new actuator of particular interest in haptics as they strike a satisfying balance: lighter than rigid exoskeletons and, indeed, more precise than electrical muscle stimulation. To understand the effect of pneumatic muscles on skill acquisition, we conducted a user study based where we compared participants' drumming performance after training with the audio or with our artificial muscles. Our haptic system was comprised of four pneumatic muscles and is capable of actuating the user's wrist to drum accurately up to 80 bpm. We found out in our study that pneumatic muscles improved participants' correct recall of drumming patterns when compared to auditory training.

A part of the ForceArm glove was also used to develop a navigation assistance prototype and tested for feasibility. The advantages of the prototype were wearability, portability and hands-free solution to navigation assistance scenario. The PGMs used

in this prototype were the same as those used in the ForceArm suit. The effectiveness of using it as a navigation assistant was evaluated using a simulated environment with Unity. Prospects of improvement and problem solving were also discussed. The main areas of possible improvement included personalizing the prototype as per user preferences, the inclusion of tactile feedback along with force-feedback and improvising the aesthetic values.

The ForceArm suit was also used for designing a PGM-based force-feedback system applicable in VR environments. The system was mainly based on the wrist flexion-extension DOF. Two types of actuation methods were used for four different types of feedback scenarios in VR. A small user study was conducted to identify the preferences of the users about the PGM-based force-feedback. The PWM-based feedback was generally more satisfying as compared to the binary control method according to the opinions of the subjects.



# Chapter 6

## Future work

There is a substantial possibility of improvement of the current version of the ForceArm prototype. Firstly, regarding the application related to accelerating motor recovery, more accurate evaluation needs to be done by involving more number of subjects with the lesser bias of age, health status and other related factors. Moreover, muscle unloading effects on the elbow and shoulder flexion in elderly participants should be identified as soon as consent is acquired. The current points of attachment of the PGMs are fixed for all subjects, which is not guaranteed to be suitable for all kinds of users with varying body dimensions and all concerned motions. Therefore, to achieve effective muscle unloading in a significant number of participants for all selected motions, we consider optimizing the lengths and attachment points of the PGMs. Optimization can be done through simulation techniques.

Moreover, a slight restriction was observed in the grasping capacity of the hand while wearing the prototype. This restriction was mainly due to the hand-wrap glove and the small part of the PGMs attached to the palm. The fingers were, however, not restricted. Therefore, to address this issue, changes need to be made in the hand part of the prototype to ensure the least restriction of natural grasping. Regarding the present control system, it is limited to providing a static air pressure input to the PGMs. We plan to improve it by introducing a dynamic control method which can realize a higher

level of compliance. Human motion-sensing also needs to be included in the dynamic control loop. The gaming task in this study was performed explicitly by two elderly subjects with and without assistance. This approach is very preliminary and can only be used for feasibility verification. Therefore, we further plan to study the effects of ForceArm-based assistance using a proper distribution of the study and control groups with a more significant number of participants. It would also be interesting to study the immediate impact of removing the assistance on users.

As future work for our motor learning-related user study, we consider attaching our soft exoskeleton on other positions, such as a whole arm or even lower limbs that could enable our body to perceive more prominent movements applicable to a broader range of tasks, beyond drumming. Besides, it is worth mentioning that our study was limited to recollection within 90 minutes, which is short for a motor learning experiment. This duration is not enough to argue that such proprioceptive feedback through wearable actuators can have long-term learning effects. Therefore more extensive studies can be done to identify such effects of long term learning.

For the navigation study, future work includes improvement of the prototype for resolving aesthetic preferences. An initial procedure of calibration also needs to be included to tune into the comfortable force range of each user. Precise navigation cues will also be attempted to be provided through variable levels of input air-pressure fed to the actuators. Such complicated cues will provide more productive and better feedback through precise information encoding. Personalizing the glove itself is a vital aspect that can add value to the wearable prototype [87]. Therefore, users can be given the ability to customize the prototype as per their convenience. Such choices will improve satisfaction as well as the concentration of the users.



The VR force-feedback case study introduced and compared two different methods to realize the forces involved in touching heavy objects. These forces were mainly rendered at the wrist joint. Since the approach was evaluated using a preliminary study only, prospects involve multiple aspects to be evaluated. The size of the study should be increased with more number of participants that will provide extended user-feedback and data that can be statistically analyzed. Moreover, the optimum rise time of air-pressure for different types of feedback needs to be identified for a more realistic experience. Additional DOFs of the elbow and shoulder joints can also be considered to enrich the different types of feedback further. Blinding the subjects by not showing any visual display will also provide us with an additional dimension of subjective feedback. Such restriction of the sensory channel will help the subjects to analyze the force-feedback types with more concentration. The PGM-based force-feedback should be compared and combined with different other methods of feedback in VR such as vibrotactile and EMS.



# Bibliography

- [1] Swagata Das, Yusuke Kishishita, Toshio Tsuji, Cassie Lowell, Kazunori Ogawa, and Yuichi Kurita. Forcehand glove: a wearable force-feedback glove with pneumatic artificial muscles (pams). *IEEE Robotics and Automation Letters*, 3(3):2416–2423, 2018.
- [2] Swagata Das and Yuichi Kurita. Forcearm: A wearable pneumatic gel muscle (pgm)-based assistive suit for the upper limb. *IEEE Transactions on Medical Robotics and Bionics*, 2(2):269–281, 2020.
- [3] Swagata Das and Yuichi Kurita. Providing navigation assistance through forcehand: a wearable force-feedback glove. In *2019 IEEE Global Conference on Signal and Information Processing (GlobalSIP)*, pages 1–5. IEEE, 2019.
- [4] Swagata Das, Chetan Thakur, and Yuichi Kurita. Force-feedback in virtual reality through pgm-based forcehand glove. In *2020 IEEE/SICE International Symposium on System Integration (SII)*, pages 1016–1021. IEEE, 2020.
- [5] Linda R Elliot, Elizabeth S Redden, Rodger A Pettitt, Christian B Carstens, Jan van Erp, and Maaïke Duistermaat. Tactile guidance for land navigation. Technical report, U. S. Army Research Laboratory, Human Research and Engineering directorate, 2006.
- [6] JJ Scott and Robert Gray. A comparison of tactile, visual, and auditory warnings for rear-end collision prevention in simulated driving. *Human factors*, 50(2):264–275, 2008.

- 
- [7] Pawel Kiper, Andrzej Szczudlik, Michela Agostini, Jozef Opara, Roman Nowobilski, Laura Ventura, Paolo Tonin, and Andrea Turolla. Virtual reality for upper limb rehabilitation in subacute and chronic stroke: a randomized controlled trial. *Archives of physical medicine and rehabilitation*, 99(5):834–842, 2018.
- [8] Isabelle Hupont, Joaquin Gracia, Luis Sanagustin, and Miguel Angel Gracia. How do new visual immersive systems influence gaming qoe? a use case of serious gaming with oculus rift. In *2015 Seventh International Workshop on Quality of Multimedia Experience (QoMEX)*, pages 1–6. IEEE, 2015.
- [9] Daniel F Keefe, Daniel Acevedo Feliz, Tomer Moscovich, David H Laidlaw, and Joseph J LaViola Jr. Cavepainting: a fully immersive 3d artistic medium and interactive experience. In *Proceedings of the 2001 symposium on Interactive 3D graphics*, pages 85–93. Citeseer, 2001.
- [10] Kurinchi Selvan Gurusamy, Rajesh Aggarwal, Latha Palanivelu, and Brian R Davidson. Virtual reality training for surgical trainees in laparoscopic surgery. *Cochrane database of systematic reviews*, (1), 2009.
- [11] Frederick P Brooks. What’s real about virtual reality? *IEEE Computer graphics and applications*, 19(6):16–27, 1999.
- [12] UN DESA. United nations, department of economic and social affairs, population division. world population prospects 2019: Highlights, 2019.
- [13] Hilde Feys, Willy De Weerdt, Geert Verbeke, Gail Cox Steck, Chris Capiiau, Carlotte Kiekens, Eddy Dejaeger, Gustaaf Van Hoydonck, Guido Vermeersch, and Patrick Cras. Early and repetitive stimulation of the arm can substantially improve the long-term outcome after stroke: a 5-year follow-up study of a randomized trial. *Stroke*, 35(4):924–929, 2004.
- [14] James Patton, Steven L Small, and William Zev Rymer. Functional restoration for the stroke survivor: informing the efforts of engineers. *Topics in stroke rehabilitation*, 15(6):521–541, 2008.

- [15] Paweł Maciejasz, Jörg Eschweiler, Kurt Gerlach-Hahn, Arne Jansen-Troy, and Steffen Leonhardt. A survey on robotic devices for upper limb rehabilitation. *Journal of neuroengineering and rehabilitation*, 11(1):3, 2014.
- [16] Kai Zhang, Xiaofeng Chen, Fei Liu, Haili Tang, Jing Wang, and Weina Wen. System framework of robotics in upper limb rehabilitation on poststroke motor recovery. *Behavioural neurology*, 2018, 2018.
- [17] Rui CV Loureiro, William S Harwin, Kiyoshi Nagai, and Michelle Johnson. Advances in upper limb stroke rehabilitation: a technology push. *Medical & biological engineering & computing*, 49(10):1103, 2011.
- [18] Seong Jun Park and Cheol Hoon Park. Suit-type wearable robot powered by shape-memory-alloy-based fabric muscle. *Scientific Reports*, 9(1):9157, 2019.
- [19] Hermano I Krebs, Mark Ferraro, Stephen P Buerger, Miranda J Newbery, Antonio Makiyama, Michael Sandmann, Daniel Lynch, Bruce T Volpe, and Neville Hogan. Rehabilitation robotics: pilot trial of a spatial extension for mit-manus. *Journal of NeuroEngineering and Rehabilitation*, 1(1):5, 2004.
- [20] Bertrand Tondu and Pierre Lopez. Modeling and control of mckibben artificial muscle robot actuators. *IEEE control systems Magazine*, 20(2):15–38, 2000.
- [21] Abhishek Gupta and Marcia K O’Malley. Design of a haptic arm exoskeleton for training and rehabilitation. *IEEE/ASME Transactions on mechatronics*, 11(3):280–289, 2006.
- [22] Abhishek Gupta, Marcia K O’Malley, Volkan Patoglu, and Charles Burgar. Design, control and performance of ricewrist: a force feedback wrist exoskeleton for rehabilitation and training. *The International Journal of Robotics Research*, 27(2):233–251, 2008.
- [23] Joel C Perry, Jacob Rosen, and Stephen Burns. Upper-limb powered exoskeleton design. *IEEE/ASME transactions on mechatronics*, 12(4):408–417, 2007.

- 
- [24] Ranathunga Arachchilage Ruwan Chandra Gopura, Kazuo Kiguchi, and Yang Li. Sueful-7: A 7dof upper-limb exoskeleton robot with muscle-model-oriented emg-based control. In *2009 IEEE/RSJ International Conference on Intelligent Robots and Systems*, pages 1126–1131. IEEE, 2009.
- [25] James A French, Chad G Rose, and Marcia K O’malley. System characterization of mahi exo-ii: A robotic exoskeleton for upper extremity rehabilitation. In *ASME 2014 Dynamic Systems and Control Conference*. American Society of Mechanical Engineers Digital Collection, 2014.
- [26] Ying Mao and Sunil Kumar Agrawal. Design of a cable-driven arm exoskeleton (carex) for neural rehabilitation. *IEEE Transactions on Robotics*, 28(4):922–931, 2012.
- [27] Tobias Nef, Matjaz Mihelj, Gabriela Kiefer, Christina Perndl, Roland Muller, and Robert Riener. Armin-exoskeleton for arm therapy in stroke patients. In *2007 IEEE 10th international conference on rehabilitation robotics*, pages 68–74. IEEE, 2007.
- [28] Nikolaos G Tsagarakis and Darwin G Caldwell. Development and control of a ‘soft-actuated’ exoskeleton for use in physiotherapy and training. *Autonomous Robots*, 15(1):21–33, 2003.
- [29] Eric T Wolbrecht, John Leavitt, David J Reinkensmeyer, and James E Bobrow. Control of a pneumatic orthosis for upper extremity stroke rehabilitation. In *2006 International Conference of the IEEE Engineering in Medicine and Biology Society*, pages 2687–2693. IEEE, 2006.
- [30] James Allington, Steven J Spencer, Julius Klein, Meghan Buell, David J Reinkensmeyer, and James Bobrow. Supinator extender (sue): a pneumatically actuated robot for forearm/wrist rehabilitation after stroke. In *2011 Annual International Conference of the IEEE Engineering in Medicine and Biology Society*, pages 1579–1582. IEEE, 2011.

- 
- [31] Sivakumar Balasubramanian, Ruihua Wei, Mike Perez, Ben Shepard, Edward Koeneman, James Koeneman, and Jiping He. Rupert: An exoskeleton robot for assisting rehabilitation of arm functions. In *2008 virtual rehabilitation*, pages 163–167. IEEE, 2008.
- [32] Ricardo Morales, Francisco Javier Badesa, Nicolás García-Aracil, José María Sabater, and Carlos Pérez-Vidal. Pneumatic robotic systems for upper limb rehabilitation. *Medical & biological engineering & computing*, 49(10):1145, 2011.
- [33] Tomoyuki Noda, Tatsuya Teramae, Barkan Ugurlu, and Jun Morimoto. Development of an upper limb exoskeleton powered via pneumatic electric hybrid actuators with bowden cable. In *2014 IEEE/RSJ International conference on intelligent robots and systems*, pages 3573–3578. IEEE, 2014.
- [34] George Andrikopoulos, George Nikolakopoulos, and Stamatis Manesis. Motion control of a novel robotic wrist exoskeleton via pneumatic muscle actuators. In *2015 IEEE 20th Conference on Emerging Technologies & Factory Automation (ETFA)*, pages 1–8. IEEE, 2015.
- [35] Zeeshan O Khokhar, Zhen G Xiao, and Carlo Menon. Surface emg pattern recognition for real-time control of a wrist exoskeleton. *Biomedical engineering online*, 9(1):41, 2010.
- [36] Christopher N Schabowsky, Sasha B Godfrey, Rahsaan J Holley, and Peter S Lum. Development and pilot testing of hexorr: hand exoskeleton rehabilitation robot. *Journal of neuroengineering and rehabilitation*, 7(1):36, 2010.
- [37] Claudio Pacchierotti, Stephen Sinclair, Massimiliano Solazzi, Antonio Frisoli, Vincent Hayward, and Domenico Prattichizzo. Wearable haptic systems for the fingertip and the hand: taxonomy, review, and perspectives. *IEEE transactions on haptics*, 10(4):580–600, 2017.

- [38] Talha Shahid, Darwin Gouwanda, Surya Nurzaman, et al. Moving toward soft robotics: A decade review of the design of hand exoskeletons. *Biomimetics*, 3(3):17, 2018.
- [39] Alan T Asbeck, Robert J Dyer, Arnar F Larusson, and Conor J Walsh. Biologically-inspired soft exosuit. In *2013 IEEE 13th International Conference on Rehabilitation Robotics (ICORR)*, pages 1–8. IEEE, 2013.
- [40] Patrik Kutilek, Jan Hejda, Pavel Smrcka, Vojtech Havlas, et al. Design of smart orthosis of upper limb for rehabilitation. In *World Congress on Medical Physics and Biomedical Engineering 2018*, pages 773–778. Springer, 2019.
- [41] Ning Li, Peng Yu, Tie Yang, Liang Zhao, Ziwen Liu, Ning Xi, and Lianqing Liu. Bio-inspired wearable soft upper-limb exoskeleton robot for stroke survivors. In *2017 IEEE International Conference on Robotics and Biomimetics (ROBIO)*, pages 2693–2698. IEEE, 2017.
- [42] Panagiotis Polygerinos, Zheng Wang, Kevin C Galloway, Robert J Wood, and Conor J Walsh. Soft robotic glove for combined assistance and at-home rehabilitation. *Robotics and Autonomous Systems*, 73:135–143, 2015.
- [43] Panagiotis Polygerinos, Stacey Lyne, Zheng Wang, Luis Fernando Nicolini, Bobak Mosadegh, George M Whitesides, and Conor J Walsh. Towards a soft pneumatic glove for hand rehabilitation. In *2013 IEEE/RSJ International Conference on Intelligent Robots and Systems*, pages 1512–1517. IEEE, 2013.
- [44] Victoria W Oguntosin, Yoshiki Mori, Hyejong Kim, Slawomir J Nasuto, Sadao Kawamura, and Yoshikatsu Hayashi. Design and validation of exoskeleton actuated by soft modules toward neurorehabilitation—vision-based control for precise reaching motion of upper limb. *Frontiers in neuroscience*, 11:352, 2017.
- [45] Nicholas W Bartlett, Valentina Lyau, William A Raiford, Dónal Holland, Joshua B Gafford, Theresa D Ellis, and Conor J Walsh. A soft robotic orthosis for wrist rehabilitation. *Journal of Medical Devices*, 9(3):030918, 2015.



- [46] Christopher J Payne, Elizabeth Gallardo Hevia, Nathan Phipps, Asli Atalay, Ozgur Atalay, Bo Ri Seo, David J Mooney, and Conor J Walsh. Force control of textile-based soft wearable robots for mechanotherapy. In *2018 IEEE International Conference on Robotics and Automation (ICRA)*, pages 1–7. IEEE, 2018.
- [47] Jianglong Guo, Chaoqun Xiang, Tim Helps, Majid Taghavi, and Jonathan Rossiter. Electroactive textile actuators for wearable and soft robots. In *2018 IEEE International Conference on Soft Robotics (RoboSoft)*, pages 339–343. IEEE, 2018.
- [48] Thomas H Massie, J Kenneth Salisbury, et al. The phantom haptic interface: A device for probing virtual objects. In *Proceedings of the ASME winter annual meeting, symposium on haptic interfaces for virtual environment and teleoperator systems*, volume 55, pages 295–300. Citeseer, 1994.
- [49] Seahak Kim, Shoichi Hasegawa, Yasuharu Koike, and Makoto Sato. Tension based 7-dof force feedback device: Spidar-g. In *Proceedings IEEE Virtual Reality 2002*, pages 283–284. IEEE, 2002.
- [50] Pedro Lopes, Patrik Jonell, and Patrick Baudisch. Affordance++: allowing objects to communicate dynamic use. In *Proceedings of the 33rd Annual ACM Conference on Human Factors in Computing Systems*, pages 2515–2524. ACM, 2015.
- [51] Omar Mubin, Fady Alnajjar, Nalini Jishtu, Belal Alsinglawi, and Abdullah Al Mahmud. Exoskeletons with virtual reality, augmented reality, and gamification for stroke patients’ rehabilitation: Systematic review. *JMIR rehabilitation and assistive technologies*, 6(2):e12010, 2019.
- [52] Richard A Schmidt, Douglas E Young, Stephan Swinnen, and Diane C Shapiro. Summary knowledge of results for skill acquisition: Support for the guidance hypothesis. *Journal of Experimental Psychology: Learning, Memory, and Cognition*, 15(2):352, 1989.

- 
- [53] Alan W Salmoni, Richard A Schmidt, and Charles B Walter. Knowledge of results and motor learning: a review and critical reappraisal. *Psychological bulletin*, 95(3):355, 1984.
- [54] Claude Ghez, James Gordon, and MARIA FELICE Ghilardi. Impairments of reaching movements in patients without proprioception. ii. effects of visual information on accuracy. *Journal of neurophysiology*, 73(1):361–372, 1995.
- [55] JAMES Gordon, MARIA FELICE Ghilardi, and Claude Ghez. Impairments of reaching movements in patients without proprioception. i. spatial errors. *Journal of neurophysiology*, 73(1):347–360, 1995.
- [56] Xiao Xiao and Hiroshi Ishii. Inspect, embody, invent: a design framework for music learning and beyond. In *Proceedings of the 2016 CHI Conference on Human Factors in Computing Systems*, pages 5397–5408. ACM, 2016.
- [57] David Feygin, Madeleine Keehner, and R Tendick. Haptic guidance: Experimental evaluation of a haptic training method for a perceptual motor skill. In *Proceedings 10th Symposium on Haptic Interfaces for Virtual Environment and Teleoperator Systems. HAPTICS 2002*, pages 40–47. IEEE, 2002.
- [58] Simon Holland, Anders J Bouwer, Mathew Dalgelish, and Topi M Hurtig. Feeling the beat where it counts: fostering multi-limb rhythm skills with the haptic drum kit. In *Proceedings of the fourth international conference on Tangible, embedded, and embodied interaction*, pages 21–28. ACM, 2010.
- [59] Emi Tamaki, Takashi Miyaki, and Jun Rekimoto. Possessedhand: techniques for controlling human hands using electrical muscles stimuli. In *Proceedings of the SIGCHI Conference on Human Factors in Computing Systems*, pages 543–552. ACM, 2011.
- [60] Michinari Kono, Takumi Takahashi, Hiromi Nakamura, Takashi Miyaki, and Jun Rekimoto. Design guideline for developing safe systems that apply electricity to

- the human body. *ACM Transactions on Computer-Human Interaction (TOCHI)*, 25(3):19, 2018.
- [61] Jose L Hernandez-Rebollar, Nicholas Kyriakopoulos, and Robert W Lindeman. The acceleglove: a whole-hand input device for virtual reality. In *ACM SIGGRAPH 2002 conference abstracts and applications*, pages 259–259, 2002.
- [62] Lisa Baraniecki, Gina Hartnett, Linda Elliott, Rodger Pettitt, Jack Vice, and Kenyon Riddle. An intuitive wearable concept for robotic control. In *International Conference on Human Interface and the Management of Information*, pages 492–503. Springer, 2017.
- [63] Ali Karime, Hussein Al-Osman, Wail Gueaieb, and Abdulmotaleb El Saddik. E-glove: An electronic glove with vibro-tactile feedback for wrist rehabilitation of post-stroke patients. In *2011 IEEE International Conference on Multimedia and Expo*, pages 1–6. IEEE, 2011.
- [64] Anthony D Kurtz. Tactile feel apparatus for use with robotic operations, July 10 2008. US Patent App. 11/650,643.
- [65] Heather Culbertson, Juan José López Delgado, and Katherine J Kuchenbecker. One hundred data-driven haptic texture models and open-source methods for rendering on 3d objects. In *2014 IEEE Haptics Symposium (HAPTICS)*, pages 319–325. IEEE, 2014.
- [66] Jun Murayama, Laroussi Bougrila, YanLin Luo, Katsuhito Akahane, Shoichi Hasegawa, Béat Hirsbrunner, and Makoto Sato. Spidar g&g: a two-handed haptic interface for bimanual vr interaction. In *Proceedings of EuroHaptics*, volume 2004, pages 138–146. Citeseer, 2004.
- [67] Kazuki Nagai, Soma Tanoue, Katsuhito Akahane, and Makoto Sato. Wearable 6-dof wrist haptic device spidar-w. In *SIGGRAPH Asia 2015 Haptic Media And Contents Design*, page 19. ACM, 2015.

- [68] Pedro Lopes, Sijing You, Lung-Pan Cheng, Sebastian Marwecki, and Patrick Baudisch. Providing haptics to walls & heavy objects in virtual reality by means of electrical muscle stimulation. In *Proceedings of the 2017 CHI Conference on Human Factors in Computing Systems*, pages 1471–1482. ACM, 2017.
- [69] Julie M Walker, Nabil Zemiti, Philippe Poignet, and Allison M Okamura. Holdable haptic device for 4-dof motion guidance. *arXiv preprint arXiv:1903.03150*, 2019.
- [70] Adam Spiers and Katherine J. Kuchenbecker. Explorations of shape-changing haptic interfaces for blind and sighted pedestrian navigation. *CHI Extended Abstracts*, 2019.
- [71] Escobar Alarcon and Francesco Ferrise. Design of a wearable haptic navigation tool for cyclists. In *2017 International Conference on Innovative Design and Manufacturing*, pages 1–6, 2017.
- [72] Matthias Hoppe, Pascal Knierim, Thomas Kosch, Markus Funk, Lauren Futami, Stefan Schneegass, Niels Henze, Albrecht Schmidt, and Tonja Machulla. Vrhaptic-drones: Providing haptics in virtual reality through quadcopters. In *Proceedings of the 17th International Conference on Mobile and Ubiquitous Multimedia*, pages 7–18. ACM, 2018.
- [73] Ferdinando Auricchio, Elisa Boatti, and Michele Conti. Sma biomedical applications. In *Shape Memory Alloy Engineering*, pages 307–341. Elsevier, 2015.
- [74] Amin Yazdanpanah Goharrizi and Nariman Sepehri. A wavelet-based approach to internal seal damage diagnosis in hydraulic actuators. *IEEE transactions on industrial electronics*, 57(5):1755–1763, 2009.
- [75] Swagata Das, Cassie Lowell, and Yuichi Kurita. Force your hand—pam enabled wrist support. In *International AsiaHaptics Conference*, pages 239–245. Springer, 2016.

- [76] Kazunori Ogawa, Chetan Thakur, Tomohiro Ikeda, Toshio Tsuji, and Yuichi Kurita. Development of a pneumatic artificial muscle driven by low pressure and its application to the unplugged powered suit. *Advanced Robotics*, 31(21):1135–1143, 2017.
- [77] Baltej Singh Rupal, Sajid Rafique, Ashish Singla, Ekta Singla, Magnus Isaksson, and Gurvinder Singh Virk. Lower-limb exoskeletons: Research trends and regulatory guidelines in medical and non-medical applications. *International Journal of Advanced Robotic Systems*, 14(6):1729881417743554, 2017.
- [78] Charles Mayo Goss. Gray’s anatomy of the human body. *Academic Medicine*, 35(1):90, 1960.
- [79] Helen Hislop, Dale Avers, and Marybeth Brown. *Daniels and Worthingham’s muscle Testing-E-Book: Techniques of manual examination and performance testing*. Elsevier Health Sciences, 2013.
- [80] Shinya Matsuda, Keiji Muramatsu, and Kenshi Hayashida. Eligibility classification logic of the japanese long term care insurance. *Asian Pacific Journal of Disease Management*, 5(3):65–74, 2011.
- [81] Hermie J Hermens, Bart Freriks, Roberto Merletti, Dick Stegeman, Joleen Blok, Günter Rau, Cathy Disselhorst-Klug, and Göran Hägg. European recommendations for surface electromyography. *Roessingh research and development*, 8(2):13–54, 1999.
- [82] Carol Barnett Lammon. *Clinical nursing skills*. WB Saunders Co, 1995.
- [83] Roberto Colombo. Performance measures in robot assisted assessment of sensorimotor functions. In *Rehabilitation Robotics*, pages 101–115. Elsevier, 2018.
- [84] Peter S Lum, Charles G Burgar, Peggy C Shor, Matra Majmundar, and Machiel Van der Loos. Robot-assisted movement training compared with conventional

- therapy techniques for the rehabilitation of upper-limb motor function after stroke. *Archives of physical medicine and rehabilitation*, 83(7):952–959, 2002.
- [85] Shinya Fujii, Kazutoshi Kudo, Tatsuyuki Ohtsuki, and Shingo Oda. Tapping performance and underlying wrist muscle activity of non-drummers, drummers, and the world’s fastest drummer. *Neuroscience letters*, 459(2):69–73, 2009.
- [86] Geoff Norman. Likert scales, levels of measurement and the “laws” of statistics. *Advances in health sciences education*, 15(5):625–632, 2010.
- [87] Matthew Pateman, Daniel Harrison, Paul Marshall, and Marta E Cecchinato. The role of aesthetics and design: wearables in situ. In *Extended Abstracts of the 2018 CHI Conference on Human Factors in Computing Systems*, page LBW518. ACM, 2018.

## Acknowledgements

I want to express my most profound acknowledgement and gratitude to my advisor, Professor Yuichi Kurita, for his valuable teaching, support, and overall guidance. He has provided me with a precious opportunity of learning about human augmentation, human modelling, haptics, human data analysis and soft actuators through his unmatched expertise and assistance. He has been a true inspiration throughout my PhD life because of his positive demeanour and optimistic character.

I would also like to thank Professor Toshio Tsuji, who is the backbone of the Biological Systems Engineering laboratory and has always supervised me during the crucial moments. He has given me some valuable pieces of advice that benefitted me through the steps of my PhD years. I also offer my sincere gratitude to Associate Professor Han Soo Lee, who has provided valuable recommendations about the implementation of my technical research with additional and necessary insight into social and cultural values.

I want to take this opportunity to thank my dearest friends and seniors Chetan Thakur, Yusuke Kishishita, Takuya Murata and Masataka Yamamoto for their valuable input and support whenever I needed. I am also appreciative to my juniors and lab members of the Biological Systems Engineering laboratory who have never failed to raise my spirit whenever I required. I am obliged to the TAOYAKA Program and its staff and members for offering valuable academic aid during my PhD education. Finally, I thank my family and friends for supporting me and giving me the courage to fulfil my desires through this academic degree.